Table des matières

RT1- Les indices de complexité

Prediction of VMAT plans deliverability to optimize patient-specific QA workload

M.L. Askoura[1], D. Dechambre[1], N. Depatoul[1], J.M. Denis[1], A. Delor[1], F. Vanneste[1]

[1]University Hospital Saint-Luc, UCL, Brussels, Belgium.

Purpose: This study aimed at reducing the patient specific QA workload of the physic team by suggesting a gamma index correlated MLC-metric to sort and prioritize the patient plans.

Introduction: The workload of physicists has considerably increased with the advent of intensity-modulated radiotherapy and subsequent pre-treatment quality assurance (QA).In a context of ever-shorter time-to-treatment, plans not passing the acceptable quality level generate extra work time (e.g. re-planning and re-measuring). As the source of error mainly comes from TPS approximation and machine deliverability, our study aimed at correlating plan complexity metric to the reference measurement results in order to predict the plans pass/fail status before QA.

Methods: 101 consecutive VMAT plans were measured using the PTW Octavius 4D/729 and retrospectively analyzed using a global 3%/3mm gamma criteria. Using RayStation V8 IronPython scripting, the modulation complexity score (MCS) was calculated according to Mc Niven *et al.,* 2010. It assesses plan complexity based on both leaf sequence and aperture area variability. Correlation between gamma passing rates (GPR, fixed at 96%passing points) and MCS values was assessed using Pearson's r-coefficient. Receiver-operating characteristic (ROC) analysis was performed to determine appropriate complexity threshold values for plan classification and assess the model prediction power.

Results: GPR ranged from 90.5 to 99.4% for class solution Breast, prostate, rectum and Glioblastoma plans.
The MCS was highly correlated with the plan pass/fail status and showed high prediction power with 0.91 area under the curve value (cf. Fig.1).

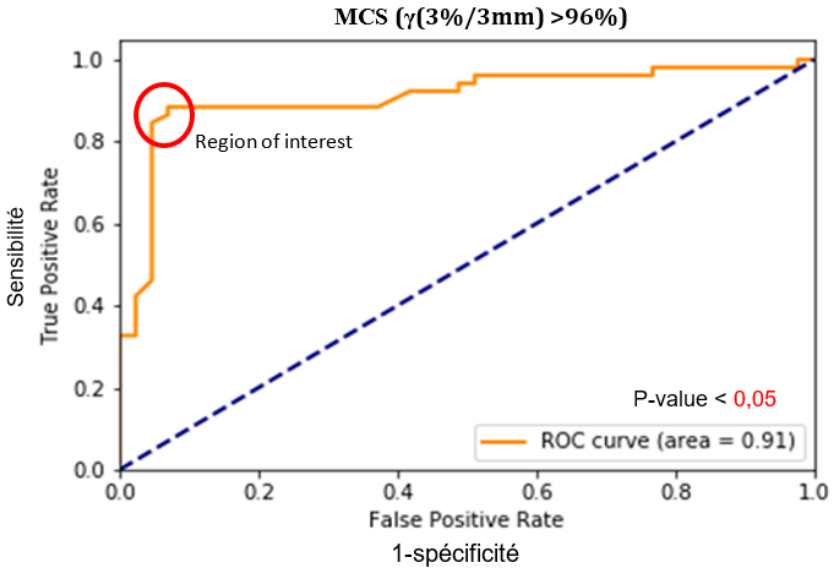

Fig. 1. ROC curve for MCS metric to predict the pass/fail status of pre-treatment QA using a 3%/3mm GPR>96%. The blue dotted line represents the random model.

Within the high sensitivity and specificity zone (red circle), 3 dose thresholds were further highlighted in Fig.2, presenting the evolution of the MCS in function of the GPR. While the 0.28 MCS threshold shows no false positive rate (FPR), it only includes 17% of the patient population (orange square). Using a MCS threshold of 0.22 allows for higher sensitivity at the cost of 5% FPR (GPR still above 95%).

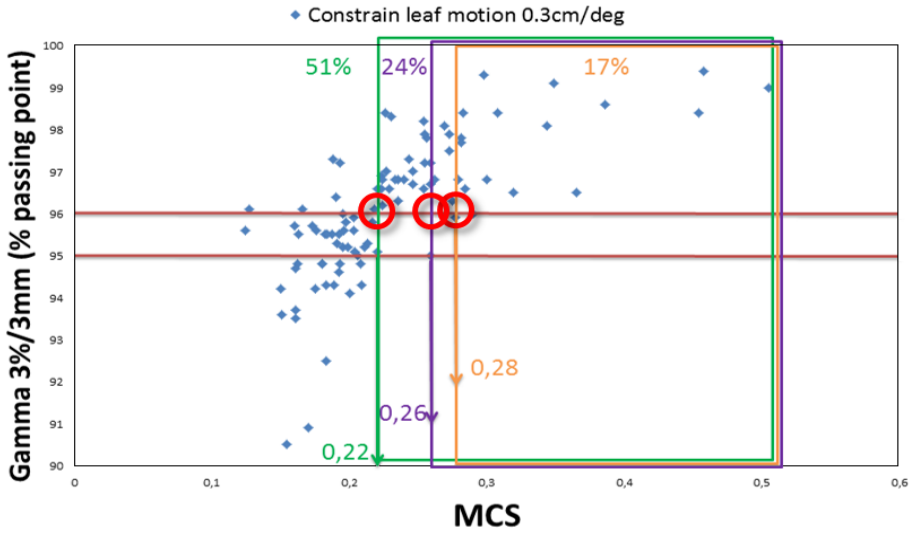

Fig. 2. Evolution of the MCS as a function of the GPR. Color box shows patient population above selected MCS thresholds.

A traffic light protocol was defined for class solution VMAT patient with MCS values <0.175 (72 % FPR) as re-planning (red-light), the [0.175, 0.22] range as "QA before treatment start" (orange light, 28% FPR) and MCS > 0.22 as "QA after start allowed" (green light, 5% FPR).

Conclusions: Plan deliverability prediction model was built on the strong correlation we found between its MCS and its QA pass/fail status. Traffic light protocol was put into place using MCS thresholds values and Raystation script was adapted with the same color code. It allowed to intercept overly-modulated plans before the QA step (red light, MCS < 0.175) and to give more flexibility to the physicist for the organization of patient specific QA (green light, MCS>0.22). This approach was successfully implemented in our daily routine.

Complexity indexes: A new approach to limit pre-treatment checks
Les index de complexité : Une nouvelle approche pour limiter les contrôles prétraitement

Z.L. Jazouli[b], S. Muraro[a], D. Julian[a], Dr. E. Beguier[a], Y.F. Alaoui[b]

[a]Centre de cancérologie du Grand Montpellier(CCGM)/L'Hérault/Montpellier/France
[b]Université Clermont Auvergne (UCA)/Auvergne/Clermont-Ferrand/France

Introduction: This study proposes a model based on complexity indexes, to predict the feasibility of treatment plans in radiotherapy with intensity modulated.

Methods: The clinical model was created in three stages. First, the development of an algorithm in python 3.7, integrating the calculation of 7 complexity scores (MCS / LTMCS) *[1] (MAD / MFA / CLS / CAS) *[2], the scores describe parameters such as moving and opening leafs for each control point (CP). An ad hoc score has been developed to integrate the variability of Monitor Units Variability (MUV). Then, a retrospective study evaluated the correlation between the scores and the Gamma Index (GI) from a database containing a sample of 700 treatment plans (1379 VMAT beams). To validate the model, a prospective evaluation was carried out on 200 VMAT treatment plans (451 beams). The model has been established to identify plans that are likely to fail the Gamma Index test as recommended by SFPM *[3].

Results: A strong correlation (R = 0.79) was found with the LTMCS / MUV combination and the GI (3% 3mm) for the normo-fractionated planes and (2% 2mm) for the stereotaxic planes. The highest found value of LTMCS is 0.57 (low complexity) and the lowest value is 0.02 (high complexity). The MUV varies between 0 (UM stable between all CPs) and 180 (Maximum variation of UM between CPs). The results showed that a LTMCS greater than 0.15 and a MUV less than 5 of a plan mean that its beams are predicted as true positives (GI> 95%). Sorting by the LTMCS and the MUV made it possible to have 75% (1035 beams out of 1379) of true positives (p-value <0.001). The scores calculated for the 25% of the remaining plans (344 beams) reflect a high complexity between each CP, and may lead to GI <95% (90 out of 344 beams). The method combining the LTMCS / MUV allowed to discriminate the risk of false positives (p-value <0.001). The prospective use of the model proved its detection efficiency of 75% of true positives (339 out of 451 beams, p-value <0.001), of the remaining 112 beams, only 25 were true negatives (GI <95%).

Conclusions: Complexity scores provide help with pretreatment controls. The study of the complexity scores and the thresholds determined are dependent on each TPS / Linac pair. The two LTMCS / MUV scores help rule out the false positives, the study continues to reduce the 15% of false negatives**.**

References

[1] Jong Min Park, So-Yeon Park and Hyoungnyoun Kim (2015). Modulation index for VMAT considering both mechanical and dose calculation uncertainties. Physics in Medicine & Biology.60.
[2] Crowe, Scott, Kairn, Tanya, Kenny, John, Knight, Richard, Hill, Brendan, Langton, Christian M., & Trapp, Jamie (2014). Treatment plan complexity metrics for predicting IMRT pre-treatment quality assurance results. Australasian Physical & Engineering Sciences in Medicine, 37(3).
[3] Report SFPM n° 34, November 2018.

Combining complexity metrics to better predict VMAT deliverability
Combinaison d'indices de complexité pour évaluer la faisabilité des plans de traitement VMAT

M. Ribeiro[a], Q. Dupuy[a], L. Bartolucci[a]

[a]Institut Curie/Paris/France

Introduction: Use of Volumetric Arc Therapy (VMAT) is constantly growing due to its ability to deliver highly conformal dose to the target faster than most of conventional techniques. However, complexity of VMAT plans has been shown to be directly linked with delivery accuracy which is one of the reasons why systematic pre-treatment QA are usually performed before clinical treatment. In order to reduce patient-specific QA workload, numerous studies have focused on complexity metrics to see whether it can be related with VMAT deliverability. However, these metrics are generally not exhaustive. In this work, we investigated (1) the complementarity of several complexity metrics to develop a more robust and effective index, and (2) the correlation with pre-treatment QA measurements.

Methods: 139 VMAT plans generated with Eclipse v13.6 for 4 treatment sites (prostate and pelvic nodes – prostate only – head and neck – breast and lymph nodes) were retrospectively analyzed. Pre-treatment quality assurance was performed using Varian PDIP (Portal Dose Image Prediction) algorithm and measured using EPID. Agreement between planned and measured dose was evaluated arc by arc using Varian Portal Dosimetry tool with global and local gamma index passing rates (GPR) with 3%/3mm and 2%/2mm criteria. Using an in-house software, 8 complexity metrics were calculated: MI_t (Modulation Index Total) [Park, 2014], MCSv (Modulation Complexity Score for VMAT), LT (Leaf Travel), LTMCS (Combination of LT and MCSv) [Masi, 2013], SAS5 and SAS10 (Small Aperture Score 5mm and 10mm) [Crowe, 2014], MU (Monitor Units), RTLS (Round-Trip Leaf Score). Complementarity between metrics was investigated by multiplying them with one another. Relationship between complexity metrics and GPR was then studied using Spearman's correlation analysis.

Results: Table 1 shows Spearman's values for the correlations, along with associated p-values. Moderate and strong correlations were observed ($p<0,001$) between local GPR and MIt, MCSv, LTMCS, SAS10 (only for 3%/3mm criteria), and the combinations MIt*MCSv, MIt*SAS10, and MIt*MCSv*SAS10. Local 3%/3mm showed better correlations than local 2%/2mm criteria, with absolute r coefficient ranging from 0,085 to 0,674 (r_mean = 0,449). Global GPR only showed at best weak to moderate correlations, with better results for 2%/2mm than 3%/3mm criteria. Overall best correlation was observed between 3%/3mm local GPR and the combination MIt*MCSv*SAS10.

Conclusions: In this study, several complexity metrics were successfully combined in order to develop a more robust and effective index for VMAT. The combinations presented in this work all show strong correlations with local GPR, especially for local 3%/3mm criteria and the combination MIt*MCSv*SAS10. It proves their great potential to predict VMAT plan deliverability more effectively than already existing metrics. Further work would consist in establishing appropriate thresholds to reduce patient-specific QA workload.

	Global				Local			
	3%/3mm		2%/2mm		3%/3mm		2%/2mm	
	rs	p-value	rs	p-value	rs	p-value	rs	p-value
MIt	-0,336	< 0,001	-0,384	< 0,001	-0,585	< 0,001	-0,581	< 0,001
MCSv	0,310	< 0,001	0,364	< 0,001	0,668	< 0,001	0,630	< 0,001
LT	-0,189	< 0,001	-0,218	< 0,001	-0,085	0,103	-0,114	0,030
LTMCS	0,171	0,001	0,186	< 0,001	0,480	< 0,001	0,429	< 0,001
RTLS	0,222	< 0,001	0,259	< 0,001	0,229	< 0,001	0,261	< 0,001
SAS5	-0,039	0,451	-0,071	0,174	-0,270	< 0,001	-0,225	< 0,001
SAS10	-0,183	< 0,001	-0,224	< 0,001	-0,404	< 0,001	-0,357	< 0,001
UM	0,206	< 0,001	0,218	< 0,001	0,252	< 0,001	0,271	< 0,001
MIt x MCSv	0,353	< 0,001	0,403	< 0,001	0,658	< 0,001	0,637	< 0,001
MIt x SAS10	0,342	< 0,001	0,390	< 0,001	0,639	< 0,001	0,620	< 0,001
MIt x MCSv x SAS10	0,338	< 0,001	0,390	< 0,001	0,674	< 0,001	0,646	< 0,001

Table 1 : Results of correlations between complexity metrics and global or local gamma passing rates with 3%/3mm and 2%/2mm criteria.

Complexity metrics combination to optimize the pre-treatment quality assurance for IMRT and VMAT plans
Optimisation du processus d'assurance qualité des plans de traitement RCMI et VMAT à partir des index de complexité

O. Bolusset[a], J. Fontaine[b], P. Retif[a,c], P. Quétin[d]

[a]Unité de Physique Médicale, CHR Metz-Thionville, Ars-Laquenexy, 57530, France
[b]Service de radiothérapie, Centre d'Oncologie de Gentilly, Nancy, 54000, France
[c]CRAN, UMR 7039, Université de Lorraine, Vandoeuvre-lès-Nancy, 54506, France; 4 CRAN, UMR 7039, CNRS, Vandoeuvre-lès-Nancy, 54506, France
[d]Service de radiothérapie, CHR Metz-Thionville, Ars-Laquenexy, 57530, France

Introduction: New radiotherapy technologies are associated with very complex treatments, with highly inhomogeneous beam fluences. However, plans whose intensity is strongly modulated may be too complex and the dose may be delivered improperly. In order to ensure the adequacy between the calculated dose and the dose delivered by the accelerator, pre-treatment quality assurance measurements are performed. When the difference between calculation and measurement is too important, plans need to be modified and recalculated.
In this study, the aim is to estimate/predict these non-compliant plans. For this purpose, several complexity metrics (indexes) are calculated in order to evaluate the correlation between the plan complexity and the pre-treatment quality assurance results, by analyzing the 3D gamma index measured with the Delta4 phantom (Scandidos, Uppsala, Sweden).
Furthermore, these indexes have been correlated with logs analysis (via LinacWatch, Qualiformed, La Roche-sur-Yon, France) to evaluate whether treatment plans failures may come from mechanical limitations of the machine or not.

Methods: Four complexity metrics are calculated to evaluate the modulation degree of the plans: the "Modulation Complexity Score" (MCS) and "Small-Aperture Score" are based on the complexity of leaves opening and movements of the multi-leaf collimator (MLC), while "Modulation Index" (MI) as well as a texture analysis, rely on the variation of fluence intensity.
The "texture analysis" is calculated by a gray level co-occurrence matrix (GLCM), on which are applied different texture features: entropy, homogeneity, variance, contrast, dissimilarity, correlation and energy.
These four complexity metrics are then calculated on H&N VMAT plans, whose the complexity has been gradually increased by two methods. One is via the "Aperture Shape Controler" option of Eclipse V15.6 (Varian Medical Systems, Palo Alto, USA), which provides 5 levels of complexity by applying constraints on the MLC and modifying the aperture area of segments during the irradiation. The other method is to use a monitor unit threshold to generate more or less complex plans.
A correlation between these complexity metrics and the local gamma index (2%, 2mm) is performed.

Results: For the plans resulting from the two methods of complexity, we observe a correlation between the values of the complexity index, the gamma passing rate of plans and the metrics derived from the log files.

Conclusion: The complexity metrics used are good indicators of the modulation degree of the treatment plans. For the next part of this study, a robustness analysis of these indices will be performed and pass/fail thresholds will be established.

VMAT modulation indexes for predicting plan delivery accuracy: the ICO experience

A. Batista Camejo[a,b], A. Moignier[a], G. Delpon[a] and S. Chiavassa[a]

[a]ICO René Gauducheau Centre, Nantes, France
[b]CHU Jean Bernard, Poitiers, France

Introduction: The delivery accuracy of volumetric arc therapy plans (VMAT) can be affected by the dose calculation model and/or by technical aspects of the accelerator such as leaves position, gantry speed or dose rate errors. For these plans, patient-specific quality assurance (PSQA) is recommended although time consuming. However, plan complexity depends on the modulation degree that can be assessed by a number of metrics commonly named modulation indexes. In this study, nine modulation indexes were studied aiming to rationalize the PSQA workload for VMAT plans.

Methods: As a first step, nine modulation indexes proposed in the literature were computed retrospectively for a total of 299 VMAT plans (72 prostates, 101 prostate beds, 56 cervix and 70 prostates and pelvic lymph nodes). All plans had been delivered with a Varian Clinac 2300iX accelerator and controlled with a PTW 2D array (seven29) and an Octavius phantom (3%/3mm criteria on local gamma index). The studied indexes were : the Leaf Travel (LT)[1], the Modulation Complexity Score for VMAT (MCSv)[1,2], the LTMCS[1], the Edge Metric (EM)[3], the number of Monitor Units per Gy (UM/Gy)[1], MI_s, MI_a and MI_t[4] and LOIC[5]. Correlation test (spearman) between indexes and gamma passing rate, ROC analysis (AUC) and sensitivity score for a given threshold were calculated. As a second step, a prospective study was made over a period of 9 months (145 plans) for the two better indexes (MCSv and LOIC) in order to confirm the initial conclusions. To this end, a script was created in Raystationv7 to easily calculate these indexes for each plan.

Results: For the initial 299 plans, the indexes MCSv, EM, UM/Gy and LOIC showed the best correlation results. The Spearman r values were 0.44, -0.50, -0.47 and -0.52, respectively. Corresponding AUC values were 0.73, 0.77, 0.74 and 0.79. After analysis of sensitivity for the prediction of DQA results, two indexes were kept: MCSv and LOIC. The threshold values found, for a specificity of 100 %, were 0.38 for MCSv (36 % sensitivity) and 1.03% for LOIC (33 % sensitivity). These conclusions have been confirmed by the prospective study made for MCSv and LOIC with Spearman r values of 0.57 and -0.61, AUC values of 0.73 and 0.80 and sensitivity of 33% and 25% for initial threshold of 0.38 and 1.03% respectively. MCSv was finally selected as index to reduce PSQA workload because of its higher sensitivity.

Conclusions: PSQA workload is reduced by more than 30% based on MCSv index. Controls are still performed for the higher modulated plans which require more attention. Moreover, MCSv can be easily calculated throughout the optimization step providing a useful guide during this process.

References

1. Masi, L et al. Med.Phys. 40 (7), 071718 (2013)
2. McNIven, AL et al. Med.Phys. 37 (2), 505-515 (2010)
3. Younge, KC et al. Med.Phys. 39 (11), 7160-7170 (2012)
4. Park, JM et al. Phys. Med. Biol. 59, 7315-7340 (2014)
5. Dechambre D et al. Radiotherapy and Oncology.127:S323 (2018)

Evaluation of a surface imaging system to perform deep inspiration breath-hold technique for external beam radiation therapy of left-sided breast cancer

Évaluation d'un système d'imagerie surfacique pour réaliser la technique d'apnée en inspiration profonde pour le traitement du cancer du sein gauche en radiothérapie externe

D. Zarate[a], N. Mathy[a], J. Mazurier[a], D. Angles[a], J. Camilleri[a], D. Marre[a], E. Caillot[a], C. Chevelle[a], D. Franck[a], O. Gallocher[a], G. Jimenez[a], I. Latorzeff[a], B. Pichon[a], B. Pinel[a]

[a] Groupe ONCORAD Garonne–Clinique Pasteur/Toulouse/France

Introduction: Deep inspiration breath-hold (DIBH) technique is used to reduce cardiac doses of left-sided breast radiation therapy. We studied the accuracy and time saving of using a 3-dimensional surface imaging technique with the AlignRT system (VisionRT) to perform DIBH instead of our usually used spirometry-based system.

Methods: We used AlignRT to setup patients and to monitor inter and intra fractional motions. It could be also used to perform DIBH radiotherapy. In our study, AlignRT system was compared with the spirometer system SDX (Dyn'R) by analyzing 10 patients per system. The treatment plans were made with opposed tangential beams and a field-in-field technique. Prior to this work, we studied and defined regions of interest of the patient surface obtained with AlignRT to get a good agreement between surface images and portal images (PIs) compared to digitally reconstructed radiographs (DRRs). The first aim of this research was to evaluate setup accuracy of breast with DIBH for both AlignRT and SDX systems. We compared translations between the initial and final setup to obtain a good agreement (less than 3 mm) between PIs and DRRs. Then, we compared the number of PIs needed to be less than 3 mm with DRRs and the treatment times. Finally, for DIBH performed with the AlignRT system, we evaluated the heart position difference between computed tomography (CT) reference image and cone beam computed tomography (CBCT) images acquired during treatment.

Results: Differences between IPs and DRRs were less than 3 mm for 71% of fractions using AlignRT system and for 51% of fractions using SDX system. The percentage of fractions with less than two PIs needed to obtain a good agreement between PIs and DRRs was 82% using AlignRT system and 67% for SDX system. Treatment times were less than 15 minutes for 70% of fractions using AlignRT and for 54% of fractions using SDX system. For AlignRT system, we evaluated that the heart position difference between the reference CT and CBCTs performed during treatment was less than 4 mm in any direction.

Conclusions: AlignRT system gives better results than our usually used spirometry-based system concerning setup accuracy and treatment times. This non-invasive imaging surface system, already in used to setup and monitor our patients, allowed us to employ DIBH technique as routine clinical practice for all eligible left-sided N0 breast cancer patients.

DoseCHECK™ algorithm evaluation used for secondary 3D dose calculation of 3DCRT and VMAT treatment plans

Evaluation de l'algorithme DoseCHECK™ utilisé pour le double calcul des unités moniteurs des traitements de radiothérapie externe en technique conformationelle et arcthérapie dynamique

J. Camilleri[a], J. Mazurier[a], D. Angles[a], D. Marre[a], N. Mathy[a], D. Zarate[a], E. Caillot[a], C. Chevelle[a], D. Franck[a], O. Gallocher[a], G. Jimenez[a], I. Latorzeff[a], B. Pichon[a], B. Pinel[a].

[a]Groupe ONCORAD Garonne - Clinique Pasteur / Toulouse / FRANCE

Introduction: DoseCHECK™ (Sun Nuclear Corporation, Miami, FL, USA) is a collapsed cone convolution/superposition algorithm developed to perform secondary 3D dose calculation of external radiotherapy treatment plans. The purpose of this work is to evaluate the accuracy of the software on 3DCRT and VMAT treatment techniques.

Methods: The model was created by the manufacturer from TPS beam data for a Novalis Truebeam STX™ (Varian Medical Systems, Palo Alto, CA, USA) and 3 photon beam energies (6, 10 and 18MV). Test plans were all calculated in our reference TPS Eclipse™ with the AAA algorithm v.13.7 and exported in doseCHECK™.
Measurements were acquired in water with a cylindrical 3D water scanning system associated with a calibrated cylindrical ionization chamber Semiflex™ 31010 (PTW, Freiburg, Germany) and converted into absorbed dose to water (according to the protocol TRS 398).
Predefined type tests of the ESTRO Booklet No.7 [1] were first used to evaluate the model in water. Then, 8 different treatment cases based on the IAEA TECDOC 1583[2] were delivered on the CIRS thorax phantom (model 002LFC) to test the model with heterogeneities.
Finally, a clinical study was conducted on 15 patients (3DCRT and VMAT techniques) by comparing doses calculated by doseCHECK™ and Eclipse™.

Results: Dose differences lower than 2% were found between measured and calculated percentage depth doses and dose profiles except for field sizes larger than 20x20cm² where significant deviations (between 3% and 5%) were observed, especially for depths higher than 20 cm.
Concerning output factors, mean deviations equal to -0.4±0.3% for the 6MV, -0.1±0.3% for the 10MV and 0.2±0.1% for the 18MV were found.
For more complex geometries, the tolerance of 2% is respected in 90% of cases (n=329) except for calculation points located behind the jaws or MLC and out of the treatment field.
Most of tolerances defined by the IAEA protocol 1583 are respected except for some points located in high and low density materials where the dose calculated by doseCHECK™ is underestimated until 4.5% in the bone and overestimated until 4% in the lung insert (tolerance level is 3% for that cases).
Differences calculated from patients study followed a Gaussian distribution with a mean value equal to 0.13 ± 0.8% at the isocenter of each tested beams both for 3DCRT (23 beams) and VMAT (45 beams) treatment techniques.

Conclusions: The model can be used as an independent secondary dose calculation both for 3DCRT and VMAT techniques by comparing doses calculated at the beam isocenter. However, differences observed for large field sizes and depths superior to 20 cm need to be more investigated before using the full 3D analysis tool.

References:

[1] Mijnheer, B. et *al.* Quality assurance of treatment planning systems – Practical examples for non-IMRT photon beams, ESTRO Booklet No. 7. *Radiother Oncol*. 73:S41 (2004).
[2] IAEA - Commissioning of radiotherapy treatment planning systems: testing for typical external beam treatment techniques, TECDOC No 1583. IAEA, Vienna (2008).

RT2- Stéréotaxie

Commissioning of 4 to 10mm conical collimators with Novalis TX® using TRS 483 protocol
Mise en service des collimateurs coniques de 4 à 10mm au Novalis TX® : application du protocole TRS 483

M. Lanaret[a], V. Chassin[a], J.B. Groslier[a], R. Gay[a], F. Magnier[a], V. Dedieu[a]

[a]Service de Physique Médicale et de radioprotection, Centre Jean Perrin, 58 rue Montalembert, 63011 Clermont-Ferrand, France

Introduction: Stereotactic radiosurgery (SRS) of very small lesions such as the trigeminal nerve, with a very high prescribed dose (80 Gy) delivered in a single focused fraction on the target, requires the use of 4mm to 10mm conical collimators. This study focuses on the acquisition of basic dosimetry data for the implementation of SRS using conical collimators in the TPS iPlan (BrainLab) with the main objective of minimizing the uncertainties about the dose delivery. The collimator output factors (OF) measurement is one of the most critical points for very small beams characterization. The purpose of this work is to compare the measured OF using different detectors by applying the TRS 483 protocol.

Methods: An essential prerequisite for dosimetric acquisitions for conical collimators is the evaluation of geometric uncertainty. The first element controlled is the overall isocenter deviation (linac and collimator mount) for gantry and couch rotation, using a Winston-Lutz test. The second condition is the verification of beam axis verticality. Quality control of the water tank in accordance with SFPM No. 35 is performed systematically before each dosimetric parameters acquisition. The OF measurements were performed by IRSN on site using LiF:Mg,Ti thermoluminescent microtubes (Harshaw) and EBT3 radiochromic films (GAFCHROMIC®) and by the Centre Jean Perrin (CJP) physics team using EBT3 films (GAFCHROMIC®) and MicroDiamond 60019 (PTW®) on Novalis TX® (Varian Medical Systems, Brainlab) equipped with 4mm, 6mm, 7.5mm and 10mm conical collimators in a 6MVSRS photon beam (rate: 1000 MU/min).

Results: The results show the importance of geometrical prerequisites respect. The maximum overall isocenter deviation (vector) is 0.6 and 0.9 mm for gantry and couch rotation respectively. The CJP OF measured values are in good agreement with the IRSN OF values. The maximum deviation between OF CJP and IRSN measurements is 3.9% for the 6mm collimator. The detector MicroDiamond 60019 has the smallest difference (-0.7%) compare to the OF average measured with the set of detectors whatever the size of the collimator.

Conclusions: Preliminary results show that for OF measurement the MicroDiamond 60019 detector leads to the smallest deviations. The OF correction factors for diode proposed in the TRS 483 protocol makes it possible to find a maximum difference of 2.2% between all the detectors. Complementary study is performed using new detectors dedicated to very small beams metrology.

Assurance Qualité des mini-faisceaux avec un détecteur scintillant multicouche et une reconstruction tomographique de champ : concept et résultats préliminaires

J. Ribouton[a], P. Pittet[b], J. Esteves[b], J-M. Galvan[b], F. Blanc[c], G. Haefeli[c], P. Hopchev[c], S. Rit[d], L. Desbat[e], G-N. Lu[b], P. Jalade[a]

[a]Service de Radiophysique et Radiovigilance, Centre Hospitalier Lyon Sud, Pierre-Bénite, France
[b]Institut des Nanotechnologies de Lyon INL, CNRS UMR5270, Université Lyon 1, Villeurbanne, France
[c]Laboratoire de Physique des Hautes Energies LPHE, EPFL, Lausanne, Suisse.
[d]CREATIS, CNRS UMR 5220 – INSERM U1206 – Université de Lyon, Villeurbanne, France
[e]TIMC-IMAG CNRS UGA CHUGA, La Tronche, France

Introduction : Le développement de protocoles d'assurance qualité pour les mini-faisceaux utilisés en radiothérapie reste délicat1 et requiert des détecteurs dosimétriques 2D présentant :
- une résolution spatiale submillimétrique pour réaliser des mesures y compris dans les zones à fort gradient de dose
- une bonne équivalence « tissu » pour ne pas être pénalisé par la perte d'équilibre électronique latérale et pour pouvoir ainsi déterminer les facteurs d'ouverture du collimateur (FOC).
Nous présentons ici une approche innovante pour l'Assurance Qualité (AQ) des mini-faisceaux basée sur un détecteur 2D scintillant multicouche et sur une reconstruction tomographique de la distribution spatiale de dose2.

Méthodes : Le détecteur scintillant SciFi mis en œuvre a été développé dans le cadre du projet LHCb du CERN. Il est constitué d'un matelas de fibres scintillantes de 250µm de cœur arrangées en 6 couches denses. Les fibres scintillantes utilisées sont équivalentes tissu. Le signal en sortie du détecteur est collecté par une caméra sCMOS et représente en temps réel une vue projetée du champ dosimétrique selon l'axe des fibres. En utilisant un empilement de détecteurs avec différentes orientations dans le champ, il est possible de reconstruire la cartographie dosimétrique 2D du champ avec une approche tomographique. Le détecteur SciFi a été caractérisé sur un système Novalis TRUBEAM STX (Varian Medical Systems, Inc) équipé de collimateurs coniques de stéréotaxie BrainLab de 4mm à 15mm.

Résultats: En utilisant des algorithmes de reconstruction algébriques, nous avons montré qu'il est possible de reconstruire la géométrie de champs simples, issus par exemple de collimateurs coniques de petite taille. Par ailleurs, les résultats de mesure sous faisceau confirment que le détecteur SciFi permet de mesurer en temps réel avec un bon rapport signal à bruit les profils projetés du champ d'irradiation avec une résolution submillimétrique. Les profils mesurés sont très cohérents avec ceux obtenus avec des films gafchromiques EBT3 y compris pour les champs de 4mm.

Conclusions : Les résultats préliminaires obtenus montrent l'intérêt de l'approche proposée, qui pourra à terme constituer une solution alternative en temps réel à l'utilisation de films gafchromiques pour l'AQ des mini-faisceaux. De plus, contrairement aux autres détecteurs actifs, ce détecteur 2D équivalent tissu permettra la mesure directe du FOC sans facteurs correctifs.

References

1. Rapport IRSN/PSE-SAN/SDOS 2018-00035 « Dosimétrie des mini-faisceaux : Mise à jour du protocole dosimétrique de détermination des FOC dans les mini-faisceaux utilisés en radiothérapie », (2018).
2. P. Pittet, GN Lu, P. Jalade, J-M Galvan, “Détecteur scintillateur multicouche et procédé de reconstruction d'une distribution spatiale d'un faisceau d'irradiation», Demande INPI n°1852480, (2018)

Evaluation of the detector response in small field conditions using spectral distribution of particle fluence
Evaluation de la réponse des détecteurs dans le cas des petits faisceaux en utilisant la distribution spectrale de la fluence des particules

T. Younes[a,b,c], J Labour[a,b], M. Chauvin[b], J. Leste[a,b], L. Simon[a,b], G. Fares[c], L. Vieillevigne[a,b]

[a] Institut Universitaire du Cancer de Toulouse Oncopole, 1 avenue Irène Joliot Curie, 31059 Toulouse Cedex 9, France
[b] Centre de Recherche et de Cancérologie de Toulouse, UMR1037 INSERM - Université Toulouse 3 – ERL5294 CNRS, 2 avenue Hubert Curien, Oncopole de Toulouse, 31037 Toulouse Cedex 1, France
[c] Université Saint-Joseph de Beyrouth, Faculté des sciences, Campus des sciences et technologies, Mar Roukos - Dekwaneh, Liban

Introduction: The aim of this study was to investigate the spectral distribution of particle fluence inside the detectors under small fields' conditions. Two PTW solid state detectors (T60019 microdiamond and T60017 E diode) and two PTW 3D PinPoint ionization chambers (T31016 and T31022) were included in this study. The investigation was carried out using Monte-Carlo simulations on a modeled TrueBeam Linac for 6MV with flattening filter beams as well as 6MV and 10 MV flattening filter free beams.

Methods: The TrueBeam multi-leaf collimator (MLC) and the four detectors were modeled using Geant4 applications for emission tomography (GATE) code. A differential fluence calculation code was implemented in GATE and verified against FLURZnrc code. Field output correction factors were determined following the IAEA TRS-483 CoP for MLC fields ranging from 0.5×0.5 cm^2 to 3×3 cm^2. In order to distinguish the impact of the volume averaging, the atomic composition, the density and the ionization potential of the sensitive volume (SV) and the extracameral components, the photons and charged particles differential fluence were determined following a chain technique [1]. By combining different configurations, the perturbation of each component was derived by comparing the fluence spectra to the one in a small water volume (0.25 mm radius and 0.5 mm height) considered as a reference.

Results: As expected the ionization chambers under-responded for fields less than 2×2 cm^2. The charged particle spectrum evaluation showed that the under-response of the ionization chambers was mainly related to the size of their SV and to lesser extent the air density. Considering the physical aspects of the SV, it was found that the density is the major parameter that influences the differential fluence in the case of an air volume. Concerning the E diode, a field output correction factor less than unity should be applied for fields smaller than 2×2 cm^2. In this case, the photons spectra revealed three peaks around 2 KeV and 25 KeV caused by characteristic X-rays of silicon and extracameral components. These photons are totally absorbed by the SV due to the high energy absorption coefficient of the silicon and cause the overresponse. As for the microdiamond, the field output correction factors were within 1% from unity. For this detector, the particle spectra calculated in SV were similar to those in the reference water volume. It was also found that the ionization potential was the main physical parameter that impacts the spectral distribution in the case of the SV of a solid state detector.

Conclusions: This study showed that the volume averaging is the limiting factor of the ionization chambers in the case of small fields dosimetry. As for the solid state detectors, their response is mainly impacted by the shielding effect caused by some extracameral components.

References

1. Bouchard, H. *et al.* Detector dose response in megavoltage small photon beams . II . Pencil beam perturbation effects. *Med. Phys.* **42,** 6048–6061 (2015).

Monte Carlo simulation of portal images for SBRT EPID-based dosimetry
Simulation Monte Carlo d'images portales pour la dosimétrie EPID de la SBRT

A.R. Barbeiro[a], J. Leste[a], T. Younes[a], L. Parent[b], L. Vieillevigne[a,b], R. Ferrand[a,b], J. Mazurier[c], A.L. Cunrath[d], D. Lazaro[d], D. Tromson[d], L. Simon[a,b] & X. Franceries[a,f]

[a]CRCT-UMR 1037, Inserm, Université Toulouse III-Paul Sabatier/Toulouse/France
[b]Dpt. Ingénierie et Physique Médicale, IUCT-Oncopole/Toulouse/France
[c]Service de Radiothérapie, Groupe Oncorad-Garonne, Clinique Pasteur/Toulouse/France
[d]LIST, CEA, Gif-sur-Yvette/France
[f]Université Toulouse III-Paul Sabatier/Toulouse/France

Introduction: Stereotactic radiation body therapy (SBRT) treatments require the implementation of robust pre-treatment and in-vivo dosimetry methods, to which electronic portal imaging devices (EPIDs) offer an attractive solution. However the development of EPID-based dosimetry models adapted to complex SBRT conditions is still challenging and is not completely supported for some EPID models and by commercial solutions. Therefore, in this work a detailed Monte Carlo (MC) model of the linac in combination with EPID is purposed to accurately predict the absorbed dose to the detector for further SBRT in-vivo dosimetry applications.

Methods: The MC simulation platform GATE/Geant4, was used to simulate the radiation transport through the detailed geometry of a previous validated model of a Varian TrueBeam STx[1], where the geometry of the aS1000 EPID was also implemented. The EPID model consisted of superimposed layers of different materials and thicknesses, according to geometry and composition provided by Varian. Varian phase-space source files (PSFs) were used to simulate 6 MV FFF photon beams and to obtain secondary PSFs at the exit of linac head for field sizes ranging from 0.5x0.5 to 15x15cm^2, defined by the MLC and/or jaws. Subsequent EPID transport simulation and absorbed dose calculation in EPID scintillator layer was then performed with variable number of secondary PSFs input particles to obtain an adequate statistical uncertainty, depending on the voxel sizes, which ranged from 1×1x0.59 to 1.96x1.96x0.52mm^3. EPID images were acquired in integrated and continuous modes for the same fields, at 150cm distance from the source and were compared to the MC calculated ones by means of relative difference maps and dose profiles.

Results: MC simulations were obtained with a statistical uncertainty < 1 and 1.5% inside and outside open field regions, respectively. Measured and simulated portal dose images showed overall good agreement, with relative dose differences lower than 2% under the open field region for the studied fields. Greatest differences up to 3.5% and 10% were however observed outside field region and for few points located at the field edge, respectively, for the 10x10cm^2 field in crossplane direction. This could be related to the resampling used for image comparison and should be further evaluated by also implementing smaller voxel sizes.

Conclusions: MC simulation of EPID dose images has been implemented and has showed the suitability of the MC model in predicting EPID response for non-transit dosimetry and integrated images for simple fields. This model is ready to be extended for transit dosimetry, where the simulation of treatment SBRT fields and continuous EPID imaging will be including for further SBRT EPID transit dosimetry.

References

1. Beilla, S. *et al.* Monte Carlo dose calculation in presence of low-density media: Application to lung SBRT treated during DIBH. *Phys. Med.* **41**, 46–52 (2017).

Phase- versus amplitude-gated therapy for lung SBRT with regular breathing patterns

M. Savanović[a,b], D. Jaroš[c], F. Huguet[a], J.N. Foulquier[a]

[a]Department of Radiation Oncology, Tenon Hospital, 75020 Paris, France.
[b]Faculty of Medicine, University of Paris-Saclay, 94276 Le Kremlin-Bicêtre, France.
[c]Affidea, International Medical Centers, Center for Radiotherapy, 78000 Banja Luka, Bosnia and Herzegovina.

Introduction: The aim of this study was to compare the dose delivery to the gross tumor volume (GTV), using phase- versus amplitude-gated therapy for lung Stereotactic Body Radiation Therapy (SBRT), for the patients with regular breathing patterns.

Methods: Respiratory gating radiation therapy (RGRT) was based on phase gating and amplitude gating. In phase gating, treatment was delivered in a certain phase of the respiratory cycle. While amplitude gating, depend on the chosen amplitude value, generally near the end-exhalation of the respiratory cycle. In this study authors performed 40 treatment deliveries (20 for phase- and 20 for amplitude-gated mode) to compare dose delivery between phase- and amplitude-gated mode using circular-breathing phantom (Varian Medical Systems, Palo Alto, CA, USA) which is modify to simulate breathing amplitude with regular patterns and to perform tumor motion in craniocaudal (CC) direction. Tumor was fabricate using Palavit (resin for permanent models, 1.32 g/cm3) with two semi-circle (ø 26 mm), inserted in the cube with medium density of 0.34 g/cm3. Gafchromic EBT-3 film with size of the GTV was placed in the tumor, to measure dose delivery to the GTV. Contouring of the GTV was performed on referent CT scan. The internal target volume (ITV) was created on the stable phases, near the end-exhalation of the respiratory cycle. While the PTV was created from the ITV, adding isotropic margins of 3 mm. Treatment was planned in Pinnacle 9.10 treatment planning system with two dynamic conformal arcs (DCA). Prescribed dose was 60 Gy to the PTV in 4 fractions. Only one fraction (15 Gy), was delivered using linear accelerator TrueBeam Novalis STx, triggered to irradiate the tumor only on the stable phases (phase mode) or near the end-exhalation (amplitude mode). To ensure tumor stability in the predetermined gating window we used cine mode to observe the tumor position during treatment delivery. The dose delivery was analyzed using Gafchromic ETB-3 film, scanned on color scanner Epson 11000XL and analyzed in Film QA Pro software.

Results: The stable respiratory motion was found between 30-60% phases, while corresponding amplitude motion was 7 (6-8) mm (about a third of amplitude), used for treatment delivery. The same breathing cycle was used for both modes (phase vs amplitude) 3.7 (2.6-5.2) s. The median dose delivered to the GTV using phase- vs amplitude-gated mode was 15.88 (12.35-17.50) Gy vs 16.22 (12.78-17.99) Gy, for the duty cycle 29 (27-31) % vs 52 (43-76) %. Treatment was delivered in each 2 (1.5-3) ° vs 4 (3-6) ° for phase vs amplitude gating modality, with 7 (6-13) MU vs 18 (12-30) MU per triggering window, respectively. Treatment time delivery was 1576 (1368-1920) s vs 796 (720-912) s, for phase- vs amplitude-gated mode, respectively.

Conclusion: We obtained better coverage of the GTV with larger duty cycle and shorter treatment delivery time using amplitude-gated mode.

Early clinical experience of lung stereotactic body radiotherapy using deep inspiration breath-hold with real-time tumour tracking

A. Dubouloz[a], M. Jaccard[a], A. Champion[a], J. Plojoux[b], P. Gasche[b], R. Miralbell[a,c], F. Caparrotti[a,*], G. Dipasquale[a,*]

[a]Department of Radiation Oncology, Geneva University Hospital / Geneva / Switzerland
[b]Department of Pneumology, Geneva University Hospital / Geneva / Switzerland
[c]Radiation Oncology, Teknon Oncologic Institute / Barcelona / Spain
[*] Equal contribution

Introduction: We report on our clinical experience implementing stereotactic body radiotherapy (SBRT) for early stage non-small cell lung cancer using deep inspiration breath-hold (DIBH) and real-time tumour tracking, via implanted electromagnetic transponders (EMT). Preliminary data for our first two patients are presented, SBRT lung treatments using real-time tracking with EMT are ongoing at our institution.

Methods: Patients were implanted with three lung-specific EMT (Calypso™) during the diagnostic bronchoscopy. For each patient, a first simulation 4DCT-scan was acquired in free breathing (FB), followed by a second CT-scan in DIBH. Dose prescription was 60Gy delivered in 8 fractions for patient 1 (pt1) and in 3 fractions for patient 2 (pt2). Plans in FB and DIBH were created and compared, especially for the ipsilateral lung. Patients were treated in DIBH with 2 half modulated-volumetric arcs. Patients' setup at the linac used the fixed EMT position from the DIBH CT-data. Orthogonal kV images and a cone beam CT followed the initial setup, aligning both EMT and the target. Treatment delivery was gated by the real-time tracking system: deviation of the EMT centroid position of more than 3mm from the planned position in any direction stopped the beam. Patient alignment and treatment delivery were analysed.

Results: The DIBH planning approach allowed for better dosimetric results compared to the FB planning. The target volumes in DIBH were 31 and 45% smaller than in FB respectively for pt1 and pt2. The ipsilateral lung volume receiving 5Gy (V_{5Gy}) decreased by 42% and 20%, the V_{20Gy} by 51% and 34% and V_{30Gy} by 56% and 43%, respectively for pt1 and pt2. Mean (±1SD) setup and treatment time per fraction were 12.1±3.1min and 5.7±4.6min respectively. EMT positions remained stable during treatments in DIBH with median (range) distance between EMT of 0.14(0-0.37)cm and 0.06(0-0.14)cm for pt1 and pt2.

Conclusions: Real-time tumour tracking using implanted EMT resulted in fast, reproducible DIBH gated lung SBRT with improved ipsilateral lung sparing.

Assessment of interplay effect using a programmable motion platform
Etude de l'effet interplay à l'aide d'une plateforme à mouvements programmables

I. Medjahed[a], J. Leste[b], F.X. Arnaud[a], L. Vieillevigne[a,b], L. Simon[a,b]

[a]Institut Claudius Regaud/Toulouse/France
[b]CRCT/Toulouse/France

Introduction: Radiation Therapy of the thoracic region is confronted to the respiratory movement. When fluency is modulated (VMAT) and high doses (SBRT) are used, an Interplay Effect (IE) can appear. This is an unfortunate combination of the respiratory and leaf movements of the Multi-leafs Collimator that could lead to under-dosing of the target or over-dosing of risk organs. In the literature, the IE has been studied and depends on a large number of parameters: dose rate, dose per fraction, number of fractions, period and amplitude of breathing, beam energy, complexity of modulation, etc. A motion platform was developed to carry phantoms and to perform programmed 3D movements. This work aims to evaluate the IE for stereotactic lung and liver treatments and study the possibility of treating our patients using VMAT SBRT.

Methods: A programmable motion platform was designed for this study (ISP-systems). This platform is able to support large QA phantom and to perform chosen motion with 4 independent axes: x, y, z directions for the main platform and a 4th axis for the vertical motion of an external marker (e.g. Varian RPM). The tray on which the phantom is placed is radio-transparent. 14 VMAT SBRT plans were created (Eclipse v13.7, Varian) on a virtual cylindrically phantom and QA measurements are achieved using a phantom (OCTAVIUS, PTW). These plans contained artificial structures: a spherical GTV (centered, diameter 2 cm) and three OARs to insure a sufficient modulation of the plans. ITVs were created by adding margins to the GTV in the superior-inferior direction. The margins were based on the knowledge of the programmable sinusoidal motion. The assessments were performed with (FF) or without flattening-filter (FFF) and for different breathing amplitudes (10, 20 and 25 mm), period times (3, 5 and 7 s), initial breathing phases, without or with gating option (plan and treatment only during phase 33% to 66%) and with or without PTV margin (5 mm). A TrueBeam STx (Varian) was used for delivery of the plans. Dose delivered at the GTV is assessed using a 3D analysis.

Results: For all plans, GTV receives more than 95% of the prescribed dose even in presence of large amplitude motion. IE was isolated from blurring effect by subtracting from measurement an "expected measure", i.e. a convolution between static computation and the motion pattern. For the worst case, IE in the GTV gave a dose difference compared to expected value of 2.6%.

Conclusions: IEs were more important for the FFF compared to the FF and more important for higher respiratory amplitudes, longer periods and more complex treatment plans. But this effect was moderate in particular because the number of respiratory cycles during the delivery is important. The change in dose distribution is more influenced by the blurring effect than by IE (fig. 1). Since the GTV is always correctly covered (95%) even in the worst scenario, VMAT SBRT treatments for lungs and liver can be envisaged.

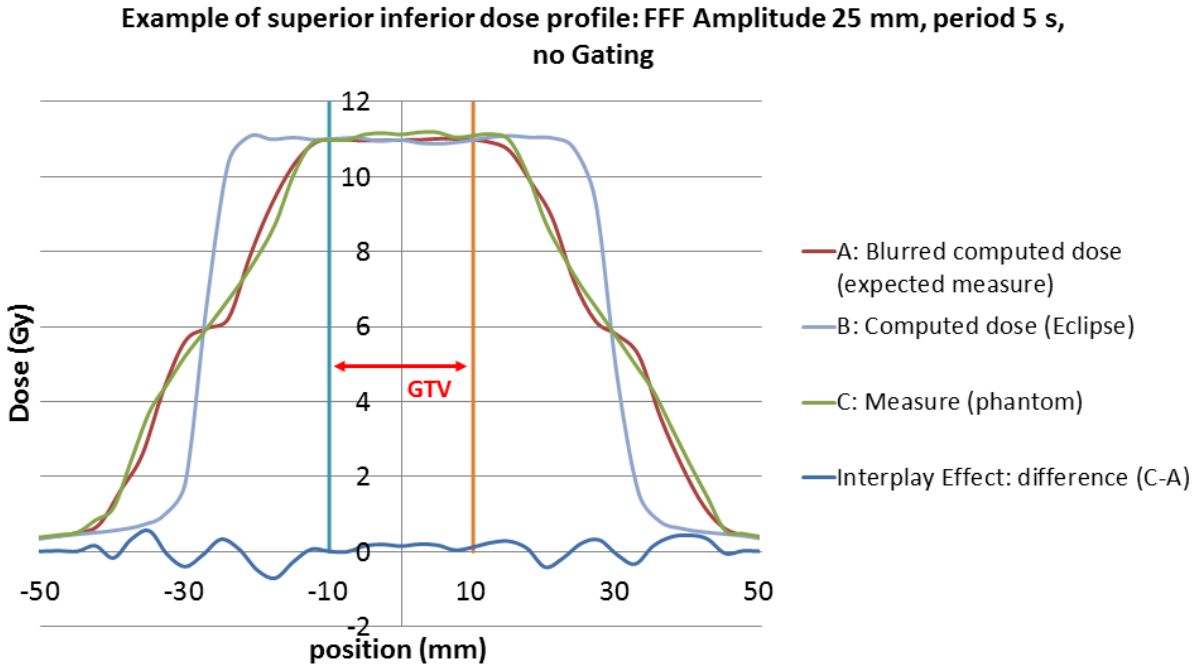
Example of superior inferior dose profile: FFF Amplitude 25 mm, period 5 s, no Gating
Dose (Gy)
12
10
8
6
4
2
0
-2
-50
-30
-10
10
30
50
position (mm)
GTV
A: Blurred computed dose (expected measure)
B: Computed dose (Eclipse)
C: Measure (phantom)
Interplay Effect: difference (C-A)

Figure 1

Healthy tissue doses in a pulmonary stereotactic treatment using the Cyberknife: application of two dosimetric methods

Doses aux tissus sains délivrées lors d'un traitement stéréotaxique pulmonaire au Cyberknife : une application de deux méthodes de détermination dosimétrique

J. Colnot[a], V. Barraux[b], C. Loiseau[b], P. Berejny[b], A. Batalla[b], R. Gschwind[c], C. Huet[a]

[a]IRSN/PSE-SANTE/SDOS/LDRI, Fontenay-aux-Roses, France
[b]Centre François Baclesse, Service de Physique Médicale, Caen, France
[c]Université de Bourgogne-Franche-Comté, LCE UMR CNRS 6249, Montbéliard, France

Introduction: Radiotherapy is a double-edged sword as this technique inevitably irradiates healthy tissues. This exposure may consequently trigger radio-induced complications. In recent years, assessing the risks induced by radiotherapy became a major concern as patients' life expectancy improves and as modern techniques irradiate a more important tissue volume[1]. Risks are directly correlated to the dose delivered to the volume of healthy organs. However, precisely determining those doses remains an important challenge[2]. In that context, two approaches were investigated at IRSN to determine normal tissue doses: a Monte-Carlo (MC) model of the Cyberknife and an experimental tool using EBT3 films. In this study, we apply those tools to determine the doses delivered in a Cyberknife stereotactic treatment of the pulmonary region.

Methods: The ATOM adult male phantom (CIRS) was scanned at the CFB (Caen). A target volume in the lung and several organs were delineated on this scan using the Multiplan TPS. A treatment plan was optimized and calculated using both RayTracing and the TPS MC algorithm. EBT3 films were prepared with a rigorous protocol and were placed between each phantom's slice. Then the phantom was irradiated following the treatment plan. From the film measurements, the doses were reconstructed in 3D with a tool developed at IRSN[3] using MatLab. Moreover, the 55 treatment beams were simulated using a PENELOPE model of the Cyberknife validated for precise out-of-field dose determination[4].

Results: RayTracing largely overestimates the healthy tissue doses whereas out-of-field doses are underestimated by MC TPS in comparison with the films. Discrepancies can be as high as 58% in the heart for MC TPS. Those discrepancies reach 33% and 256% for MC TPS and RayTracing respectively regarding the mean head and neck dose (measured at 9.1 cGy) and 32% and 623% respectively in the kidney (measured at 5.0 cGy). The pelvic mean dose (area not included in the CT scan) is estimated at 1.8 cGy with the films.

Conclusions: This study enables to show the incorrect evaluation of the Multiplan TPS regarding out-of-field doses. The MC simulations are currently ongoing and will complete the results of this experimental study. Those dose evaluations could be used to estimate adverse effects risks induced by the treatments.

References

1. Harrison, R. M. Introduction to dosimetry and risk estimation of second cancer induction following radiotherapy. *Rad.Meas.* **57,** 1-8 (2013).
2. Kry, S. F. *et al*. AAPM TG 158: Measurement and calculation of doses outside the treated volume for external-beam radiation therapy. *Med. Phys.* **44**(10), 391-429 (2017).
3. Colnot, J. *et al*. Development of an experimental tool to evaluate normal tissue 3D doses in external-beam radiotherapy. *Phys. Med*. **56**(1), 44 (2018).
4. Colnot, J. *et al.* A Monte Carlo simulation of a Cyberknife system: a model for the precise determination of out-of-field doses. *Phys. Med. Biol.* (2019, under submission)

Comparison of paraspinal metastasis SBRT plans: Cyberknife® versus VMAT
Irradiation des métastases paravertébrales en conditions stéréotaxiques : comparaison de plans de traitement Cyberknife® versus VMAT

F. Mahinc[a], M. Ayadi[a], P.Dupuis[a], M.C. Biston[a,b]

[a] Léon Bérard Cancer Center, University of Lyon/F-69373 Lyon/France
[b] Université de Lyon, CREATIS, CNRS UMR5220, Inserm U1044, INSA/ F-69622 Lyon/France

Introduction: The irradiation of paraspinal tumors requires the use of highly modulated plans due to the restricted dose to the spinal cord. The objective was to compare the performances of new generation linear accelerator (Linac) versus robotic radiation system dedicated for the stereotactic treatment of paraspinal tumors. Cyberknife® plans were compared to volumetric modulated arc therapy (VMAT) plans delivered with a Versa HD®. The impact of the tumor location on the plan quality was considered.

Methods: Twelve patients previously treated with the Cyberknife® on vertebrae (4 cervical, 4 dorsal, 4 lumbar) were selected. Gross target volume (GTV)-to-Planning target volume (PTV) margins as well as planning-organs at risk volumes (PRV) were 2 mm in all directions. The delivered doses were 30-35Gy in 5 fractions prescribed at the 80% isodose. The original treatments were planned with Multiplan® treatment planning system (TPS) (V3.2.0, Accuray) and were delivered on a Cyberknife® (Accuray) using 2 or 3 fixed-size collimators. The same plans were replanned in VMAT with Monaco TPS (V5.11.02, Elekta). They were simulated using 6-MV photons with an Elekta Versa HD® Linac equipped with an Agility® MLC (80 paired leaves each measuring 5 mm in width at the isocenter). The first objective was to find the optimal arc geometry for VMAT delivery. Hence several combinations of parameters were amended (number of arcs, collimator, gantry and table angles) on one patient. Then VMAT and Cyberknife® dose distributions were compared using Paddick conformity index (PCI); gradient index (GI); mean doses to the PTV and CTV/GTV; volume of PTV and GTV/CTV covered with the prescribed isodose ($V_{30\text{-}35Gy}$); mean and maximum doses (D2%) to the spinal cord.

Results: The VMAT ballistic using a combination of 2 arcs with 80° and 280° collimator rotations gave the best results in terms of PTV coverage and OARs preservation than other ballistics tested (non-coplanar arcs, partial arcs, or 2 arcs with 0-90° collimator rotations). In all the treatment plans resulting from both techniques, the dose constraints to the spinal cord were respected (Table 1). The delivered dose to the targets showed that both techniques resulted in similar PTV coverage and similar mean dose whatever the localization. In contrast, CTV/GTV coverages, GI and PCI were found substantially better for Multiplan than for Monaco for dorsal and cervical localizations (Table 1). However, for lumbar vertebrae, both techniques gave similar results.

Conclusions: VMAT plans offer a dose distribution comparable to Cyberknife® plans, particularly for metastases located at the lumbar level. Therefore, this technique can be a good alternative to the Cyberknife® in the treatment of deep-seated paravertebral metastases. Further work is in progress to examine the impact of patient positioning errors during the treatment delivery, on the treatments plans results.

Table 1: Comparison of the dose delivered to the target volumes and to the spinal cord for the irradiation of dorsal, lumbar and cervical metastasis

Vertebrae	TPS	PTV coverage (%)	Dmean PTV (Gy)	CTV/GTV coverage (%)	Dmean CTV/GTV (Gy)	GI	PCI	D2% PRVspinal (Gy)	Dmean PRVspinal (Gy)
Cervical	Multiplan	92.7 ± 2.7	34.4 ± 3.3	94.8 ± 2.3	34.6 ± 3	4.1 ± 0.3	0.72 ± 0.04	26.9 ± 1.2	8.2 ± 5.2
	Monaco	91.7 ± 5.5	34.6 ± 3.2	92.9 ± 4.4	35.6 ± 3.2	5 ± 0.4	0.64 ± 0.08	26.7 ± 1.3	9.3 ± 5.5
Dorsal	Multiplan	91.7 ± 7.1	33.2 ± 0.6	92.1 ± 11.1	34.1 ± 0.5	4.6 ± 0.7	0.77 ± 0.05	24.3 ± 4.8	8.3 ± 8.3
	Monaco	92.3 ± 6.9	33.7 ± 0.8	90.7 ± 11.9	34.3 ± 1	4.4 ± 1.2	0.67 ± 0.08	26.4 ± 1.6	8.3 ± 8.5
Lumbar	Multiplan	93.5 ± 3.9	37.5 ± 2.9	94.7 ± 5.3	38.4 ± 3.2	3.8 ± 0.8	0.78 ± 0.05	26.4 ± 1.4	7.5 ± 5.2
	Monaco	93.9 ± 2.1	37.9 ± 2.9	93.1 ± 4.9	38.9 ± 3	3.8±0.3	0.77 ± 0.04	26.3 ± 1.1	6.6 ± 3.4

Dosimetric comparison of two treatment techniques (with and without intensity modulation) according to two commercial software for the treatment of brain metastases in stereotactic conditions

A-S. Lucia [a], S. Guillerm[a], G. Goaduff[a], S. Key [a], S. Karimi[a]
[a]Service de Radiothérapie Morvan / CHRU Brest / France

Introduction: Stereotactic radiotherapy is a treatment technique indicated for patients with one or more brain metastases. It uses a series of small converging beams to irradiate a small target volume (cm3) receiving high dose with millimetric spatial accuracy. The objective of the present study was to compare dosimetric planning between two treatment techniques, with and without intensity modulation, using two commercial software packages, for one or two brain metastases.

Methods: In this study a total of fifteen patients were selected: five with a single isolated metastasis, five with two metastases and five with a metastasis attached to the brainstem. For each patient, a scanner and T1 Gado MRI acquired in the treatment position were merged to facilitate contouring. On this basis, two dosimetric plans were carried out using a dynamic arctherapy technique. In the first case Pinnacle v9.10 software (Philips) and intensity modulation were used. In the second case, Iplan RT 4.5 software (Brainlab) was used, with conformal arctherapy dynamic technique without intensity modulation. The prescribed dose was 33Gy at the isocenter for one or two metastases and 30Gy at the isocenter for single metastases stuck to the brainstem (70% isodose at the periphery of the PTV). Comparison criteria were based on dose distributions (isodose curves, DVH, dosimetric indices: gradient, Paddick conformation, RTOG conformation), number of MUs and irradiation time.

Results: For single or double metastasis treatments, planning with Iplan and Pinnacle provided good coverage of target volumes ($V_{99\%prescibed\ dose}$ > 99%) and the constraints on organs at risk were respected. However, we noticed that $V_{3.3Gy}$ was doubled and dosimetric indices were lower with the intensity modulation technique: $I_{Gradient}$ = 4.55 (Pinnacle) vs 2.58 (Iplan); $I_{paddick}$ = 0.87 vs 0.89; I_{RTOG} = 1.12 vs 1.11. With Iplan and contrary to Pinnacle, peripheral isodose (21Gy) did not cover the target volume for single metastases stuck to the brainstem. Also, in general, there was a threefold increase in delivery time when using ballistics from Iplan (on average 2min30s vs 7min30s).

Conclusion: In summary, both treatment techniques can be used in cases of isolated single metastases and double metastases. However, the intensity modulation technique used with Pinnacle software is recommended for single metastases in contact with the brainstem.

RT3- Evaluation des systèmes

Intégration du Cyberknife M6 dans la plate-forme Monte Carlo Moderato et prédiction des paramètres faisceaux par machine learning

A. Wagner[a,b], K. Brou Boni[a,c], E. Rault[a], F. Crop[a], T. Lacornerie[a], N. Reynaert[a,d]

[a]Centre Oscar Lambret, Unité de Physique Médicale/Lille/France
[b]Université libre de Bruxelles, Faculté de Médecine/Belgique
[c]Univ. Lille, CNRS, CRIStAL, Centrale Lille/Lille/France
[d]Institut Jules Bordet, Unité de Physique Médicale/Bruxelles/Belgique

Introduction : Cette étude décrit dans un premier temps la modélisation du système Cyberknife M6, doté d'un collimateur multi-lames. La machine est intégrée dans la plate-forme *Moderato* et des plans de patients sont re-calculés afin de valider le modèle en clinique. Enfin, une nouvelle méthode est introduite afin de prédire par machine learning les paramètres du faisceau d'électrons lors de la modélisation d'accélérateurs.

Méthodes : Des mesures de profils de dose dans l'eau sont utilisées pour réaliser la modélisation du M6 dans le système BEAMnrc/DOSXYZnrc. La géométrie primaire de la tête et le faisceau d'électrons sont d'abord ajustés à partir des collimateurs fixes de 5 et 60 mm, puis ceux-ci sont remplacés par le MLC afin d'optimiser la partie secondaire de la machine. Ce modèle est ensuite intégré dans *Moderato*[1], une plate-forme Monte Carlo permettant une vérification indépendante des distributions de dose calculées par le TPS. Des plans de patient sont recalculés et les doses comparées pour les deux algorithmes disponibles dans le TPS (*Finite-Size Pencil Beam* FSPB et *Accuray Monte Carlo* AMC) et pour *Moderato*. Dans la dernière partie de l'étude, une nouvelle méthode de machine learning est proposée pour la prédiction de l'énergie et de la taille du faisceau d'électrons. A partir d'une série de profils de dose et de rendements en profondeur simulés en faisant varier la taille (1 à 4 mm) et l'énergie (4 à 8 MeV) du faisceau, un algorithme de régression est entraîné et testé par validation croisée.

Résultats : La meilleure correspondance dans les profils de dose simulés et mesurés a été obtenue avec un faisceau d'électrons monoénergétique de 6.75 MeV présentant une distribution spatiale gaussienne de 2.4 mm de largeur à mi-hauteur. L'évaluation sur des plans de patients montre une correspondance satisfaisante (< 2 %) entre les trois algorithmes. Cependant quelques déviations significatives (> 5 %) apparaissent pour des situations incluant de nombreux faisceaux « périphériques ». Des mesures sont en cours afin d'évaluer l'origine de ces différences. Enfin, une validation croisée à 10 plis a démontré que l'algorithme de prédiction permettait de prédire l'énergie et la taille de spot avec une erreur absolue moyenne (MAE) de 0.1 MeV et 0.2 mm respectivement.

Conclusions : Ce travail a permis d'intégrer le Cyberknife M6 dans la plate-forme *Moderato* et de fournir une validation indépendante des plans calculés sur cet appareil. D'autre part, une nouvelle méthode basée sur le machine learning a montré la possibilité de prédire les paramètres du faisceau d'électrons à partir de profils de dose. L'étude se poursuit afin de réduire les incertitudes de prédiction et d'appliquer la méthode à d'autres appareils.

Références

1. Reynaert, N. *et al.* Clinical implementation of a Monte Carlo based treatment plan QA platform for validation of Cyberknife and Tomotherapy treatments. *Phys. Medica* **32,** 1225–1237 (2016).

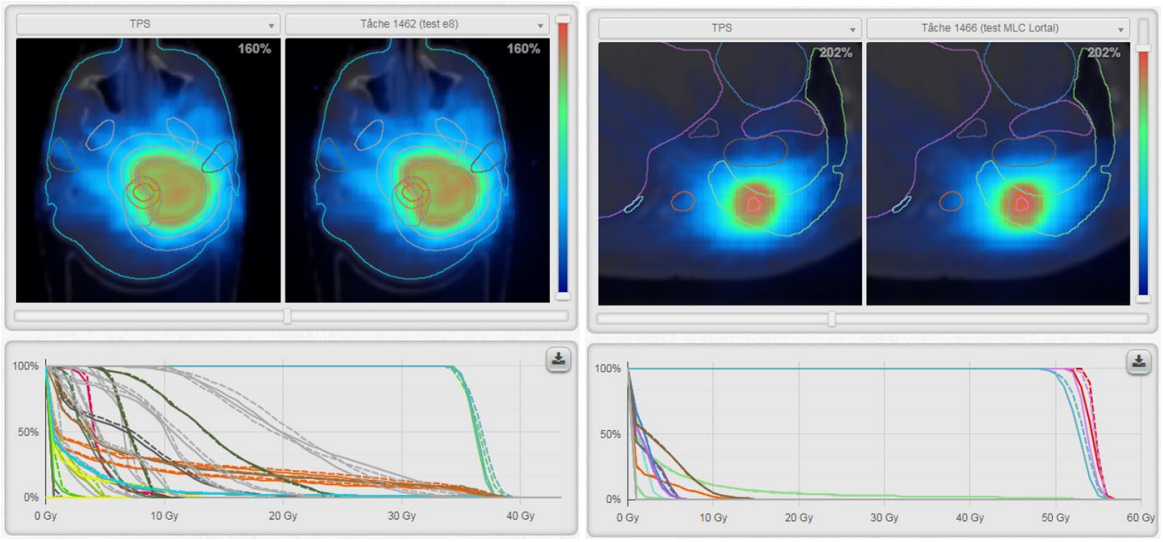

Figure : *Recalcul de traitements Cyberknife du cerveau et du poumon. La dose médiane au PTV dévie de moins de 2 % dans les deux cas (le calcul du TPS utilise un algorithme FSPB pour le cerveau et AMC pour le poumon).*

Portal dosimetry prediction using collapsed-cone convolution model for clinical quality assurance applications
Dosimétrie portale avec le model collapsed cone convolution pour contrôles qualité prétraitement

Y.Cerbah[1.2],C.Popotte[1], R.Belshi[1], M.Fawzi[1]

[1]Curie Institute/Saint-Cloud/France
[2]Univesity Grenoble Alpes/Grenoble/France

Introduction: Quality assurance (QA) of a volumetric modulated arc therapy (VMAT) plan can be performed using an amorphous silicon electronical portal imaging devices (EPIDs) to improve the QA efficiency. In our clinical routine, dosimetric plannifications are calculated with clinical treatment planning system (TPS) Pinnacle (Philips Medical Systems, Madison, WI) and transferred to Eclipse (Varian Medical Systems, Palo Alto, CA). Then a 3D recalculation is required in order to use the portal dose image prediction (PDIP) algorithm, which extends the files preparation time. The aim of this work is to use Pinnacle to create a model dedicated to portal pre-treatment dose verification.

Methods: Approach involves Pinnacle physics tools to create a dedicated machine model that matches the EPID acquisitions. VMAT dose plannifications are calculated based on the Pinnacle convolution–superposition algorithm according to the work of Montero et al.[1] and Papanikolaou et al.[2]. Portal images were acquired for a variety of rectangular fields according to the works of Khan *et al*.[3] using an amorphous silicon flat panel portal imager aS1200 (Varian Medical Systems) irradiated with a 6MV photon beam from a Truebeam linear accelerator (Varian Medical Systems). The measured images were post processed using ARIA (Varian Medical Systems) to extract in-plane, cross-plane profiles and relative output factors[1] (square fields from 1cm² to 30 cm²) then imported into Pinnacle. Assuming an effective depth of 3 cm, our model fit measured profile with predefined clinical parameters[3] : energy spectrum 6MV, primary source size (0.0893cmX0.0831cm), secondary source size (FWHM=1.179cm) and strength (0.07270cm),jaws and MLC transmission(0,001 and 0,014). To validate the model, planar doses were calculated in Pinnacle and compared to EPID measurements using local gamma index criteria implemented in Verisoft (PTW, Freiburg, Germany).

Results: For jaws-only collimated fields, a good accordance between the measured and calculated profiles in central-axis and off-axis areas were obtained, even for the small square fields sizes (1cm², 2cm², 3cm²). Processed-measured output factors ratio were between 0,97-1,021. The passing points were respectively 99.6% and 98.2% for routine local gamma index of 3% 3mm and 2% 2mm, with 10% of maximum dose threshold. For modulated clinical treatment plans (prostate, pelvis, ENT, lung, breast) the mean gamma index results yield respectively 98.7% and 97.3% of points passing for 3% 3mm and 2,5mm 2,5% criteria, with 10% of maximum dose threshold.

Conclusions: The output factors ratio averaging 1 confirms our model efficiency. The resulting model predicts the EPID response with good agreement compared to the model used in Eclipse. Therefore the model can be employed to predict a planar dose map of the EPID. Further work will be done to evaluate the impact of each parameter in the Pinnacle model. Also, further validation tests will be performed using a 3D dose verification phantom and EBT3 Gafchromic films. Nevertheless, our method is expected to find an application as a pre-treatment QA in our clinical VMAT routine.

References :

1. Sánchez Montero R et al. A portal dosimetry dose prediction method based on collapsed cone algorithm using the clinical beam model. *Medical Physics, 44.* January 2017.
2. Papanikolaou et al. *Investigation of the convolution method for polyenergetic spectra*. *Int. J. Radiat. Med Phys. 1993;20(5):1327–1336*.
3. Khan. *et al* .Rao F.H.. An empirical model of electronic portal imager response implemented within a commercial treatment planning system for verification of intensity-modulated radiation therapy fields Rao. *JOURNAL OF APPLIED CLINICAL MEDICAL PHYSICS, FALL 2008*.

Intrafraction portal dosimetry for volumetric modulated arc therapy
La dosimétrie portale intra-séance pour l'arcthérapie volumétrique avec modulation d'intensité

J. L. Bedford[a], I. M. Hanson[a]

[a]Joint Department of Physics, The Institute of Cancer Research and The Royal Marsden NHS Foundation Trust/London/UK

Introduction: The use of in vivo portal dosimetry is widespread for the verification of delivered dose during radiotherapy. Normally this process is used for a whole fraction of radiotherapy, but if an error is encountered, a significant incorrect dose may be delivered (Woodruff et al. 2015, Spreeuw et al. 2016). This is particularly relevant for hypofractionated treatments, which are forming an increasingly large proportion of treatment courses. This work therefore describes a method for portal dosimetry during delivery of a treatment fraction, with prompt notification of a discrepancy.

Methods: A forward projection method was used for this study (Bedford et al. 2014), in which predicted and measured images from the portal imager were compared. Predicted images were created and stored for each control point of the volumetric modulated arc therapy (VMAT) beam. An in-house program (AutoDose v1.0, see Figure 1) was used to compare these predicted images, at the time of treatment delivery, with those measured using an iViewGT portal imager on a Versa HD accelerator (Elekta AB, Stockholm, Sweden). The method was retrospectively investigated for 46 fractions in 13 prostate patients. For three patients, the method was also used for treatments calculated and delivered on a water-equivalent phantom. The sensitivity of the method to deliberately introduced monitor unit, multileaf collimator opening, multileaf collimator shift and path length errors was determined.

Results: The software is able to read and process each acquired image in around 100 ms, but there is a delay of around 2s before the necessary image information is stored by the iViewGT system, so practical measurement frequency is approximately 0.5 Hz. The mean percentage difference between predicted and measured images, for a running section of 10 control points, relative to the predicted image maximum, has a median of 5.3% (range 2.2% - 11.9%). Using an action level of 12%, which is sufficiently large that all of the normal patient and phantom deliveries pass, the method is able to detect a 10% error in monitor units, a 4 mm error in aperture size, a 6 mm error in aperture position, and a 40 mm x 50 mm air gap in the three patients investigated. In general, the errors are detected soon after 10% of the arc segments are delivered.

Conclusions: The proposed method provides an effective means of detecting erroneous treatments in a short timeframe, so that action can be taken before delivering a whole fraction of treatment.

References

Bedford JL *et al*. Portal dosimetry for VMAT using integrated images obtained during treatment. *Med. Phys.* **41**, 021725 (2014).

Spreeuw H, *et al.* Online 3D EPID-based dose verification: Proof of concept. *Med. Phys.* **43**, 3969-3974 (2016).

Woodruff HC, *et al*. First experience with real-time EPID-based delivery verification during IMRT and VMAT sessions. *Int. J. Radiat. Oncol. Biol. Phys.* **93**, 516-522 (2015).

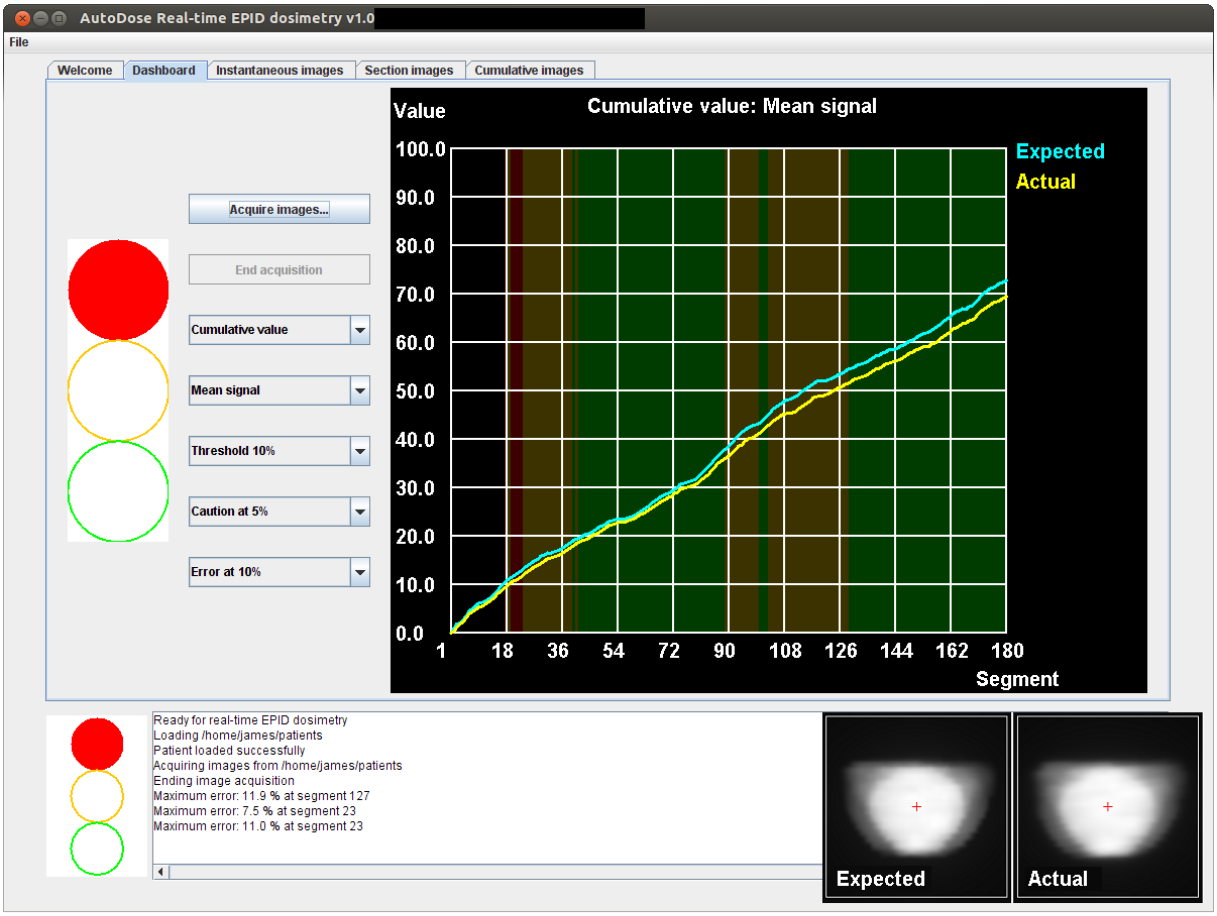

Figure 1. AutoDose software showing intrafraction analysis of cumulative images.

Personalized pretreatment QA for intracranial stereotactic treatments using gel dosimetry and 3D printing of phantom: a feasibility study
Contrôles prétraitements personnalisés en stéréotaxie intracrânienne mettant en œuvre la dosimétrie par gel et l'impression 3D de fantôme: étude de faisabilité

J. Colnot[a], S. Chiavassa[b], G. Delpon[b], C. Huet[a]

[a]IRSN, PSE-SANTE/SDOS/LDRI, Fontenay-aux-Roses, France
[b]Institut de Cancérologie de l'Ouest, Département de Physique Médicale, Site Saint-Herblain, France

Introduction: In stereotactic radiotherapy, pretreatment patient-specific quality controls (PSQA) are performed on generic phantoms to check the agreement between the dose calculated by the treatment planning system (TPS) and the measured dose by a point or 2D detector. For those controls, gel dosimetry seems a promising technique as it presents several advantages compared with conventional dosimeters such as 3D absolute dose determination with high spatial resolution[1]. Thus, we investigated the feasibility of gel dosimetry in combination with a patient-based 3D printed phantom for personalized PSQA.

Methods: CT images of a patient treated by intracranial stereotactic radiotherapy were processed to generate a STL file. Phantom was 3D printed at scale 1:1 using an Ultimaker 3 extended 3D printer. The phantom consisted in a 1.2mm thick wall made of PET and the nose was printed separately to be used as a plug. This phantom filled with water includes a cylindrical insert at the target location to place a radiochromic gel jar. It was scanned with the patient's stereotactic mask and the patient plan was recalculated using the phantom CT on the iPlan TPS (BrainLab). The radiochromic gels were manufactured and calibrated according to a protocol developed at IRSN[2]. One treatment fraction was delivered on the phantom with the gel in place using a Novalis TrueBeam STX accelerator. Gels were optically read following the protocol and data analysis was performed using MatLab.

Results: A good agreement is found between the dose distribution measured with the gel and calculated with the TPS. For a coronal slice at the center of the gel dosimeter, the local 2D 3 mm-3% gamma-index was evaluated within the central 85% of the cylinder diameter. The gamma passing rate reaches 86.5%. In the same region, the local 3D 3 mm-3% gamma-index passing rate is 95.2%. Within the central 85% of the cylinder volume, 87.2% and 96.2% of points pass the local 2 mm-2% and the global 1 mm-2% gamma-index 3D respectively.

Conclusions: This study presents promising results for personalized PSQA for stereotactic radiotherapy and this work could be extended to end-to-end tests. Other cases are currently investigated in order to benchmark the methods and the reproducibility of the measurement protocol.

References

1. Babic, S. *et al.* Three-dimensional dose verification for IMRT in the Radiological Physics Centre head-and-neck phantom using optical CT scans of Ferrous Xylenol-Orange gel dosimeters. *Int. J. Radiat. Oncol. Biol. Phys.* **70,** 1281–1291 (2008).
2. Colnot, J. *et al*. Characterisation of two new radiochromic gel dosimeters TruView and ClearView in combination with the Vista Optical CT Scanner: A feasibility study. *Phys. Med.* **52**, 154-164 (2018).

Intercomparaison des recettes de six accélérateurs linéaires halcyon (varian) avec les données du modèle préconfiguré

V. Bernard[a], S. Fafi[a], P. Coutand[b], S. Bedjeguelal[b], Y. Jacob[c], E. da Eira[c], C. Barca[c], F. Bogalhas[c], D. Nguyen[d], G. Largeron[d], M. Khodri[e]

[a]Département de radiothérapie, Clinique Charcot, Groupe ORLAM/Lyon/France
[b]Département de radiothérapie, Clinique Mermoz, Groupe ORLAM/Lyon/France
[c]Département de radiothérapie, Bayard, Groupe ORLAM/Villeurbanne/France
[d]Département de radiothérapie, Centre Oncologie-Radiothérapie Macon, Groupe ORLAM/Macon/France
[e]Département de radiothérapie, Groupe ORLAM/Lyon/France

Introduction : Six accélérateurs linéaires de dernière génération Halcyon (Varian Medical Systems, *Palo Alto*, CA) ont été installés dans le groupe ORLAM entre Lyon et Macon. La tête de l'accélérateur est montée sur un anneau. Elle se caractérise par l'absence de mâchoires et, pour chaque banc, par un double MLC (proximal et distal) de 29 et 28 lames de largeur 1cm à l'isocentre et décalés de 5mm afin de minimiser la transmission. La vitesse maximale des lames est de 5cm/sec. La taille de champ maximale est de 28x28cm^2. L'Halcyon dispose d'une énergie unique de 6XFFF d'un débit de dose maximal de 800UM/min.

Méthodes : Les données dosimétriques d'acceptance ainsi que l'ensemble des données préconfigurées dans le TPS Eclipse ont été mesurées dans une grande cuve à eau Blue Phantom^2 et HALO (IBA) en utilisant les détecteurs CC13 (IBA), EDGE (SunNuclear) et Farmer (PTW) conformément à celles effectuées par Varian. Ces mesures de courbes de rendement en profondeur, profils, profils diagonaux, FOC, facteur de transmission et DLG ont été comparées entre les six machines et aux données préconfigurées.

Résultats : La profondeur moyenne du maximum pour un rendement d'un champ 10x10cm^2 est de 13.2±0.46mm et la dose à 10cm D10=63.1±0.36% (tolérances constructeur respectives : 13±2mm et 63±1%). La dose moyenne à 10cm le long d'un profil 28x28cm^2 est de 79±0.25% et la symétrie est de 0.48±0.15% (tolérances constructeur respectives : 79±2% et 2%).
Pour les rendements en profondeur : la différence moyenne après Dmax est de -0.62±0.3% par rapport aux données Varian. La différence la plus importante est de -1.2% pour le champ 2x2cm^2. La profondeur de Dmax moyenne est comprise entre 11.1±0.9mm (28x28cm^2) à 12.7±0.3mm (6x6cm^2). Le D10 moyen est respectivement de 53.3%, 56.1%, 58.3%, 60%, 61.3%, 64.5% et 65.4% pour les tailles de champs 2x2, 4x4, 6x6, 8x8 ,10x10, 20x20, 28x28cm^2. La différence maximale de -0.5% pour le champ 2x2cm^2. Une bonne corrélation entre les profils et profils diagonaux inter-Halcyon et par rapport au modèle est observée. La différence la plus importante est pour le champ 2x2cm^2.
La différence moyenne des FOC pour l'ensemble des tailles de champ et machines est de 0.17±0.18%. La différence la plus importante est pour les champs où Y=1cm (0.33±0.06%). Les transmissions moyennes, mesurées à DSP 95cm sous 5cm, pour les bancs distal et proximal sont en moyenne de 0.455% et 0.46%. La transmission moyenne à travers les deux bancs est de 0,005%. La moyenne des DLG pour le banc distal est de 0.09±0.01mm. La différence maximale par rapport au modèle (DLG=0.1mm) est de 0.02mm.

Conclusions : Une très bonne corrélation inter-machines est observée. Celles-ci sont en excellente concordance avec le modèle préconfiguré qui a été conservé sans modifications pour l'ensemble des six Halcyons.

Treatment overrides: How to decrease them?
Outre passements de messages d'alerte à la machine : Comment les éviter ?

V.Roosen[a], A. Vaandering[a], F. Vanneste[a], D.Dechambre[a]

[a]Cliniques Universitaires St-Luc/Bruxelles/Belgique

Introduction: Alarm/alert fatigue occurs when a person is exposed to a large frequency of them and consequently becomes desensitized, thus potentially leading to error. It has been found that RTTs are frequently exposed to pop-ups/alerts and as a result have to override various elements regularly. This generates weariness and a decrease in the attention to their content. An analysis of the overrides number in the Mosaiq V2.6 was launched in order to determine the content and action level of the overwritten elements and whether they led to an incident (= unjustified override). As a result of this analysis, procedures were put in place to improve our practices and avoid mistakes due to alarm fatigue.

Methods: An overrides report was generated for all patients treated over a 12-month period. Those that occured during patient positioning (Site Setup) and treatment field selection were differentiated using Excel 2010. By analyzing these data, it allowed us to determine which elements were overwritten, their frequency and the reason behind. After this analysis, specific process changes were implemented to decrease the frequency of overrides needing to be realized. A new analysis was carried out one year after making the adaptations to evaluate the impact of these process changes.

Results : 72% of these concerned treatment field parameters while 28% concerned site setup parameters. 2 unjustified overrides were made and impacted treatment delivery: One for the MLC position and one for the couch rotation. Site setup overrides mostly concerned manual validation of patient ID and accessory overrides that were solved by the introduction of a barcode reader. Simulation practices were standardized as there is no longer use of an isocenter, but only a reference point from which the RTTs displace the patient systematically. For field overrides, localization and immobilization system-based table tolerances were created. At the beam level, manual manipulations of Monitors Units to compensate for the imaging doses were eliminated as they created the highest risk of error. Cumulative and daily dose tolerances were adjusted to include imaging dose as a background of the treatment. One year after their implementation, the number of by-passed items decreased by 69.3%.

Conclusions: In order to make Mosaiq's warnings relevant, it was necessary to adjust the tolerances to make them consistent with real errors risk and decrease the potential fatigue alert. In this study, it was possible to quantify the number of pop-up/alerts that appeared in our MOSAIQ workflow. Though the number of overrides analysis was carried out over a short period, the use of automatic validation tools (e.g., via a barcode reader) and personalized threshold levels allowed to decrease the number of alerts. Further reduction is still possible by rising the awareness among the RTTs.

Performance assessment of the Calypso® system
Evaluation des performances du système Calypso®

D. Cirella[a], J. Prunaretty[a], P. Debuire[a], N. Aillères[a], A. Morel[a], S. Simeon[a], S. Valdenaire[a], P. Fenoglietto[a]

[a]Institut du Cancer de Montpellier, Service Radiothérapie/Montpellier/France

Introduction: The Calypso® 4D localization system (Calypso® Medical Technologies, Seattle, Wa) is a real-time electromagnetic tracking system. It is used to continuously monitor implanted Beacon® transponders for patient alignment and target position tracking during the treatment. The purpose of the study was to assess the performances, the accuracy and the stability of this system.

Methods: A series of tests were performed using a quality assurance (QA) fixture containing three embedded radiofrequency transponders. The tracking accuracy of the system was established by positioning the QA fixture at the treatment isocenter, tracking the phantom and then, shifting it by known values. Isocenter data output from the Calypso® system was compared against the expected position of the phantom. 63 translational offsets with a resolution of 0.5 mm/measurement were applied. System repeatability was performed by repeating 10 times localization tests. And system reproducibility was carried out by repeating 10 times localization test after switching the Calypso® system on and off. Next, the system stability was assessed by tracking the phantom for a period of 30 min, once without irradiation and another time with successive irradiation. Finally, a comparison with On Board Imaging (OBI) system was achieved by positioning the QA fixture at the treatment isocenter, shifting it by known values and evaluating the distance between the shifts calculated for both systems.

Results: The tracking accuracy test showed a maximum deviation of 0.5 mm. It represents the display resolution of the Calypso® system in the tracking mode. The repeatability test showed standard deviations of 0.3%, 0.4% and 0.5% for lateral, longitudinal and vertical directions, respectively. Transponders were localized with a maximum deviation up to 0.1 mm. The reproducibility test showed standard deviations of 0.8%, 0.6% and 0.4% for lateral, longitudinal and vertical directions, respectively. Transponders were localized with a maximum deviation up to 0.2 mm. Continuous measurements during a period of 30 min led to stable measurements within a deviation of 0.7 mm and 1.1 mm, respectively for measurements without irradiation and under irradiation conditions. Moreover, no tracking interruption was observed for both tests. The mean deviations between the Calypso® and the OBI systems in lateral, longitudinal and vertical directions are 0.4 ± 0.3 mm, 0.1 ± 0.1 mm and 0.2 ± 0.3 mm.

Conclusions: The Calypso® 4D localization system was largely assessed. The results showed that this system can provide with submillimeter accuracy and it appears to be stable and reproducible. The comparison with the OBI system highlights the achieved accuracy. These features allow treatment margins reduction for prostate treatment.

RT4: Session SFPM / SFRO : modulation d'intensité dans le sein

A multi-center study of breast irradiation techniques
Etude régionale comparative des traitements du sein par radiothérapie externe

F. Jouyaux[a], O. Henry[a], E. Biron[b], F. Coste[c], S. Danhier[d], M. Benchalal[a], P. Gesnouin[a], M. Getain[e], G. L'Haridon[f] P. Le Dorze[g], C. Le Prince[h], P. Lecoeur[d], C. Leleu[i], C. Llagostera[j], F. Le Vigouroux[k], E. Martin[l], S. Martineau[m], J. Palisson[f], S. Perrot[n], T. Prodhomme[n], A. Vela[d], S. Collet[d]

[a]Centre Eugène Marquis/Rennes/France
[b]Institut de Cancérologie de l'Ouest/Nantes/France
[c]Clinique mutualiste de l'Estuaire/Saint Nazaire/France
[d]Centre François Baclesse/Caen/France
[e]Centre d'oncologie St Vincent/St Gregoire/France
[f]Centre Mallet Proux/Laval/France
[g]CH Bretagne Sud/Lorient/France
[h]Centre de la Baie/Avranches/France
[i]CH Cornouaille/Quimper/France
[j]Institut de Cancérologie de l'Ouest/Nantes/France
[k]Centre d'oncologie Saint-Yves/Vannes/France
[l]CHU Morvan/Brest/France,
[m]ILC Maurice Tubiana/Caen/France
[n]CARIO/Plérin/France

Introduction : In France, several treatment techniques are approved for irradiation of breast and regional nodes (Hennequin et al. Recorad, 2016). A regional association of medical physicists suggested to make an inventory of the common clinical practices among its members. The study aimed to identify the irradiation techniques used and their dosimetric impact on clinical cases.

Methods : With common CT images and structures set, each of the eleven institutions participating to the study produced treatment plans approved by a radiation oncologist for two clinical left breast cases. Treatment phase A prescriptions were 50 Gy to the whole breast for case 1, and 50 Gy to the whole breast, the internal mammary chain (IMN) and supra and infraclavicular nodes for case 2. Phase B was a 16 Gy boost on tumor bed for both cases. All the irradiations techniques used were identified and a qualitative and quantitative analysis of dose distributions was done. Dosimetric evaluation of organ at risk and planning target volume through minimum, maximum value [minimum-maximum] and standard deviation (S.D) was done.

Results : For case 1, eight centers planned phase A with 3D conformal radiotherapy (3DCRT) using wedged tangential photons beams (wTG), three centers used intensity modulated techniques with static tangential beams (IMTG). Nine centers planned phase B with 3DCRT using two wTG, with an additional oblique photons beams for one center and an additional electron beam for one center, two centers used two IMTG. For case 2, five centers planned phase A with 3DCRT using both anterior photons and electrons beams for IMN irradiation, two used RC3D with IMN included in large wTG, one used two IMTG, two used volumetric modulated arctherapy (VMAT), and one Tomotherapy ® (TM). Ten centers planned phase B with 3DCRT and one with VMAT. Qualitative dose distribution comparison on axial slices is illustrated on figure 1. Quantitative analysis on DVH values showed : For case 1, PTV breast, V95% : [96.5%-99.6%] (S.D= 0.9%), tumor bed, V95% : [99.4%-100%] (S.D= 0.2%), PTV breast, V105% : [0%-49%] (S.D=19.1%), heart mean dose : [3.2 Gy-6.2 Gy] (S.D=1.0 Gy), left lung mean dose : [2.3 Gy–5.1 Gy] (S.D=0.9 Gy). For case 2, PTV breast and nodes V95%: [85.8%-97.5%] (S.D= 3.7%), PTV tumor bed V95% : [52.2%-98.4%][S.D=21.0%], heart mean dose : [4.3 Gy-10.6 Gy] (S.D=2.1 Gy), left lung mean dose : [13.6 Gy–20.9 Gy] (S.D=1.9 Gy). VMAT and TM techniques had on average a 40% better conformal index, but a mean augmentation of 2.3 Gy of contralateral breast mean dose and 68% of 5 Gy isodose volume.

Conclusions : The study showed the discrepancies among the common techniques used for breast irradiation and their impact on dose distribution. The dosimetric differences increased with the plan complexity. The study should be continued to encompass the volume delineation and the dose prescription differences.

The Growing Role of Intensity Modulated Irradiation Techniques (IMRTs) in the Management of Breast Cancer: The Radiation Oncologist's Point of View

La place Grandissante de techniques d'irradiation avec modulation d'intensité (IMRT) dans la prise en charge du cancer du sein: le point de vue d'oncologue radiothérapeute

Y. Kirova[a]
[a]Department of Radiation Oncology, Institut Curie, 75005 Paris, France

Introduction: Adjuvant breast radiation therapy is standard of care after breast conserving surgery in early breast cancer, improving disease free survival and overall survival (OS)[1]. Benefit of lymph node irradiation [internal mammary chain (IMC) and supra and infra clavicular nodes (SN)] in patients with axillary lymph node involvement or at high risk of relapse has been shown by a meta-analysis of three randomised trials [2]. In recent years, intensity modulated radiation therapy (IMRT) has been developed to lessen organs at risk (OAR) exposure to high doses. Static breast cancer IMRT significantly reduced acute and late skin toxicity compared to standard techniques in 3 phase III randomised trials [3-5]. Then static IMRT techniques moved to helical tomotherapy (HT) or volumetric modulated arc therapy (VMAT) for pelvic and head and neck cancers. These two techniques (VMAT and HT) have been recently performed and assessed in breast cancers. Dosimetrics studies showed that HT or VMAT improved target volume coverage, allowed better dose homogeneity and decreased high doses to OAR compared to 3D-CRT, therefore they are used frequently [6-9]. At the other hand these two techniques increased low doses to OAR suggesting the possibility of greater risk for secondary malignancies [10-13]. The purpose of this work is to report the clinical and dosimetrics results for patients treated with IMRT in the setting of complex adjuvant breast and nodes irradiation and discuss the negative and positive points.

Methods: The history of safe 3D techniques, going to highly performing IMRT with or without DIBH (deep inspiration breath hold) have been studied in terms of dosimetric findings, clinical results nd future directions have been studied in the available literature.
Results: Using conventional techniques in breast and nodes irradiation, there could be suboptimal target coverage or great dose exposure to the normal structures.
At the same time, numerous 3D simple and safe techniques are available as the breast alone treatment in lateral position, as well in prone, or using field in the field technique (14-16). These are technique that shown perfect dose distribution and good sparing of the organs at risk (17).
Previously published studies suggested that helical tomotherapy (HT) and volumetric modulated arc therapy (VMAT) plans provide excellent target volume coverage and reduces high doses to organs at risk with an acceptable acute toxicity. At the same time, HT and VMAT deliver lower doses to larger volumes of normal tissues, suggesting in some cases an increased risk of second cancer. Nevertheless, the risk to benefit ratio seems to be in favour of HT and VMAT as opposed to three-dimensional conformal radiation therapy in complex target volumes, such as funnel chest, tumour in the inner quadrant when internal mammary chain and tumour bed boost are indicated, large breast size or unfavourable cardiac anatomy (6-8). But in some cases the improved sparing of the heart with IMRT at cost of increased dose to the normal tissue (e.g. contralateral breast) and in other cases the sparing of the heart can be more efficient with 3D conformal RT with respiratory control (3D_DIBH) than with IMRT with free breathing. Therefore probably the future direction for highly selected population will be the use of protons with respiratory control in case of young patients with or without BRCA mutations.

Conclusions: Most of the patients irradiated to the breast only can be treated using safe alternative techniques as radiotherapy in lateral or prone position as well as field in the field simplified IMRT with or without DIBH. In case of complex anatomy (funnel chest), lymph node irradiation, the IMRT become a very attractive option, but different important criteria must be evaluated as the age of the patient, family history, doses to OAR, as well as the low doses received by the contralateral breast and OAR.

References:
1. Darby S, McGale P, Correa C, Taylor C, Arriagada R, Clarke M, Cutter D, Davies C, Ewertz M, Godwin J, et al. Effect of radiotherapy after breast-conserving surgery on 10-year recurrence and 15-year breast cancer death: meta-analysis of individual patient data for 10,801 women in 17 randomised trials. Lancet. 2011;378:1707–1716.
2. Budach W, Kammers K, Boelke E, Matuschek C. Adjuvant radiotherapy of regional lymph nodes in breast cancer - a meta-analysis of randomized trials. Radiat Oncol. 2013;8:267.

3. Mukesh MB, Barnett GC, Wilkinson JS, Moody AM, Wilson C, Dorling L, Chan Wah Hak C, Qian W, Twyman N, Burnet NG, et al. Randomized controlled trial of intensity-modulated radiotherapy for early breast cancer: 5-year results confirm superior overall cosmesis. J Clin Oncol. 2013;31:4488–4495.
4. Pignol JP, Olivotto I, Rakovitch E, Gardner S, Sixel K, Beckham W, Vu TT, Truong P, Ackerman I, Paszat L. A multicenter randomized trial of breast intensity-modulated radiation therapy to reduce acute radiation dermatitis. J Clin Oncol. 2008;26:2085–2092.
5. Donovan E, Bleakley N, Denholm E, Evans P, Gothard L, Hanson J, Peckitt C, Reise S, Ross G, Sharp G, et al. Randomised trial of standard 2D radiotherapy (RT) versus intensity modulated radiotherapy (IMRT) in patients prescribed breast radiotherapy. Radiother Oncol. 2007;82:254–264.
6. Lauche O, Kirova YM, Fenoglietto P, Costa E, Lemanski C, Bourgier C, Riou O, Tiberi D, Campana F, Fourquet A, Azria D. Helical tomotherapy and volumetric modulated arc therapy: New therapeutic arms in the breast cancer radiotherapy. World J Radiol. 2016 Aug 28;8(8):735-42. doi: 10.4329/wjr.v8.i8.735. PubMed PMID:27648167; PubMed Central PMCID: PMC5002504.
7. Massabeau C, Fournier-Bidoz N, Wakil G, Castro Pena P, Viard R, Zefkili S, Reyal F, Campana F, Fourquet A, Kirova YM. Implant breast reconstruction followed by radiotherapy: can helical tomotherapy become a standard irradiation treatment? Med Dosim. 2012 Winter;37(4):425-31. doi: 10.1016/j.meddos.2012.03.006. Epub 2012 Apr 24. PubMed PMID: 22534136.
8. Arsene-Henry A, Foy JP, Robilliard M, Xu HP, Bazire L, Peurien D, Poortmans P, Fourquet A, Kirova YM. The use of helical tomotherapy in the treatment of early stage breast cancer: indications, tolerance, efficacy-a single center experience. Oncotarget. 2018 May 4;9(34):23608-23619. doi: 10.18632/oncotarget.25286. eCollection 2018 May 4. PubMed PMID: 29805760; PubMed Central PMCID: PMC5955102.
9.Arsene-Henry A, Fourquet A, Kirova YM. Evolution of radiation techniques in the treatment of breast cancer (BC) patients: From 3D conformal radiotherapy (3D CRT) to intensity-modulated RT (IMRT) using Helical Tomotherapy (HT). RadiotherOncol. 2017 Aug;124(2):333-334. doi: 10.1016/j.radonc.2017.07.002. Epub 2017 Jul 18. PubMed PMID: 28733052.
10. Bazire L, De Rycke Y, Asselain B, Fourquet A, Kirova YM. Risks of second malignancies after breast cancer treatment: Long-term results. Cancer Radiother. 2017 Feb;21(1):10-15. doi: 10.1016/j.canrad.2016.07.101. Epub 2016 Dec 26. PubMed PMID: 28034681.
11. Kirova YM, Gambotti L, De Rycke Y, Vilcoq JR, Asselain B, Fourquet A. Risk of second malignancies after adjuvant radiotherapy for breast cancer: a large-scale, single-institution review. Int J Radiat Oncol Biol Phys. 2007 Jun 1;68(2):359-63. Epub 2007 Mar 26. PubMed PMID: 17379448.
12: Kirova Y, Vilcoq JR, Asselain B, Sastre-Garau X, Campana F, Dendale R, Bollet M, Fourquet A. [Radiation-induced sarcomas after breast cancer: experience of Institute Curie and review of literature]. Cancer Radiother. 2006 Feb-Mar;10(1-2):83-90. Epub 2005 Nov 21. Review. French. PubMed PMID: 16300982.
13: Kirova YM, Vilcoq JR, Asselain B, Sastre-Garau X, Fourquet A. Radiation-induced sarcomas after radiotherapy for breast carcinoma: a large-scale single-institution review. Cancer. 2005 Aug 15;104(4):856-63. PubMed PMID: 15981282.
14. Fournier-Bidoz N, Kirova YM, Campana F, Dendale R, Fourquet A. Simplified field-in-field technique for a large-scale implementation in breast radiation treatment. Med Dosim. 2012 Summer;37(2):131-7. doi: 10.1016/j.meddos.2011.03.002. Epub 2011 Sep 25. PubMed PMID: 21945169.
15. Kirova YM, Hijal T, Campana F, Fournier-Bidoz N, Stilhart A, Dendale R, Fourquet A. Whole breast radiotherapy in the lateral decubitus position: adosimetric and clinical solution to decrease the doses to the organs at risk (OAR). Radiother Oncol. 2014 Mar;110(3):477-81. doi:10.1016/j.radonc.2013.10.038. Epub 2013 Dec 13. PubMed PMID: 24342456.
16. Formenti SC, Truong MT, Goldberg JD, Mukhi V, Rosenstein B, Roses D, Shapiro R, Guth A, Dewyngaert JK. Prone accelerated partial breast irradiation after breast-conserving surgery: preliminary clinical results and dose-volume histogram analysis. Int J Radiat Oncol Biol Phys. 2004 Oct 1;60(2):493-504. PubMed PMID:15380584.
17. Bronsart E, Dureau S, Xu HP, Bazire L, Chilles A, Costa E, Logerot C, Falcou MC, Campana F, Berger F, Fourquet A, Kirova YM. Whole breast radiotherapy in the lateral isocentric lateral decubitus position: Long-term efficacy and toxicity results. Radiother Oncol. 2017 Aug;124(2):214-219. doi:10.1016/j.radonc.2017.07.001. Epub 2017 Jul 19. PubMed PMID: 28734546.

VMAT technique and imaging on patients with breast cancer: the daily repositioning challenge
Le VMAT et l'imagerie pour le cancer du sein: le défi du repositionnement quotidien

B. Baron[a], R. Msika[a], I. Birba[a], E. Costa[a]

[a]Institut Curie/Paris/France

Introduction: Daily session positioning in radiotherapy for patients with breast cancer is a crucial step towards a better treatment delivery. Studies have demonstrated that the radiographers can use surgical clips of the tumoral bed as matching structures for patient repositioning. They evaluated the coverage for breast and tumoral bed volumes but excluded the lymph nodes from the studies. The purpose of this work is to evaluate the variation in the position of the isocenter and to compare the coverage of all target volumes using different matching structures and imaging techniques available.

Methods: A group of 10 patients that benefits from the VMAT technique for breast cancer treatment was studied retrospectively. We selected one orthogonal kilovoltage (kV-kV) pair of images and the respective CBCT performed the same day, adding up to 53 radiotherapy sessions. Four matching techniques were tested. The first matching with kV-kV was realized using the bony anatomy while the second matching with kV-kV was performed based on the surgical clips only. The first CBCT matching was performed with a ROI including the breast tissue and other soft tissues while the second CBCT matching was performed by selecting a ROI of 6mm around the delineated tumoral bed (surgical clips included). The translations in all 3 directions were compared for each pair of matching technique. A preliminary study for dosimetric evaluation on the coverage of target volumes re-delineated on the CBCT (breast, L2 to L4 lymph nodes and the internal mammary nodes) was realized by transposing the original planning treatment on each CBCT and applying the translations to the isocenter that were previously acquired.

Results: We determined that in more than 90% of the radiotherapy sessions, the matching using the surgical clips was equivalent and, in more than 80% of them, the anatomic matching was equivalent for either imaging technique (distance between isocenter < 5mm). In addition, in almost 10% of the cases, the difference in isocenter position is superior to 1cm when comparing clips and bony matching on kV-kV. Finally, the dosimetric evaluation of the target volume coverage indicates that the matching using the surgical clips with both imaging techniques leads to a decrease of more than 10% to the D95% value for more radiotherapy sessions compared with other matching. No significant differences on the D95% value were noted between the uses of the two imaging techniques for anatomic matching.

Conclusions: The use of kV-kV images with bony matching is a reliable solution for daily patient repositioning when considering all the volumes treated with the VMAT technique. The differences in isocenter positioning when compared with the anatomic CBCT matching were minimal and dosimetric calculations tend to demonstrate a decline in the coverage of all target volumes for the matching with surgical clips. However, CBCT imaging remain our gold standard to evaluate a volume loss in soft tissues.

Comparison of matching procedures : number of sessions with differences of the isocenter position < 5mm or > 10mm

		KV clips /kV bone	CBCTclips / CBCT soft tissues	kV clips / CBCT clips	KV bone / CBCT soft tissues
Differences in isocenter position between 2 matching procedures	< 5mm	51,0%	66,0%	**92,0%**	**81,0%**
	>10mm	**9,4%**	1,9%	3,8%	0,0%

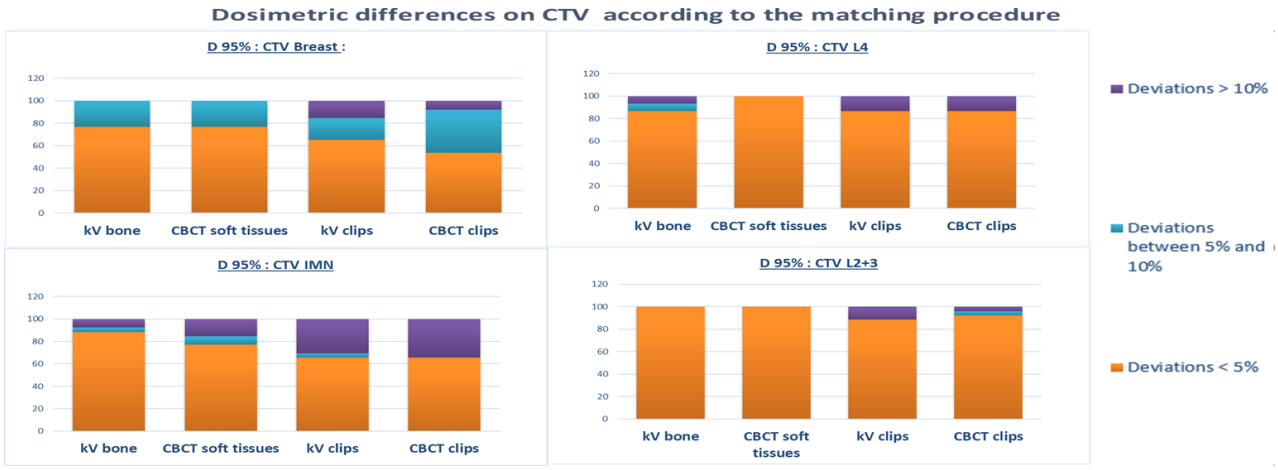

Evaluation de la méthode de contrôle du positionnement des patientes pour le traitement des cancers du sein en VMAT
Assessment of the positioning control method of patients treated for breast cancers with VMAT technique

K. Herlevin-Gérard[a], P. Royer[b], A. Ropers[b], I. Gehin[b], F. Saunier[a], C. Monod[b], V. Marchesi[a], I.Buchheit[a], C. Brunaud[b]

[a]Medical Physics Unit, Institut de Cancérologie de Lorraine, Vandoeuvre-lès-Nancy, France
[b]Radiotherapy Department, Institut de Cancérologie de Lorraine, Vandoeuvre-lès-Nancy, France

Introduction: Breast treatments with volumetric modulated arc therapy (VMAT) require an accurate positioning of the patients. The aim of this study was to assess the quality and reproducibility of our set-up method and to verify if the 5mm margin between the CTV and the PTV was appropriated.

Methods: The 20 first patients treated with VMAT for a postoperative loco-regional radiation therapy for breast cancer were included in our study. The treated volumes were the breast, the internal mammary nodal chain, the supra-clavicular nodes +/- the I, II and III axillary nodal levels. The dosimetry planning was calculated on the Eclipse TPS (v.11) with AcurosXB algorithm and the VMAT optimization has been done using an “expanded breast PTV” defined with a 1cm margin beyond the body outline. Treatments were performed on Varian iX linear accelerators in 6MV. Patients were positioned in the supine position with both arms above the head, without thermoplastic mask. Two orthogonal kilovolt (kV) control images were performed daily to adjust the isocenter position, and one tangential kV image was added to verify the inclusion of the mammary gland in the “expanded breast PTV”. Those images were analyzed on-line by the radiation therapists. Once a week, at the end of the treatment session, these patients also had a CBCT scan to assess the position of the node target volumes, that was analyzed by the breast specialized radiation oncologist. In this study, for each patient, a minimum of 3 sessions has been analyzed. The breast specialized radiation oncologist performed the registrations on the kV images in a blinded way and they were compared to those of the radiation therapists.

Results: A total of 82 sessions have been analyzed (0°/270° kV, tangential kV and CBCT). The mean shift obtained by the radiation therapists on the kV orthogonal images was 5mm in vertical (SD 4mm), 5mm in longitudinal (SD 4mm) and 3mm in lateral (SD 2mm). The mean discrepancy between the radiation therapists and the radiation oncologist’ registration was inferior to 1mm in vertical, longitudinal and lateral (respective SD inferior to 1mm). For 22% of the sessions, the mammary gland went outside the external contours but was still inside the “expanded breast PTV” volume. For 100% of the sessions, the CTV nodes were included in the PTVs.

Conclusions: This study showed that our patients’ set-up method for VMAT treatments is reproducible and accurate and that the radiation therapists perform on-line registrations of quality comparable to the radiation oncologist. It confirmed the need to use an “expanded breast PTV” volume to take into account the breast positioning differences from one session to another and that the 5mm margin between the CTVs and the PTVs is adapted to our positioning technique. Finally, the CBCT acquisition is not systematically performed anymore since we showed that kV images bring enough information. It is just used to take decisions in case of difficulties with the positioning.

Intensity modulated therapy on breast : dosimetric and clinical results
Retour d'expérience sur les irradiations mammaires et ganglionnaires par modulation d'intensité

J.Ramos[a], F.Vincent[a], G. Bernadou[a], T. Boisserie[a], P.E. Cailleux[a], M.L. Maillet[a]

[a]CORT37 / Chambray-les-Tours / France

Introduction: This study presents the clinical and dosimetric results of 80 patients treated for breast cancer using intensity modulation.

Methods: Volumes drawn according to the Radiation Therapy Oncology Group (RTOG) standards included the mammary gland or thoracic wall and nodes groups. The prescribed doses were 47.25Gy for the mammary gland or 45Gy for the thoracic wall and 45Gy for the nodes regions (2.25Gy per fraction – 4 fractions per week). Fixed field IMRT was performed for the treatment. An extended CT data with a virtual bolus extended 1cm outside the body was used for optimization and pre-calculation of treatment plan[1]. The final plan is calculated on the original CT data. This method minimizes skin overdosage and accounts for position uncertainty, breathing and morphological variations during the treatment. A conformational technique was used for the tumour bed irradiation.

Results: The target volumes receiving 95% of the prescribed dose was 98.4% for the mammary gland/thoracic wall; 94.7% for internal mammary nodes; 98.3% for the superior lymphatic nodes (including subclavicular, supraclavicular, axillary and interpectoral nodes depending on the case).
For the ipsilateral lung : medium dose = 14.3Gy, volume receiving 20Gy = 26%, volume receiving 30Gy = 11% ; contralateral lung: medium dose = 4.5Gy, volume receiving 10Gy = 4.5% ; heart: medium dose = 8.3Gy, volume receiving 10Gy = 30%, volume receiving 20Gy = 6.5% ; contralateral breast : medium dose = 4Gy, max dose = 15.7Gy ; trachea : volume receiving 20Gy = 10%, volume receiving 30Gy = 2% ; esophagus : volume receiving 20Gy = 10%, volume receiving 30Gy = 2%.
During treatment, 19% of patients had a grade 2 skin toxicity and 9% had a grade 1 esophagus toxicity. No other toxicities were reported.

Conclusions: IMRT allows excellent coverage of target volumes while preserving the organs at risk as much as possible and limits acute toxicities. The planning strategy using a virtual bolus remains complex but guarantees an optimal treatment quality.

References

1. Nicolini, G. *et al.* Planning strategies in volumetric modulated arc therapy for breast. *Med. Phys.* 38(7), July 2011

RT5 : Dosimétristes, planification, curiethérapie

Planning study of RA and DCA for the boost of the breast treatment
Etude dosimétrique du traitement des lits tumoraux du sein en RA et DCA

C. Cavet[a], T. Lacaze[a]

[a]Institut Universitaire du Cancer de Toulouse/Toulouse/France

Introduction: In our institute, electron Conformal Radiotherapy (eCRT) usually used to treat breast boost is not optimal due the size and depth of the Planning Target Volume (PTV). In those cases photon CRT (xCRT) is used but without being satisfactory due to the tunnel effect. This study proposes to assess the feasibility of planning with two other techniques: RapidArc (RA) with one or two arcs and Dynamic Conformal Arc (DCA). Results of these techniques are compared to eCRT and xCRT.

Methods: With Eclipse v13.7 and for a Clinac 2100 C/D accelerator (Varian), data of 13 previously treated patients were used. Patients are treated with 50 Gy on the breast followed by 16 Gy on the boost (tumor bed). For each patient, the plans of the boost are achieved with 4 techniques: eCRT, xCRT, RA and DCA. A direct field using an adapted energy depending on boost depth is used for the eCRT. For xCRT, 2 or 3 fields (6 or 18 MV) are used. For RA and DCA, a partial arc shaped to the target with 5 mm margin was planned with the beginning and ending angulations of the breast treatment tangential fields. Prescription is made at maximum depth for eCRT and at the isocenter for xCRT. For RA, normalization is made on the median of the PTV of the boost (PTVboost) volume. In DCA, dose prescription was made on the reference point (sometimes different from the isocenter). For 5 patients, supplementary RA plans using 2 arcs are achieved to assess the interest of using a second arc. Plans are summed (50 + 16 Gy). D95%(boost), the dose received by 95% of the PTVboost and V55Gy(breast), the breast volume receiving 55 Gy (110% of 50 Gy) are compared for the 4 techniques to assess the boost coverage and the breast overdose respectively. Doses in the organs at risk (OAR) heart, lungs and spinal canal are also compared.

Results: For all patients, the mean value of D95%(boost) is 63.5 Gy, 64.3 Gy, 63.9 Gy, and 64.6 Gy and the mean value of V55Gy(breast) is 33.3%, 35.7%, 23.6%, and 26.3% for eCRT, xCRT, DCA and RA respectively. For all techniques, mean dose to the heart and to the controlateral lung are less than 3.5 Gy and 0.5 Gy respectively. Maximal dose received by the spinal cord are less than 3 Gy.

Conclusions: In order to assess the planning feasibility of the tumor bed boost treatment with RA and DCA, these techniques were compared to those routinely used in our department: eCRT and xCRT. RA appears to be the best solution according to every measured indicator (PTV boost coverage, OAR doses) except V55Gy in breast volume. On the other hand DCA technique does not provide any amelioration compared to CRT regarding these indicators. Few differences were observed between RA plans with 1 or 2 arcs (but it would take more time to deliver 2-arcs plans). Thus, 1-arc RA is envisaged for the treatment of breast tumor beds.

Evaluation des pratiques et validation des compétences en dosimétrie : Exemple de la planification ORL en Tomotherapy

A. Garnier[a], E. Biron[a], P. Cadot[a], G. Delpon[a], M. Doré[b], A. Grégoire[a], N. Guillaume[a], A. Lisbona[a], A. Moignier[a], Y. Seroux[a], M. Voyeau[a], N. Wiazzane[b], C. LLagostera[a]

[a]Institut de Cancérologie de l'Ouest, service de physique médicale/Saint-Herblain/France
[b]Institut de Cancérologie de l'Ouest, service de radiotherapie/Saint-Herblain/France

Introduction : Le développement et le maintien des compétences est un enjeu important notamment lorsque les équipes s'étoffent ou qu'une nouvelle technique de traitement est mise en service. L'acquisition d'une nouvelle compétence nécessite une formation, incluant une validation. Dans notre institution, une partie de la validation consiste à évaluer la variabilité inter-planificateur pour un cas clinique représentatif. Cette stratégie de formation permet à la fois de vérifier le niveau atteint par le nouvel opérateur et l'homogénéité de la pratique au sein du groupe de planificateurs accrédités. Nous présenterons le travail effectué pour un cas ORL en Tomotherapy.

*Méthodes :*Les membres de l'équipe (11 au total) ont réalisé la planification du même cas. Nous avons tout d'abord comparé les paramètres choisis pour la planification (pitch, collimation, facteur de modulation) ainsi que les caractéristiques de l'irradiation qui en découle (temps de traitement, facteur de modulation final). Ensuite, une comparaison dosimétrique basée sur les objectifs cliniques a été effectuée. Tous les plans ont également été présentés aux médecins référents en présence de tous les opérateurs pour validation.

Résultats : Le groupe se compose de 11 opérateurs (1 apprenti, 3 occasionnels et 7 confirmés). Le choix des paramètres d'optimisation montre une bonne homogénéité du groupe. Seuls les 3 plans préparés par les opérateurs occasionnels comportent des déviations par rapport aux paramètres recommandés. La plus grande variabilité est observée pour le facteur de modulation. D'un point de vue dosimétrique seuls 9 plans sont considérés comme acceptables. En effet, pour 2 plans produits par des opérateurs occasionnels, les objectifs dosimétriques au tronc et à la moelle sont respectés mais jugés trop élevés par rapport à la pratique habituelle. Le plan de l'apprenti est un des plus modulés mais protégeant le moins les OAR. Des choix arbitraires de protection ou non de certains OAR considérés comme non critiques (niveau 3) apparaissent.

Conclusions : Ce travail a permis d'évaluer le nouvel opérateur et de vérifier le maintien de l'homogénéité des pratiques. Les plans comportant des déviations sont ceux des opérateurs occasionnels ce qui montre l'importance du maintien des compétences par une pratique régulière. Les observations médicales nous ont permis de redéfinir la conduite à tenir pour les OAR de niveau 3. Enfin, on remarque qu'avec l'expérience les plans produits sont moins modulés pour le même voire un meilleur résultat dosimétrique.

Reducing contouring time of organs at risk in the thoracic and pelvic regions with innovative contouring software

Réduire le temps de délinéation des organes à risques dans les régions thoraciques et pelviennes grâce à l'utilisation de logiciels de délinéation innovants

A. Munoz[a], G. Beldjoudi[a]

[a]Centre Léon Bérard/Lyon/France

Introduction: Inverse planning requires delineating a large number of Organs at Risk (OAR) which is a time consuming process in radiotherapy. In Centre Léon Bérard (CLB), our team uses MonacoSim for more than 10 years and has a real expertise with the available tools. MiM Maestro (MiMSoftware) and Syngo.via (Siemens) were recently purchased and the associated new features (auto-contouring atlases, advanced contouring tools) were evaluated. The objective of this study is to evaluate the saving of time allowed by these new tools for OAR contouring in thoracic and in pelvic regions.

Methods: Five CT scans of thorax and five of pelvis were selected and contoured with the three contouring software. One dosimetrist, trained for OAR contouring, measured the time spent for contouring or adjusting the contours of OAR in each software. When an atlas was used to generate a first set of contours, the computing time to produce the contours was not measured as it does not mobilize human resources.
With MonacoSim, only manual contouring was done as ABAS tool is not used in the CLB because of its non-integration in Monaco. With Syngo.via, atlases provided by Siemens were used and the results were edited with the tools directly in the software. With MiM, a custom built atlas was run for thoracic CT scans and an atlas provided by MiM was used for pelvic CT scans: results were corrected with MiM tools.
An intercomparison of the delineated volumes was performed: Jaccard index and MDA (Mean Distance to Agreement) were calculated by using MonacoSim contours sets as reference.

Results: In the pelvic area, on average on all OAR, Jaccard indexes are of 0.86±0.10 and of 0.88±0.11 and MDA are of 1.45±1.09mm and of 1.03±0.85mm for contours performed respectively with Syngo.via and with MiM. In the thoracic area, Jaccard indexes are of 0.75±0.20 and of 0.75±0.22 and MDA are of 2.18±2.08mm and of 2.93±5.05mm for contours performed respectively with Syngo.via and with MiM.
In the pelvic region, the mean contouring time was measured at 10min27s ±1min27s in MonacoSim, at 6min28s ±47s in Syngo.via and at 3min28s ±1min29s in MiM. In the thoracic region, the mean contouring time was measured at 14min04s ±2min5s in MonacoSim, at 6min15s ±49s in Syngo.via and at 1min39s ±44s in MiM.

Conclusions: A good relationship was obtained between the contours performed with MonacoSim, Syngo.via and MiM for organs with well-defined anatomic limits (heart, lungs, bladder, etc.). For non-finite organs (trachea, bronchus, spinal cord) contours on a different number of upper or lower slices could have been done and results in a lower relationship based on the evaluated indexes.
The results of the contouring time measurements show a large advantage in favor of MiM Software thanks to its integrated and potentially custom-built atlases associated with real innovative tools. This combination allows, for a radiotherapy service, considerable time saving for OAR contouring of pelvic and thoracic regions.

4DCT motion artifacts: volumetric and dosimetric impacts on VMAT plans

D. Om[a], B. K. Dubois[a], G. Moliner[a]

[a]Centre Hospitalier Universitaire de Nîmes/Nîmes/France

Introduction: 4DCT is widely used for treatment planning of lung tumors, particularly to determine the necessary internal target volume (ITV). Benefits of 4DCT are limited by the presence of artifacts resulting from the acquisition and postprocessing. The aim of this study was to evaluate the volumetric and dosimetric impacts of motion artifacts on treatment planning of lung cancers.

Methods: QUASAR™Programmable Respiratory Motion Phantom–which contains a lung-equivalent insert- was used to acquire CT images with motion artifacts. 4DCT series with 5 breathing rate (BR) (6, 10, 15, 20, 24 BPM) and 3 pitches (0.1, 0.08, 0.04) were acquired. A thresholding method was used to delineate target volume. The threshold was mathematically estimated according to the phantom geometry and motion. For each acquisition, ITV_{acc} (sum of all clinical target volumes from each respiratory phase) and ITV_{MIP} (ITV delineated by thresholding on the maximum intensity projection) were determined. Deviations on target volumes in cm^3 (compared to theoretical volume) were compared to evaluate the volumetric influence of 4DCT motion artifacts.
VMAT plans using two arcs were calculated on Eclipse V15.5. For each 4DCT, 2 plans were calculated on the average serie, respectively with the ITV_{MIP} and the ITV_{acc} as target volume. Minimum dose (D_{min}), maximum dose (D_{max}) and the percent volume that received at least 95% of the prescription dose (V_{95}) were compared to evaluate the dosimetric influence of motion artifacts.

Results: With adapted pitch, mean deviation on ITV_{acc} volume is 6.2% [4.3 – 8.2]. For 6 BPM and pitch 0.04, deviation on ITV_{acc} volume is -55.4%. For 10 BPM ≤ BR ≤ 24 BPM, deviations increase when the pitch deviates from the adapted pitch (average absolute deviation: 8.3% [-24.7 – +7.2]) and overlapping artifacts are observed. With low pitch (0.04) and BR ≥ 20 BPM, deviations on ITV_{acc} volume are low [6.0 – 6.7 %] but spiral artifacts are observed. ITV_{MIP} volumes are 2.2%(mean) higher than ITV_{acc} volumes. High dose deviations are found on 6 BPM plans (+16.2% on D_{min} from pitch 0.04 to pitch 0.08). For BR ≥ 10 BPM, mean deviations are 5.8% on D_{min}, 0.5% on V_{95} and 2.7% on D_{max}. When the pitch is too high, D_{min} decreases while D_{max} increases. When the pitch is too low, D_{min} and D_{max} increase.

Conclusions: No artifacts are seen when the pitch is adapted. Motion artifacts are observed with unadapted pitches. Dose deviations occur when the chosen pitch is too high regarding the BR (the patient has a slower respiration during the acquisition). It is a common situation in clinical routine. For BR ≥ 10 BPM, dosimetric impact of movement artifacts is: 5.8% deviation on D_{min}. Respiratory synchronized acquisitions can not be performed properly on patients with BR ≤ 10 and leads to relevant dose deviations. With our process, it seems difficult to treat patients with BR ≤ 10 BPM (uncommon cases). Dosimetric results need to be confirmed by performing dose measurements in a 4D-phantom.

Evaluation of Acuros XB dose calculation algorithm in metallic implants
Évaluation de l'algorithme de calcul de dose Acuros XB dans les implants métalliques

R. Chipana[a], A. Arnoul Jarriault[a], T. Younes[a,b], L. Vieillevigne[a,b]

[a]Department of Medical Physics, Institut Claudius Regaud, Institut Universitaire du Cancer de Toulouse, Toulouse, France
[b]Centre de Recherche en Cancérologie de Toulouse, UMR 1037 INSERM, Université Toulouse 3, ERL5294 CNRS, Oncopole Toulouse, France

Introduction: The metallic fixations affect negatively the treatment planning of radiation therapy by causing difficulties to delineate the target volume and reducing the patient absorbed dose calculation accuracy. Acuros XB (AXB) discretizes deterministically the angle, energy and space variables into grids and iteratively solves the linear Boltzmann transport equation (LBTE). The aim of this work was to evaluate Acuros XB (AXB) in presence of metallic elements, such as hip prosthesis and dental implants. Comparisons against GATE (Geant4 Application for Tomography Emission) Monte Carlo (MC), Anisotropic Analytical Algorithm (AAA) calculations and measurements were undertaken.

Methods: Firstly, AXB calculations were performed in simple virtual phantoms and were compared with AAA and GATE Monte Carlo. AXB and MC dose calculations were reported to dose-to-medium Secondly, measurements were undertaken in water tank phantom containing the prosthesis. The prostheses were scanned with MAR software and their contours were checked in all dimensions. Radiation photon beams were selected to transit through metallic elements. The PTW PinPoint 3D chamber was used to measure profiles, percent depth doses (PDD) and absolute doses. Measured doses were then compared to the predicted ones by AXB and AAA. In addition, dose differences (Δ) were calculated.

Results: In the virtual phantom, AXB calculations were in good agreement with GATE. AAA failed predicting the backscatter in front of water/Titanium or water/stainless steel and exhibited differences up to 11%. Beyond 2 mm after the metallic heterogeneity, AXB differed by -2% and -4% for Titanium and stainless steel respectively, whereas AAA differed by -6% and -12%. The PinPoint 3D dose profiles presented good agreement (<2% on average) compared with AXB calculations, in contrary to AAA calculations. The absolute dose measurements (around 2 cm after the metallic implants) for 6 and 10 MV photons beams indicated maximum differences of 1.4% and 5.8% for AXB and AAA, respectively.

Conclusions: Even when the beams transited through the metallic implants, AXB has been shown to handle perturbations as well as Monte Carlo calculations. AXB calculations were in good agreement with profile and absolute dose measurements, highly better than AAA calculations.

Evaluation of Auto-Planning module in Pinnacle^3 of VMAT for prostate and head and neck
Evaluation de l'outil Auto-Planning de Pinnacle^3 pour la planification dosimétrique en VMAT de la Prostate et de l'ORL

H.Miloudi[a], J.Le Bourhis[a], T.Y.P.Dinh [a], H.Huet De Froberville[a]

[a]Centre Clinique de la Porte de Saint Cloud/Boulogne-Billancourt/France

Introduction: The French Health Authority (HAS) has recommended Volumetric Modulation Arctherapy Treatment (VMAT) for prostate and head and neck (HN) tumors. At the Centre Clinique de la Porte de Saint Cloud, these two localization are the most common for VMAT. This technique uses inverse-planning approach, which can lead to a difference in the treatment results between two users. In order to harmonize practices and automate treatment planning, Philips propose the Auto-Planning (AP) tool for treatment planning in Pinnacle3 TPS. The objectives of this study are to show feasibility as well as benefits of treatment plans performed using this module.

Methods: Treatment planning are done for ten patients with and without AP in Pinnacle3 (Philips, v.16.2) for prostate and HN treatments. The treatment planning are performed on Elekta linac with an Agility multi-leaf collimator. The study evaluate the planning target volume (PTV) coverage, the dose gradient, the dose administered to the organs at risk (OAR) and the units monitors (UM). To assess the consistency between calculation and measurement, pre-treatment quality assurance (QA) are performed using the Octavius phantom and a 2D array detector (PTW). The analysis is given for a passed gamma index criteria of 3 %/3mm local and a threshold of 10%.

Results: The PTV coverage follows the ICRU 83 recommendations and the dose gradients are closed with and without AP. For the prostate, the doses for the bladder wall and the rectum wall are similar and follows the RECORAD recommendations. For HN, there is a reduction of the maximum dose with AP of 11 Gy (± 6 Gy) for the brainstem and 4 Gy (± 2 Gy) for the spinal cord. For the parotid glands, thyroid and larynx, the doses are similar. The AP provide an average increase of 23 UM (± 21 UM) for prostate and 82 UM (± 43 UM) for HN. The pass rates of pre-treatment AQ of AP are decreasing by 1,3 % (± 1.2 %) for prostate and 1,3 % (± 2,2 %) for HN.

Conclusions: Auto-Planning maintains a proper coverage of the target volume while respecting the constraints of dose administered to the OAR. For some OAR, AP even allows to reduce the dose. Moreover, it allows a practice harmonization and facilitates planning since the operator does no longer need to manage the optimization part in TPS. However, AP process provides more UM and there is a slight reduction in the consistency between calculation and measurement but the results of the pre-treatment AQ meet the international recommendations. Finally, considering the significant use of VMAT in the clinic for prostate and HN, the use of AP for treatment planning has a significant benefit.

MCO in VMAT treatment planning for locally advanced head and neck cancer
MCO dans la planification du traitement VMAT pour le cancer de la tête et du cou localement avancé

J. Rolland[a], B. Farnault[b], P. Fau[b], A.Tallet[b], V. Favrel[b]

[a]Department of Radiotherapy oncology, Centre Hospitalier Intercommunal des Alpes du Sud, Gap, France
[b]Department of Radiotherapy oncology, Institut Paoli Calmettes, Marseille, France

Introduction: Efficacy of inverse planning is becoming increasingly important for advanced radiotherapy techniques, and especially for head and neck cancer to decrease radiation therapy toxicity. However, the inverse planning process can create a suboptimal plan despite meeting all constraints. Multicriteria optimization (MCO) may improve doses at organs at risk (OARs) and provide better treatment planning without being time consuming. The aim of this study was therefore to evaluate the benefit of VMAT with multi-criteria optimization (MCO) in RayStation (v6.1.1.2 & v8A, RaySearch Laboratories, Sweden) for head and neck cancer patients and compare the DVH difference between MCO VMAT plans and standard optimization (SO) VMAT plans.

Methods: SO VMAT plans and MCO VMAT plans were created for 15 patients with head and neck cancer. Three levels of dose were prescribed to all patients. PTV 70Gy, 63Gy, 56Gy in 35 fractions. Acceptable SO VMAT plans with minimal average dose to OARs were chosen for comparison with deliverable MCO VMAT plans. All the plans were reviewed, and the dose-volume parameters were compared between the MCO plan and the SO plans. VMAT pretreatment QA are performed comparing measured and calculated dose distribution in phantom (ArcCheck, SunNuclear) by means of gamma index (3% 3mm, Threshold 10%). A complexity metric of the MLC, calculated as a function of the shape and the aperture of MLC, and the monitor units (MU) number were compared.

Results: For both types of optimization, the dose values required to validate target coverage (D98% and D2%) are respected (< 1% difference). The dose to OARs and the conformation number (CN) for each PTV were compared, and a Wilcoxon signed-rank test was performed. MCO provided statistically significant reduction of Dmean (10% to 20%) for : parotid gland , larynx, oral cavity and Dmax for brainstem ($p < 0.05$) in which the magnitude was linked to the overlapping volume of the corresponding OAR and targets. The CN with MCO allowed a gain between 5% and 15%, and especially on the PTV 56 Gy ($p < 0.05$). For the spinal cord and the brachial plexus, the study did not show a significant difference ($p > 0.05$). The active planning time was the same. The QA passing rate with gamma analysis was > 99% for both type of optimization. The complexity metric and the MU number are higher with MCO plans compared to SO plans (5% and 10% respectively).

Conclusions: MCO is feasible in head and neck cancer treatment and MCO plans significantly reduced the dose of OARs, without compromising the target coverage comparing to standard VMAT optimization. All the plans are deliverable by a Linac. MCO, with the navigation of Pareto plan, enables physician to provide greater active clinical input into the VMAT planning process.

Validation de l'utilisation des images IRM pour la reconstruction d'un applicateur en titane en curiethérapie gynécologique

S. Jan[a], D. Autret[a], C. Di Bartolo[a], S. Dufreneix[a], M. Ferre[a], A-S. Gautier[a], M. Posnic[a], N. Mesgouez-Nebout[b], M.Brémaud[a]

[a]Service de physique médicale - Institut de Cancérologie de l'Ouest-Site d'Angers - France
[b]Service de radiothérapie - Institut de Cancérologie de l'Ouest-Site d'Angers - France

Introduction : Selon les recommandations du GEC-ESTRO *(Haie-Meder et al. 2005)*, l'IRM est la modalité d'imagerie de référence pour la délinéation des volumes cibles et des OAR en curiethérapie utéro-vaginale. Néanmoins, l'utilisation d'applicateurs en titane peut entraîner l'apparition d'artefacts métalliques rendant difficile leur reconstruction sur ces images. Une étape de validation de leur reconstruction est donc nécessaire avant leur mise en oeuvre en clinique.

Méthodes : L'applicateur gynécologique utilisé est un modèle Fletcher en titane (Varian). Les reconstructions sont réalisées à partir d'images TDM (GE LightSpeed) et IRM (Siemens Aera 1.5T). Les images tomodensitométriques servent de référence pour la reconstruction géométrique de l'applicateur. Les séquences d'acquisition IRM sont optimisées pour limiter l'impact des artefacts métalliques sur la qualité de l'image (séquence T2 WARP à large bande passante). Les reconstructions sont effectuées sur le TPS Brachyvision v13.6 (Varian). L'étude est divisée en 2 étapes :

- L'applicateur est placé dans un repère géométrique fixe et imagé en TDM puis IRM. 8 opérateurs d'expériences différentes reconstruisent l'applicateur sur chaque modalité. Les images TDM et IRM sont fusionnées et les écarts en distance entre les reconstructions TDM et IRM sont évalués afin d'estimer la possibilité de reconstruire l'applicateur de manière précise sur les images IRM.
- Une seconde étude est réalisée sur dix patientes ayant eu IRM et TDM afin d'évaluer la précision de la reconstruction en condition clinique. La reconstruction de l'applicateur est réalisée par 4 opérateurs expérimentés. Les écarts en distance entre les différentes reconstructions sont évalués et comparés à la reconstruction de référence sur le scanner utilisé pour le traitement.

Résultats : Les reconstructions de l'applicateur dans le repère fixe ont montré une bonne correspondance entre les différents opérateurs (écarts inférieurs à 1mm) et entre les deux modalités (écarts inférieurs à 1.5mm). Les résultats sont similaires quel que soit l'orientation des séquences IRM de base utilisée. L'étude sur patients a montré un écart maximal de 2.9mm entre les reconstructions IRM et la reconstruction validée en traitement. Néanmoins, 93% des écarts entre les reconstructions sur IRM et la reconstruction de référence sur TDM sont inférieurs à 2mm et 97.3% des écarts sont inférieurs à 1.5mm.

Conclusions : La faisabilité de la reconstruction de l'applicateur sur les images IRM est validée, les écarts observés sur les différentes études étant inférieurs à 2mm. Ces écarts sont à mettre en perspective avec les autres incertitudes dosimétriques présentes dans ce type de traitement (précision de positionnement de la source : 2mm ; incertitude de délinéation des organes: 3 à 6mm (Primoz et al. 2013).

Interstitial high dose rate brachytherapy : commissioning and first clinical results
Curiethérapie interstitielle à haut débit de dose : mise en place et premiers résultats cliniques

C.Dupuy[a,c], I.Sibide[b], M.Voyeau[a], E.Rio[b], C.Llagostera[a]

[a]Service de physique médicale/ Institut de Cancérologie de l'Ouest/Saint-Herblain/France
[b]Service de radiothérapie/Institut de Cancérologie de l'Ouest/Saint-Herblain/France
[c]Service de radiothérapie/Unité de physique médicale/Institut Bergonié/Bordeaux/France

Introduction: At Institut de Cancérologie de l'Ouest, ear, nose and throat (ENT) tumors used to be treated by brachytherapy with ^{192}Ir wires. Since the wire production has been stopped, ^{192}Ir source with High Dose Rate (HDR) afterloader method has replaced the use of wires. Its implementation is evaluated by the measurement of the first dwell position of the new applicator and dosimetric comparison between the previous and new methods. A review is done for patients treated from 2013 to 2018 for lip or nose basal or squamous cell carcinoma.

Methods: The applicator used is the OncoSmart system (Elekta) whose implementation follows the Paris system recommendations. It consists of 4FProGuide tubes of 240mm length, which fits into flexible needles during the computed tomography (CT) and treatment, stop buttons, nuts and clamps. EBT3 radiochromic films determine the most distal position. On other hand, a delivered dose control with five EBT3 radiochromic films ensures that the system delivers the correct dose. The irradiation time is calculated from the TPS OncentraBrachy (Elekta) for one catheter for 2Gy prescribed at 1cm. Last patients treated with wires were planned also with HDR method. The dose distribution is compared for both techniques.
28 patients were treated between 2013 and 2018 for lip or nose basal or squamous cell carcinoma with 36Gy dose delivered in 8 or 9 fractions (bi-fractionated) prescribed on the 85% isodose. Treatment plans were calculated on CT images without optimization from the TPS.

Results: The reference distance is 1239mm for all applications with this system. After EBT3 radiochromic films calibration (6% of uncertainty), the average of the five films irradiated was 2.04Gy +/- 0.1Gy. The comparison of the two techniques showed deviations of less than 5% for $V_{100\%}$ and $V_{150\%}$ and deviations of 0.3cc for $V_{250\%}$.
The patients had a consultation at 1 month of the end of treatment and then every 6 months for 2 years then once a year. The median follow up is 37 months (69-6). Among the 28 patients treated, only one presented a local recurrence treated by surgery and 2 cervical lymph nodes metastases (treated with external radiotherapy). Good tolerance was observed in the month following end of treatment with 2 patients with a grade 3 radioepithelite (7, 4%), 6 with grade 2 (20.4%) and 20 with grade 1 (71.4%). The average healing delay was 4 weeks. There are good esthetical and functional results among all patients. All patients are alive in March 2019.

Conclusions: After validation of the Oncosmart applicator for clinical use, the film dose measurement and the dosimetric comparison of the two techniques validate the replacement of the ^{192}Ir wires by the Oncosmart applicator connected to the HDR afterloader. The doses and fractionation are adjusted to the new dose rate and procedures are written to optimize the treatment conditions. Treatment is well tolerated with good clinical results (carcinological, esthetical and fonctionnal).

Custom applicators made by 3D printer in brachytherapy: experience of the F. Baclesse centre (Caen- France)
Applicateurs personnalisés réalisés par imprimante 3D en curiethérapie : expérience du centre F. Baclesse (Caen)

C. Loiseau[a],V. Barraux[a], P. Berejny[a], A. Batalla[a], H. Austins[c], C. Ollivier[b], A. Piantino[b], C. Nicolas[b], D. Stefan[b], W. Kao[b], M. Silva[b], D. Lerouge[b]

[a] Medical Physics Department / Centre de Lutte Contre le Cancer François Baclesse / Caen / France
[b] Radiotherapy Department / Centre de Lutte Contre le Cancer François Baclesse / Caen / France
[c] Biomedical Service / Centre de Lutte Contre le Cancer François Baclesse / Caen / France

Introduction: Brachytherapy is a localized radiotherapy technique that uses the movement of a radioactive source near the tumor to treat it. Conventional solutions for delivering this type of treatment are the use of non-personalized applicators or the creation of personalized molded applicators, the source being guided into these applicators by catheters. The manual manufacturing process is long, tedious, with a precise positioning of the catheters in the applicator that can become a real challenge. The objective of this work is to improve and extend the possibilities by creating custom applicators by 3D printing. In order to guarantee quality treatment, these applicators must be positioned precisely, reproducibly and individually to the patient's anatomy. We present the technical implementation of this method.

Methods: From a millimetric tomodensitometric acquisition, the position of the catheters is optimized during a preplanning process. Dicom data is converted to digital format "stl" by the 3DSlicer software. The virtual applicator is designed in the Rhinoceros 3D software, with the Grasshopper plug-in added. The digital object is exported to the Simplify3D software to generate the file for the printer. The applicator is manufactured by a low-cost 3D printer (Creatr HS-XL, leapfrogs), by depositing molten filament in layers of 0.1 mm thick. A second scanner is performed with the 3D applicator in place to plan the final treatment. Processing is planned by inverse optimization. 15 patients received brachytherapy treatment with this technique: 10 skin carcinomas, 3 post-operative endometres, 1 utero-vaginal cervix and 1 penile carcinoma.

Results: The first observations are in favour of improving the immobilisation, repositioning of the devices and better adaptation to the patient's anatomy (minimisation of aerial interfaces). Brachytherapy is improved using these 3D tools for superficial and endocavitary complex lesions. The detailed study of 2 skin treatments has been the subject of an article, to be published soon.

Conclusions: 3D printing can be applied for many types of brachytherapy treatments. Geometric accuracy and improved processing using these new techniques will require the use of dosimetry in a heterogeneous environment to ensure dose distribution. This last point will be further quantified in future studies.

Reference

1. Lecornu, M. *et al.* Intérêt de l'impression 3d pour la planification de curiethérapie de contact des tumeurs cutanées inopérables. *Can. Rad. to be published.*

Simulation of micro-nanodosimetry spectra and free radicals with Geant4-DNA, LQD, PHYCHEML, CHEM for ion beams

L. Auzel[a], Y. Ali[b], C.Monini[b] , J.M. Létang[c], E. Testa[b], M. Beuve[b], L. Maigne[a]

[a]LPC / 4, avenue Blaise Pascal, TSA 60026, CS 60026, 63178 - Aubière Cedex / France
[b]IPNL/Campus LyonTech-la Doua, Bâtiment Paul DIRAC - 4, rue Enrico Fermi, 69622 – Villeurbanne Cedex / France
[c]Creatis/7, avenue Jean Capelle, 69621 – Villeurbanne / France

Introduction: Hadrontherapy treatments rely on the estimation of the relative biological effectiveness (RBE). Biophysical models, such as the Microdosimetric Kinetic Model (MKM) [1] and the Nanodosimetry Oxidative stress model (NanOx) [2], evaluate the RBE using the calculation of specific energy spectra at micrometric scale (MKM, Nanox) and/or nanometric scale (LEM, Nanox). For the NanOx formalism, the chemical energy based on free radical production during irradiation is also considered. This study aims at benchmarking Geant4-DNA and LQD/PHYCHEML/CHEM for the simulation of specific and lineal energy spectra and radiolysis species. Physical and chemical data are estimated for electron [1-100 keV], proton [1-250 MeV] and carbone ion [1 MeV/n- 400 MeV/n] monoenergetic beams.

Methods: Geant4-DNA physics lists are tested with the different options available. These options are recommended for discrete particle interactions and use different electron elastic and inelastic models. LQD [3] uses CDW-EIS calculation for ionizations induced by ions. Three-dimensional energy transfer points are calculated in thin liquid water slices. Transfer points are analyzed with the TED code to calculate, in micrometric and nanometric targets, the specific and the lineal energy. Radiochemical species (, OH., .,.), are calculated with the Geant4-DNA chemistry module and with PHYCHEML/CHEM modules associated to LQD. Results are then extrapolated to SOBP by superposing appropriate monoenergetic ion tracks.

Results: The comparison of the results obtained with Geant4-DNA and LQD will be presented for monoenergetic beams as well as for SOBP. The radiochemical species yields will be calculated as well at the nanometric level with Geant4-DNA and PHYCHEML/CHEM softwares.

Conclusions: This study is preliminary to a full implementation of MKM and NanOx biophysical models into the GATE platform for the evaluation of Relative Biological Effectiveness (RBE) in hadrontherapy treatments.

References

[1] Hawkins RB. Med Phys. 1998;25: 1157-1170.
[2] Cunha M, et al. PMB, 2017;62: 1248-1268.
[3] Gervais B, et ak. RPC, 2005;75: 493-513.

RT6 : Radiothérapie adaptative

Implementation of MIM Software (adaptive module, Tomotherapy) and assessment of the planned versus delivered dose distributions for breast irradiation
Implémentation du logiciel MIM Software (module adaptative, Tomotherapy) et évaluation de l'irradiation mammaire en comparant la distribution de dose planifiée à la distribution de dose administrée

A. Djibo Sidikou[a], U. Niewoehner[b], J. Fontaine[c], P. Retif[a,d], P. Quétin[b].

[a]Unité de Physique Médicale, CHR Metz-Thionville, Ars-Laquenexy, 57530, France
[b]Service de radiothérapie, CHR Metz-Thionville, Ars-Laquenexy, 57530, France
[c]Unité de Physique Médicale, Centre d'Oncologie de Gentilly, Nancy, 54000, France
[d]CRAN, UMR 7039, Université de Lorraine, Vandoeuvre-lès-Nancy, 54506, France; 4 CRAN, UMR 7039, CNRS, Vandoeuvre-lès-Nancy, 54506, France

Introduction: Assessing breast irradiation is a critical issue: acute and late toxicity assessment, dose homogeneity in target volumes and delivered to organs at risk. For the Tomotherapy (Accuray®) system, the adaptive module MIM software (2017 MIM Software Inc.) - allows daily monitoring and evaluation of the dose delivered using the MVCT of each treatment session. The purpose of this project is to ensure that MIM software is reliable and then to evaluate its clinical relevance to verify the quality of the treatment by analyzing fractions administered by Tomotherapy. Clinically, treated patients are reviewed as part of a follow-up 1 – 6 and 12 months after the treatment to assess side effects.

Methods: The MIM reliability assessment is divided into three steps: 1. Verification of the correspondence between mass and electronic densities of kVCT and MVCT using the solid cylindrical Cheese phantom (Gammex RMI, Middelton WI, U.S.A), filled with inserts of different electronics densities which are known. 2. Dosimetry is done on a virtual target volume in a homogeneous zone (A) then heterogeneous zone (B), on the Cheese with water equivalent inserts -on the PreciseART™ TPS. 3. A dosimetry for right breast irradiation's scenario is made on an anthropomorphic phantom (zone C) with the same TPS. The dose distributions obtained are compared with those computed by MIM, by using dose-volume histograms, target coverage (TC) and Homogeneity Index (HI) (ICRU reports 16 and 17). This method is applied to a cohort of 30 patients treated for breast cancer.

Results: The comparison of mass and electronic densities kVCT and MVCT shows no significant difference from reference values except for the CorticalBone insert. For this last, the mass density for kVCT is 1.66 g/cm3 and the electronic density is 1.55, for MVCT 1.81 g/cm3 and 1.69 respectively. The ratio of target volume average doses computed on the kVCT and the MVCT is equal to, respectively for zones A, B and C, 1.0, 1.01 and 0.99. The relative discrepancy of HI between kVCT and MVCT, compared to kVCT, is equal, respectively for zones A, B and C, -4.39%, -13.72% and -4.79%. For treated patients, the average value of TC and HI ratio (kVCT/MVCT) are equal respectively 1.01 ± 0.08 and 1.10 ± 0.21 ($\sigma = 1$).

Conclusions: The assessment of MIM gives very satisfying results. The underestimation found for the CorticalBone insert is probably related to the fact that a CIRS 62 phantom that was used to establish the initial IVDT curve of the kVCT. Variations in dose distributions for both phantoms are due to the presence of heterogeneities and artifacts caused by their own components. The results obtained for the patients by MIM are also very satisfactory. The next step is to evaluate the relationship between the clinical observations of the physician and the results obtained by MIM.

Making decision for plan adaptation in rotational delivery era
Prise de décision pour l'adaptation du plan à l'ère de l'irradiation par la rotation

S. Yartsev[a]

[a]London Regional Cancer Program, London, Ontario, Canada

Introduction: Patient's anatomy may change significantly during radiation treatment. A simple modification of the number of monitor units to be delivered by a particular static beam can be easily evaluated based on the change in effective depth. This approach cannot be applied in the case when radiation is delivered continuously from different angles in rotational techniques as VMAT or helical tomotherapy. Our routine practice for evaluating the necessity for plan adaptation is presented.

Methods: Megavoltage CT (MVCT) scan is performed prior to every fraction of radiation treatment on helical tomotherapy unit in our centre for aligning the patient as close as possible to his/her position during planning CT. Planned Adaptive software is used for QA purpose and calculation of the dose distribution in the MVCT study imbedded into original planning CT. In the case of significant changes observed by radiation therapists, Planned Adaptive procedure is repeated and both dose-volume histograms and point dose values are compared with the ones obtained for the first fraction. The treating radiation oncologist has a quantitative voxel-wise evaluation of the impact of observed anatomy changes on the dose to the targets and organs at risk.

Results: Many Head and Neck cancer patients exhibited visibly significant anatomy changes. For the Head and Neck cases treated with VMAT on Varian linacs in 2018, 16.5% of patients were re-scanned and new plans were created. For the patients treated in the same period on tomotherapy with implementation of the proposed Planned Adaptive evaluation, only 2.9% of head and neck cancer patients were required to be re-scanned and new plans developed. Off-line consultation with the treating radiation oncologist was crucial in determining the need for plan adaptation. Both patient's clinical status and the number of remaining fractions were taken into account for the final decision on whether to adapt the initial plan. Re-contouring of the organs with changed anatomy was done only in the projects of evaluating volume change as a function of time, but was not necessary for decision of adaptation.

Conclusions: Planned Adaptive software was shown to be an effective tool for evaluation of the dosimetric significance of observed anatomy changes during radiation treatment on helical tomotherapy. A comparative analysis of dose distributions calculated for the first fraction and for the fraction of suspected large variation in anatomy can save resources in a busy clinic.

Assessment of dose calculation efficiency on corrected cone-beam CT images

P. Onoma[a], G. Delpon[a], S. Josset[a], C. Llagostera[a], A. Lisbona[a], A. Moignier[a], M. Voyeau[a] and S. Chiavassa[a]

[a]Medical Physic department, ICO/Nantes/France

Introduction: Cone-beam CT (CBCT) images present an important interest in monitoring delivered dose and adapting treatment to patient anatomical changes. However, the accuracy of CBCT-based dose calculation is limited by image quality, Hounsfield unit (HU) variation and restricted field of view (FOV). A new method based on corrected CBCT images is under development in Raystation7 (Research version - RaySearch Lab). This study aims to evaluate this method of correction (CORR-M) for dosimetric evaluation on CBCT images in case of prostate, pelvis and breast modulated treatments.

Methods: CORR-M uses an iterative approach to convert the CBCT intensity scale into the planning CT (pCT) intensity scale. Low frequency artifact corrections and data completion in case of FOV limitation are made based on a rigid or deformable image registration between the pCT and the CBCT. A corrected CBCT, corresponding to a pseudoCT, is then created and CT image value-to-density table (CT-IVDT) is applied. CORR-M was assessed on cheese phantom (CP) with inserts of various densities (Accuray) and patient data. For CP, 3 CBCT images were acquired: CP centered (case 1), anterior part of CP outside the CBCT FOV (case 2) and CP centered but with 2 inverted inserts (case 3). CORR-M was also assessed on 10 patients without anatomical changes and 4 with significant changes. These last cases include 2 pCTs: before (pCT1) and after (pCT2) changes. Data were classified into 2 groups: with (iFOV) and without (oFOV) ROIs included in the FOV. CORR-M was compared with two HU conversion methods: threshold (TH-M) and CBCT-IVDT (IVDT-M). For all studied cases, the same plan was calculated on each image, and mean density and mean dose in given ROIs were compared using pCT as reference.

Results: In case 1, maximal differences in mean density (Δ-density) were 0.14, 0.29 and 0.07g/cc for CORR-M, TH-M and IVDT-M. Corresponding maximal differences in mean dose (Δ-dose) were 1.4, 5.1 and 6.3% respectively. In case 2, CORR-M compensated for the missing part and the resulting artefacts, leading to small differences in density (≤0.07g/cc) and dose (≤1.2%), while the two other methods failed (≤0.73g/cc and 47%). In case 3, the inversion of the two inserts did not impact TH-M and IVDT-M results but slightly impacted CORR-M.
On patient data without anatomical changes and with iFOV, the 3 methods produced results close to the reference: Δ-density was 0.03g/cc, 0.15g/cc, 0.15g/cc and Δ-dose was 0.4%, 1.7%, 1.5% for CORR-M, TH-M and IVDT-M respectively. In case of oFOV, only CORR-M reflected the constancy in patient anatomy with Δ-dose≤0.5% while TH-M and IVDT-M presented Δ-dose≤21.3%.
Patients with significant changes were 4 breast cases with some ROIs outside the CBCT FOV. In these cases, CORR-M was the only efficient method, providing results close to pCT2 with Δ-density≤0.03g/cc and Δ-dose≤0.8%.

Conclusion: When registration is relevant, CORR-M overcomes the main limitations of dose calculation on CBCT allowing a rapid estimation of anatomical changes impact on dose distribution.

Evaluation and comparison of CT-CBCT deformable image registration quality of two software for cervical cancer treatment

Evaluation et comparaison de la qualité du recalage déformable CT-CBCT de deux logiciels dans le cadre d'une radiothérapie du cancer du col de l'utérus

S. Tahri[a], A. Barateau[b], M. Gobeli[a], J. Leseur[a], D. Williaume[a], R. de Crevoisier[b], C. Hervé[a], E. Trifard[a] C. Lafond[b], N. Perichon[a]

[a]Centre Eugène Marquis – CRLCC Eugène Marquis – Avenue Bataille Flandres-Dunkerque 35042 RENNES CEDEX, France
[b]Univ Rennes, CLCC Eugène Marquis, Inserm, LTSI – UMR 1099, F-35000 Rennes, France

Introduction: During radiotherapy for cervical cancer, anatomical modifications can occur. Daily cone beam CT (CBCT) acquired for positioning issue, could be used to calculate the daily dose. Besides, using a cumulative strategy, it might also allow to calculate the delivered dose during treatment. For this purpose, a CT-CBCT deformable image registration (DIR) is required. The aim of this study was to investigate the quality of DIR for two software.

Methods: Twenty patients treated for cervical cancer with intensity-modulated RT (IMRT) were included in this study. For each case, three planning CTs, with three different bladder volumes: empty, intermediate, and full bladder; were registered. Nine to sixteen CBCTs (Elekta *XVI*) per patient were performed, resulting in 240 CBCTs in total. The CBCTs were delineated (CTV T, bladder, rectum) by a radiation oncologist. For each CBCT, a CT-to-CBCT automatic DIR was performed, with the most similar CT (based on the bladder volume). Two DIR algorithms were compared: MIM Software (v.6.2) and Admire (Elekta, v.3.3.1 research). Image registration accuracy was assessed using Dice Similarity Coefficient (DSC) and Mean Distance to Agreement (MDA) metrics, between deformed contours and initial contours from the CBCT. A paired Wilcoxon signed-rank test was carried out to compare the software (significant for p-value < 0.05). A Spearman test was performed to evaluate the correlation between the structures volume difference on the CT and on the CBCT, and the DSC values.

Results: Mean DSCs values of CTV T, bladder, rectum were 0.551, 0.514 and 0.482 respectively, with MIM; 0.596, 0.583 and 0.543, respectively, with ADMIRE. DSC results between the two software were significantly different ($p<0.001$). Mean MDAs values of CTV T, bladder, rectum were 6.9 mm, 7.5 mm and 6.1 mm respectively, with MIM; 5.8 mm, 6.7 mm and 5.2 mm respectively, with ADMIRE. No statistical differences were found. Spearman correlation coefficients were lower than |0.2|. For the rectum, with ADMIRE, the patient with the highest volume difference between CT and CBCT had the lowest DSC value. Conversely, the patient with the lowest volume difference has the highest DSC value.

Conclusions: For cervical radiotherapy, the geometric reliability of CT-to-CBCT DIR was evaluated with MIM and ADMIRE. In a first approach, using automatic DIR, comparison based on delineations gives better results with ADMIRE software. Moreover, the volume difference between CT and CBCT affects the registration accuracy for the rectum. The next step is to cumulate and monitor the dose during treatment, based on daily CBCT images.

Report of the IRSN/SFPM Task Group on the implementation of an MR-linac for radiotherapy
Rapport du GT IRSN/SFPM sur l'installation et la mise en œuvre d'un IRM-linac en radiothérapie

S. Derreumaux[a], J. Caron[b], N. Reynaert[c], R. Oozeer[d], A. Petitfils[e], V. Dedieu[f]

[a] Institut de Radioprotection et de Sureté Nucléaire (IRSN)/PSE-SANTE/SER/UEM/Fontenay-aux-Roses/France
[b] Institut Bergonié/Département de Radiothérapie/Unité de Radiophysique/Bordeaux/France
[c] Institut Jules Bordet/Département de Physique Médicale/Bruxelles/Belgique
[d] Radiation Therapy Consulting/Marseille/France
[e] Centre Georges-François Leclerc/Service Radiophysique/Dijon/France
[f] Centre Jean Perrin/Service de Physique Médicale et Radioprotection/UMR 1240 Inserm/IMOST/UCA/Clermont-Ferrand/France

Introduction: In the frame of the marketing of new radiation therapy devices coupling a linear electron accelerator to a magnetic resonance imaging system (MR-linac), the French Nuclear Safety Authority asked IRSN to conduct a study on the implementation of these systems. The aim was to establish the state of the art for this technology and to identify any points requiring vigilance. In particular, the study focuses on the impact of the presence of a magnetic field on the operation of a radiotherapy department (other accelerators and work organization), management of the dose delivered to the patient, including quality control of equipment, and specific issues related to patient care workflow.

Methods: The study was performed by a task group (TG) of medical physicists from the French Society of Medical Physics lead by the IRSN. The TG has performed auditions (MR-linac manufacturers, first French center installing a machine, national metrology laboratory, medical physicists with expertise in the area of deformable registration or risk management in an MRI environment), tours of facilities and discussions with pioneer teams in Europe, exchanges with the MR-linac manufacturers and analysis of their documentation, review of recent scientific literature.

Results: The various observations and recommendations of the TG concern the impact of the magnetic field on the operation of accelerators in neighboring rooms, impact of the quality of MRI images on treatment quality, impact of the magnetic field on the measurements of beam characteristics (commissioning and quality control), in particular on the beam calibration, impact of the magnetic field on the dose distribution in the patient, expected performance, commissioning and quality control of the treatment planning system (dose calculation, deformable registration), independent dose verification (second calculation and in vivo dosimetry), and finally the impact of the use of an MR-linac on department organization and human resources (in particular training of professionals, adaptive radiotherapy specific organization and risk management regarding electromagnetic fields).

Conclusions: The report of the TG presents a review of the data and reference documents concerning the implementation of an MR-linac in a radiotherapy department. The TG raises questions that any team in charge of implementing this type of device should consider and make numerous recommendations, especially for medical physicists. Finally, the report indicates technical solutions that already exist or are in development, in particular regarding dosimetry issues.

Intelligence artificielle

Deep learning in radiotherapy in 2019: what role for the medical physicist?
Deep learning en radiothérapie en 2019 : quel rôle pour le physicien médical ?

P. Meyer[a], V. Noblet[b], A. Lallement[b], C. Niederst[a], D. Jarnet[a], N. Dehaynin[a], C. Mazzara[a]

[a]Medical Physics Department, Paul Strauss Center/Strasbourg/France
[b]ICUBE Laboratory, IMAGeS team/Strasbourg/France

At early 2010's, the emergence of algorithms based on deep-learning (DL) techniques revolutionized the field of artificial intelligence [1]. Since then, a growing number of research works using DL for radiotherapy applications have been published [2].
Radiotherapy is indeed an unavoidable playground for DL developments and, through the many published works, it can be noticed that all steps of patient workflow are related to potential applications [3]. Automatic segmentation of medical structures with DL-based algorithms is the most obvious example, already widely studied in the literature, for almost all organs/tumors and many imaging modalities [4]. Other classic radiotherapy fields have been the subject of recent publications in which deep-learning methods have been used. Without being exhaustive, one can mention the processing of simulation and positioning images (MRI to pseudo-CT images creation [5], metal artifact correction [6], image quality improvement [7]...), deformable multimodal imaging registration [8], automatic treatment planning [9] or quality assurance [10]. It should be noted that the combination of some of these different applications could facilitate the adoption of adaptive radiotherapy in clinical routine. Algorithms based on deep-learning have also been developed for the management of the patient's movement and anatomy during treatment [11]. Finally, several studies have shown that deep-learning is an interesting tool for outcome modelling and toxicity prediction [12].
However, these numerous research projects are still not transferred to clinical routine: apart from a few automatic segmentation applications, there is currently no commercial application using deep-learning in radiotherapy. Several reasons may explain the slowness and difficulty of this shift from research works to hospital tools. Among these reasons, the main obstacle could be related to the lack and the quality of training data, which is an essential part of deep learning algorithms. It is precisely through the creation of clean and structured databases that the medical physicist has an important role to play, at the interface between the clinical and the research fields.

References

[1] LeCun Y, Bengio Y, Hinton G. Deep learning. Nature 2015;521:436–44. doi:10.1038/nature14539.
[2] Sahiner B, Pezeshk A, Hadjiiski LM, Wang X, Drukker K, Cha KH, et al. Deep learning in medical imaging and radiation therapy. Med Phys 2019;46:e1–36. doi:10.1002/mp.13264.
[3] Meyer P, Noblet V, Mazzara C, Lallement A. Survey on deep learning for radiotherapy. Comput Biol Med 2018;98:126–46. doi:10.1016/j.compbiomed.2018.05.018.
[4] Cardenas CE, Yang J, Anderson BM, Court LE, Brock KB. Advances in Auto-Segmentation. Semin Radiat Oncol 2019;29:185–97. doi:10.1016/j.semradonc.2019.02.001.
[5] Kazemifar S, McGuire S, Timmerman R, Wardak Z, Nguyen D, Park Y, et al. MRI-only brain radiotherapy: Assessing the dosimetric accuracy of synthetic CT images generated using a deep learning approach. Radiother Oncol J Eur Soc Ther Radiol Oncol 2019;136:56–63. doi:10.1016/j.radonc.2019.03.026.
[6] Hegazy MAA, Cho MH, Cho MH, Lee SY. U-net based metal segmentation on projection domain for metal artifact reduction in dental CT. Biomed Eng Lett 2019. doi:10.1007/s13534-019-00110-2.
[7] Jiang Z, Chen Y, Zhang Y, Ge Y, Yin F-F, Ren L. Augmentation of CBCT Reconstructed from Under-sampled Projections using Deep Learning. IEEE Trans Med Imaging 2019. doi:10.1109/TMI.2019.2912791.
[8] Yan P, Xu S, Rastinehad AR, Wood BJ. Adversarial Image Registration with Application for MR and TRUS Image Fusion. ArXiv180411024 Cs 2018.
[9] Fan J, Wang J, Chen Z, Hu C, Zhang Z, Hu W. Automatic treatment planning based on three-dimensional dose distribution predicted from deep learning technique. Med Phys 2019;46:370–81. doi:10.1002/mp.13271.
[10] Nyflot M, Thammasorn P, Wootton L, Ford E, Chaovalitwongse W. Deep learning for patient-specific quality assurance. Med Phys 2019;46:456–64. doi:10.1002/mp.13338.
[11] Hirai R, Sakata Y, Tanizawa A, Mori S. Real-time tumor tracking using fluoroscopic imaging with deep neural network analysis. Phys Med 2019;59:22–9. doi:10.1016/j.ejmp.2019.02.006.

[12] Bibault J-E, Giraud P, Housset M, Durdux C, Taieb J, Berger A, et al. Deep Learning and Radiomics predict complete response after neo-adjuvant chemoradiation for locally advanced rectal cancer. Sci Rep 2018;8:12611. doi:10.1038/s41598-018-30657-6.

RT7: Utilisation statistique des données et machine learning

Gamma Index Pass Rate control limit determination using Bayesian statistical inference: application to pre-treatment quality controls[...]

Détermination de la limite de contrôle du taux d'indice Gamma par inférence statistique bayésienne : application aux contrôles pré-traitement

T. Tiplica[a], S. Dufreneix[b], C. Legrand[b]

[a]LARIS Systems Engineering Research Laboratory, University of Angers, France
[b]Integrated Center for Oncology, Medical Physics Department, Angers, France

Introduction: Statistical Process Control (SPC) and control charts have been successfully implemented in radiotherapy in order to detect special causes of variation in processes and thus to increase their quality[1,2]. Furthermore, the Gamma Index Pass Rate (GIPR), characterized by a Beta distribution, is a widely used parameter for analyzing measurements in medical physics[3,4]. This study presents two methodologies to determine the GIPR control limit (CL). The first one is based on Bayesian inference and defines an adaptive CL to each GIPR measurement. It can thus be used from the first record without any prior information. The second one employs a fixed CL defined as a quantile of the Beta distribution fitted over a reference sample of GIPR.

Methods: An application of these two methodologies was provided for pre-treatment quality controls measured with an aS1200 electronic portal imager (EPID) device on a TrueBeam v2.5 (Varian). Statistical computations were performed with R (v.3.5.1) software. Pre-treatment quality controls compared the dose distribution acquired with the EPID with the calculated dose distribution using the GIPR metric generated by Portal Dosimetry v13.7. The following settings were used: local 3 % / 3 mm, threshold 30 %, ROI defined as MLC + 5 mm.

Results: For the first 100 measurements the adaptive CL (first methodology) varied from 98.5 to 94.5 % and converged to 95.1 %. These first 100 arcs were considered as a reference sample for the second methodology. It was best characterized by a Beta distribution and the resulting fixed CL was 95.1 % assuring continuity between the two methodologies.

Conclusions: A simple SPC methodology for monitoring GIPR was precisely described and CLs were calculated from the first arc. As a first step, Bayesian inference was used until a sufficient amount of data was collected and, in a second step, a fixed control limit was calculated. The strong points of this method lie in using the true GIPR's distribution that minimizes both: false positive and no detection of special causes. This methodology should be very useful for those who wish to set an individual control chart to follow any GIPR values.

References

1. Pawlicki T. et al. Statistical process control for radiotherapy quality assurance. *Med Phys,* 32, 2777-86 (2005)
2. Miften M. et al. Tolerance limits and methodologies for IMRT measurement-based verification QA: Recommendations of AAPM Task Group No. 218. *Med Phys* (2018)
3. Low, D. A. *et al.* A technique for the quantitative evaluation of dose distributions. Med Phys, 25, 656-61 (1998)
4. Kearney V. *et al.* Correcting TG 119 confidence limits. *Med Phys,* 45, 1001-1008 (2018)

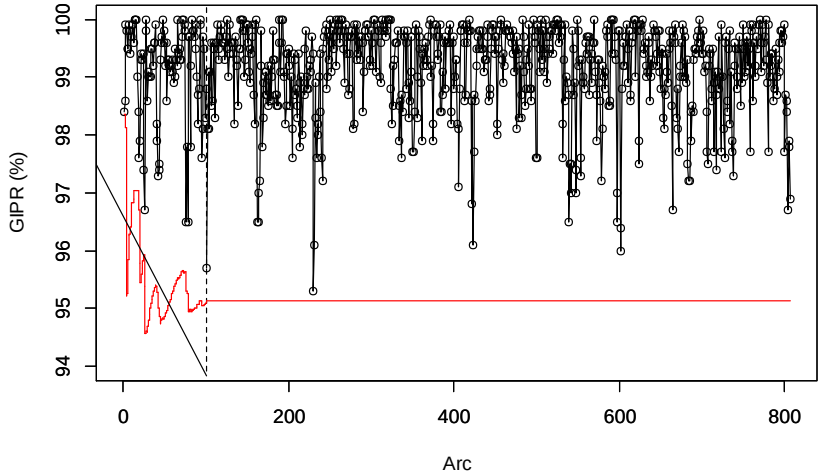

Control chart for the GIPR based on Beta distribution (first 100 GIPR values correspond to the reference sample – before the vertical dashed line).

From creation to clinical use of knowledge-based optimization model for breast and lymph node irradiations in volumetric modulated arc therapy, VMAT
De la création à l'utilisation clinique d'un modèle d'optimisation basé sur les connaissances et pour les irradiations du sein et des aires ganglionnaires réalisées en arcthérapie dynamique, VMAT

T. Richir[a], E.Costa[a], M.Robilliard[a], P.Poortmans[a]

[a]Department of Radiation Oncology, Institut Curie/Paris/France

Introduction: Treatment planning is a complex process that can result in a large number of possible dosimetric solutions. The final dose distribution depends on the geometry of organs at risk with respect to the target, differences in treatment technique, planner experience … Our work aims to describe the first steps of the creation and clinical validation of a knowledge-based treatment planning model for breast cancer irradiation using VMAT.

Methods: This work is based on a panel of VMAT treatment plans made for patients treated for left-sided loco-regional breast irradiation. As a first step, we used the PQM[1] index and analyzed the volumetric and dosimetric data of the breast, heart and lungs to select the plans to build the model. As a second step, we generated a left-sided breast model using RapidPlan™ (Varian). As a third step, to verify the model, we analyzed dosimetric outliers to review the dose distribution and to remove the structures perceived as geometric outliers. Finally, we evaluated the model following two loops: 1/ Testing on the plans that we used to create it (closed loop), and 2/ Applying it for a panel of new patients (open loop).

Results: The analysis of the 168 available plans allowed us to select 58 plans for the construction of the left-sided breast model by rejecting the plans with too high doses to OARs or with structures that were removed based on the Gaussian distribution of the population (Fig 1.a). We adjusted the dose distribution of 8 plans with a negative PQM as well. This step is essential to ease the validation step by immediately removing dosimetric outliers. After creating the model of 17 structures (± 25h), the verification required about 7h. During this step, we removed structures degrading the model (11% of the total number of structures injected) (Fig 1.b). During closed loop validation, the dosimetric results of the 58 plans generated were equivalent to the original ones for the majority of the PTVs, with a slight degradation of breast PTV coverage and a small increase in OAR dose. Following the manual resumption of the last stages of optimization of the plans generated by the model (± 0.25h), we obtained PTV coverage equivalent to the original plans as well as a significant reduction of OAR doses ($p<0.05$) (Fig 1.c). Dose distributions obtained in the open loop validation equates to clinically validated treatment plans (Fig 1.d). Using the model reduces the optimization time by half (0.75h versus 1.5h).

Conclusions: Using the model in clinical practice allowed us to improve the quality of dosimetric plans without an increasing time. A third loop of validation will study the flexibility of the model and thus standardize practices for breast treatment by evaluating the model's response for different treatment geometries. Applying complexity indices enabled us to identify acceptance thresholds and thereby to limit pre-treatment QA.

References

1. Nelms and al., Practical Radiation Oncology 2, (2012): 296–305.

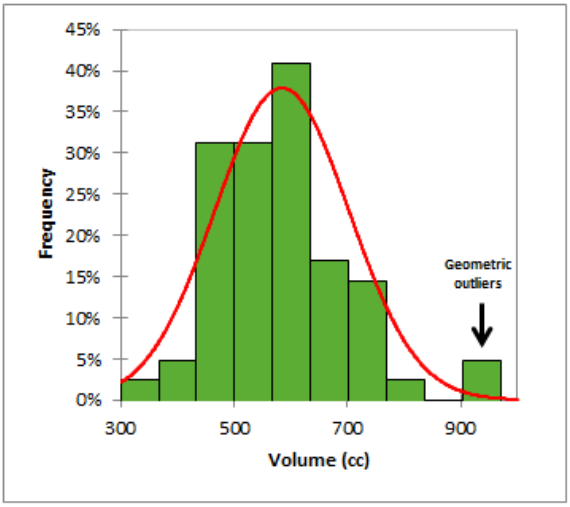

Fig 1.a. Distribution of heart volumes of the plans taken into account for the creation of the left breast model.

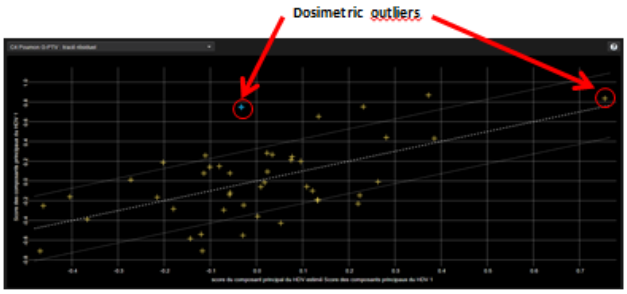

Fig 1.b. Identification of dosimetric outliers during the verification step with RapidPlan.

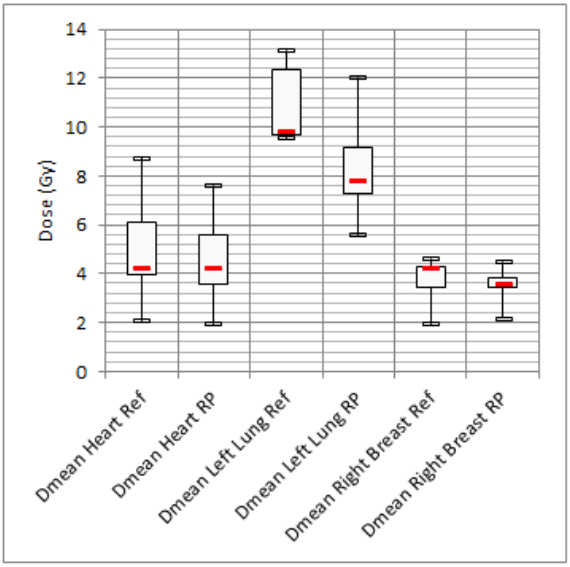

Fig 1.c. Closed loop: Dosimetric improvement of the heart, left lung and right breast structures for 10 plans generated by the model with manual reoptimization (RP) compared to the originals (Ref) (Paired stutend t-test : p<0.05).

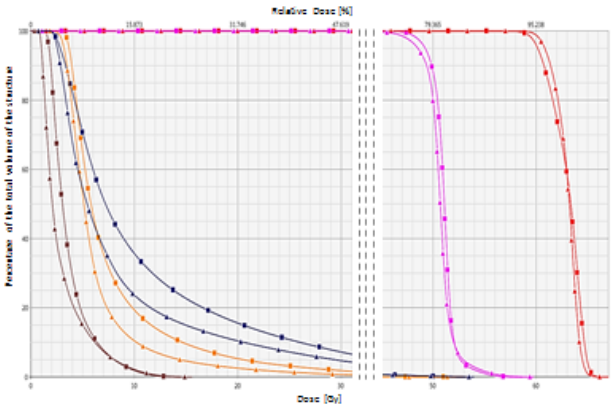

Fig 1.d. Open loop: Comparison between a plan generated by the model with manual optimization (triangle) and the original plan (square) of a patient. The structures considered are: right breast (brown), right lung (turquoise), heart (orange), left lung (blue), PTV left breast (purple), PTV tumoral bed (red).

Assessing the impact of key preprocessing concepts on the pseudo CT generation
Impact de concepts clés dans le processus de génération de pseudo CT

E. Alvarez Andres[a,b], L. Fidon[b,c], M. Vakalopoulou[c], G. Noël[d], A. Beaudre[e], S. Niyoteka[a], N. Benzazon[e,f], D. Lefkopoulos[e], E. Deutsch[a,f,g], N. Paragios[b], C. Robert[a,e,f]

[a]U1030 Molecular Radiotherapy, Paris-Sud University - Gustave Roussy - Inserm - Paris-Saclay University/Villejuif/France
[b]TheraPanacea/Paris/France
[c]Centre for Visual Computing, Paris-Saclay University/Gif-sur-Yvette/France
[d]Department of Radiotherapy, Paul Strauss Institute/Strasbourg/France
[e]Department of Medical Physics, Gustave Roussy - Paris-Saclay University/Villejuif/France
[f]Paris-Sud University, Paris-Saclay University/Le Kremlin-Bicêtre/France
[g]Department of Radiotherapy, Gustave Roussy - Paris-Saclay University/Villejuif/France

Introduction: Magnetic Resonance Imaging (MRI) only radiotherapy workflows have been increasingly appealing as they ensure a reduction of the dose received by the healthy tissues and thus a higher patient safety. We used state-of-the-art 3D neural networks (1) to map any high-resolution T1-weighted MRI (T1) or enhanced T1 weighted MRI (T1Gd) to a pseudo Computed Tomography (pCT). The goal of this study was to quantify the impact of critical preprocessing steps on the 3D pCT generation.

Methods: The global dataset was composed of 402 rigidly-registered pairs of brain CT and T1 or T1Gd. Experiment 1 consisted in evaluating the impact of the MRI input sequence. To this aim, two datasets composed of 222 and 220 T1-only and T1Gd-only MR images respectively were constituted and distributed between the training, validation and test sets. A second experiment was conducted to quantify the impact of the training set size. Five models were used, with 242, 121, 60, 30 and 15 patients respectively in the training set. The validation and test sets remained the same and were composed of 81 and 79 patients respectively. A last experiment to assess the role of MR standardization was performed. 242, 81 and 79 patients were included in the training, validation and test sets respectively. Three different approaches were investigated: no standardization (NS), a histogram-based (HB) (2) and zero mean-unit variance (ZMUV) standardizations. To evaluate the quality of all generated pCT, the Mean Absolute Error (MAE) was computed within four areas (whole head, air, bone and water components). T-tests were conducted for statistical evaluation.

Results: For the first experiment, a p-value of 0.72 was achieved between the T1-only and T1Gd-only models suggesting that the two sequences can be used without any distinction. The MAE obtained for the second experiment are presented in Figure 1. We showed that more than 100 patients must be used in the training set to reach optimal performances. The last experiment led to head MAE of 92HU +/- 23HU, 83HU +/- 22HU and 96HU +/- 23HU for the HB, ZMUV, NS approaches respectively. Differences between HB/ZMUV and ZMUV/NS methods were found to be significantly different, with p-values of 0.013 and 0.00038 respectively.

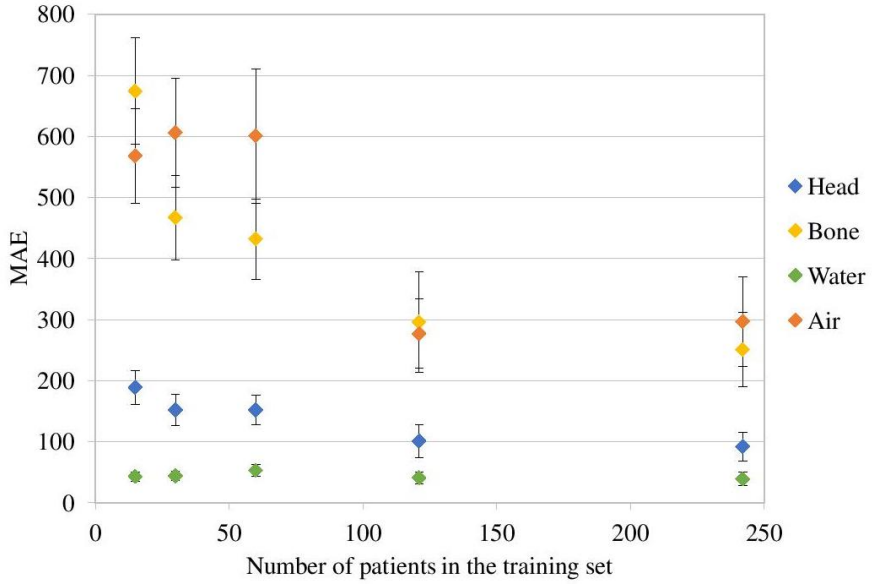

Figure 1: MAE as a function of the size of the training set

Conclusions: We evaluated pseudo-CT generated with a highly performing deep learning architecture from MRI. To our knowledge, it is the first study to adopt a 3D approach based on a large dataset (402 patients).

References

1. Li W, Wang G, Fidon L, Ourselin S, Cardoso MJ, Vercauteren T. On the Compactness, Efficiency, and Representation of 3D Convolutional Networks: Brain Parcellation as a Pretext Task. ArXiv170701992 Cs. 2017;10265:348-60.
2. Nyúl LG, Udupa JK, Zhang X. New variants of a method of MRI scale standardization. IEEE Trans Med Imaging. févr 2000;19(2):143-50.

A comparison of pseudo-CT generation methods for prostate MRI-based dose planning: deep learning, patch-based, atlas-based and bulk-density methods

Comparaison de méthodes de génération de pseudo-CT pour une planification dosimétrique à partir d'IRM : deep learning, basée patches, atlas et assignement de densités

A. Largent[a], A. Barateau[a], J. Nunes[a], C. Lafond[a], P.B Greer[b,c], J. A Dowling[d], J. Baxter[a], H. Saint-Jalmes[a], O. Acosta[a], R. de Crevoisier[a]

[a]Univ Rennes, CLCC Eugène Marquis, INSERM, LTSI - UMR 1099, F-35000 Rennes, France
[b]School of Mathematical and Physical Sciences University of Newcastle/Newcastle/Australia
[c]Department of Radiation Oncology, Calvary Mater, Newcastle, Australia
[d]CSIRO Australian e-Health Research Centre, Herston/Queensland/Australia

Introduction: Deep learning methods (DLM) have recently been developed to generate pseudo-CT (pCT) from MRI for radiotherapy dose calculation. The main advantage of these methods is the speed of pCT generation. This study aims to evaluate the accuracy of two DLMs proposed to generate pCT from MRI in prostate radiotherapy: a generative adversarial network (GAN) DLM using a perceptual loss, the classical U-Net DLM and compare them with three current state-of-the art methods: a patch-based method (PBM), an atlas-based method (ABM) and a bulk density method (BDM).

Methods: Thirty-nine patients received VMAT for prostate cancer (78 Gy in 39 fractions). T2-weighted MRIs were acquired in addition to the planning CTs. pCTs were generated from these MRIs by two DLMs: GAN, U-Net; and by three current state-of-the art methods: PBM [1], ABM [2] and BDM (water-air-bone density assignment). The GAN DLM was used with a perceptual loss instead of standard loss functions. The PBM was performed with feature extraction and approximate nearest neighbor search. DLMs and PBM were trained with data from 25 patients. The five methods were compared in a cohort of 14 patients. Imaging endpoints were mean absolute error (MAE) and mean error (ME) of Hounsfield units (HU) computed between pCT and reference CT. Dose uncertainties of the methods were defined as the absolute mean differences between DVH parameters of the organs at risk and PTV calculated from the reference CT and from the pCTs for each method. 3D gamma index analyses (local, 1%/1mm) were also performed. The Wilcoxon test was used to compare the uncertainties.
Results: In the whole pelvis, the GAN DLM showed significantly lower MAE (mean value of 37 HU) compared to the PBM (41 HU), ABM (43 HU and) and BDM (99 HU) and similar MAE compared to the U-Net DLM (37 HU). The ME obtained from the PBM (-1 HU) was lower compared to those of the GAN DLM (-9 HU), U-Net DLM (-10 HU), ABM (-8 HU) and BDM (-18 HU). The GAN dose uncertainties were: 0.7% for the prostate PTV $V_{95\%}$, 0.5% for the rectum V_{70Gy}, and 0.2% for the bladder V_{50Gy}. The figure shows the dose uncertainty of each method along the whole DVH for the rectum. DVH differences were significantly lower when using the DLMs and the PBM, than the ABM and BDM. All the mean gamma values were significantly lower with the DLMs and the PBM, compared to the ABM and BDM. The mean calculation times to generate one pCT were 15 s for the two DLMs and 62 min for the PBM.
Conclusions: In order to generate pCT from MRI for dose calculation, the five assessed methods provide clinically acceptable uncertainties (<1%). The GAN DLM appears a good compromise considering the dose accuracy and calculation time (< 1 min).

References

1. Largent, A. *et al.* Pseudo-CT Generation for MRI-Only Radiation Therapy Treatment Planning: Comparison Among Patch-Based, Atlas-Based, and Bulk Density Methods. *IJROBP* (2018).
2. Dowling, DA *et al.* An atlas-based electron density mapping method for magnetic resonance imaging (MRI)-alone treatment planning and adaptive MRI-based prostate radiation therapy. *IJROBP* (2012).

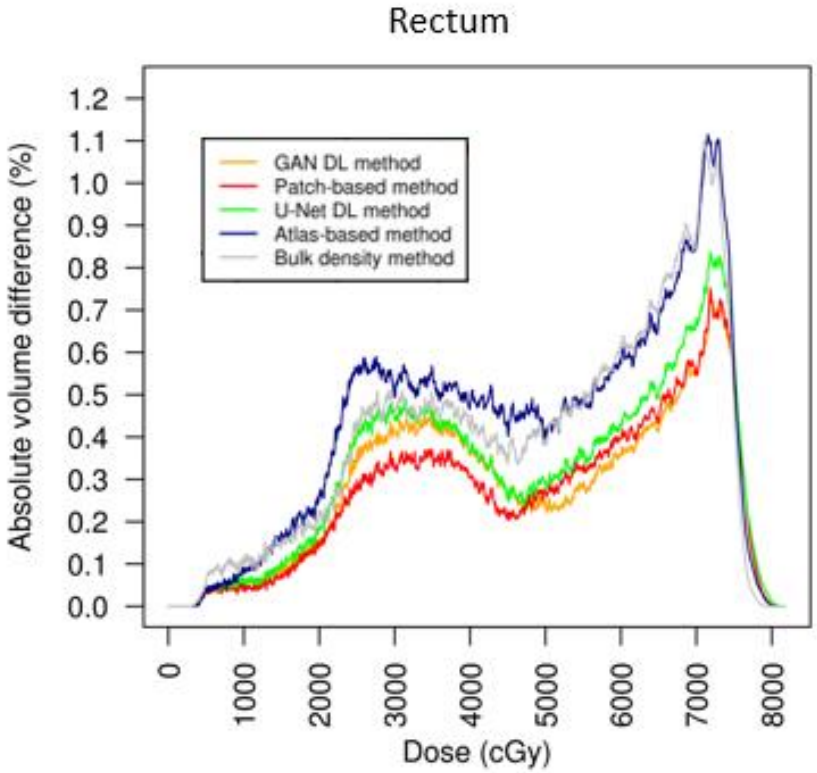

Fig. Dose uncertainties along the whole DVH for rectum using 5 methods in the same cohort of patients: GAN DLM, U-Net DLM, PBM, ABM and BDM

Deep MR to CT synthesis using paired data in the pelvic area
Synthèse d'un CT avec des images MR-CT alignées par apprentissage profond dans la région pelvienne

K.N.D. Brou Boni[a,b], L. Vanquin[a], A. Wagner[a], J. Klein[b], D. Pasquier[c,b], N. Reynaert[d,a]

[a] Centre Oscar Lambret, Service de Physique Médicale/Lille/France
[b] Univ. Lille, CNRS, CRIStAL, Centrale Lille/Lille/France
[c] Centre Oscar Lambret, Département de radiothérapie/Lille/France
[d] Institut Jules Bordet, Service de Physique Médicale/Bruxelles/Belgique

Introduction: The establishment of a MRI-only workflow in radiotherapy depends on the ability to generate an accurate synthetic-CT (sCT) for dose calculation. Previously proposed methods have used a Generative Adversarial Network (GAN) to generate a fast sCT in order to simplify the clinical workflow and reduce uncertainties. We used a conditional Generative Adversarial Network (cGAN) framework called pix2pixHD[1] which addresses the two main issues of a GAN: the difficulty of generating high-resolution images and the lack of details in the previous high-resolution results. In this work, we trained this cGAN with paired MR-CT images in the pelvic area in order to have a fast, simple and accurate sCT generation.

Methods: This study included T2-weighted MR and CT images of 8 patients in treatment position from a public dataset[2]. All voxels outside the body were set arbitrarily at the same value, CT as well as MR images.
GAN are characterized by an image generator followed by a discriminator whom it tries to fool. The cGAN proposed by Wang et al.[1] used in this work contains a coarse-to-fine generator and a multi-scale discriminator. The implementation provided by the authors was fitted to use 16-bits greyscale images allowing the use of the whole CT and MR range of values. We enforce the Hounsfield units (HU) consistency by adding a L1-loss. A leave-one-patient-out cross-validation was used by training the network with 7 patients to generate a sCT of the last one. The Mean Absolute Errors (MAE) for each patient were evaluated between real and synthetic CT. To compare with an existing solution, we implemented the vanilla cGAN introduced by Maspero et al.[3] and tested it on our dataset.

Results: It takes an average of 11 s to generate a complete sCT (80 slices) for a patient (Figure 1). The MAE in HU between the sCT and actual patient CT (within the body contour) was 35 ± 5 HU with our method, thus outperforming the vanilla cGAN implementation (60 ± 13 HU). A dosimetric evaluation is in progress to assess the clinical impact of these HU differences on patient dose distributions.

Conclusions: This study demonstrated that a sCT can be generated with a unique MR sequence, reducing the pre-processing step while being fast and accurate. Future work implies the combination of a cGAN with a Recurrent Neural Net to mitigate the discontinuities across slices.

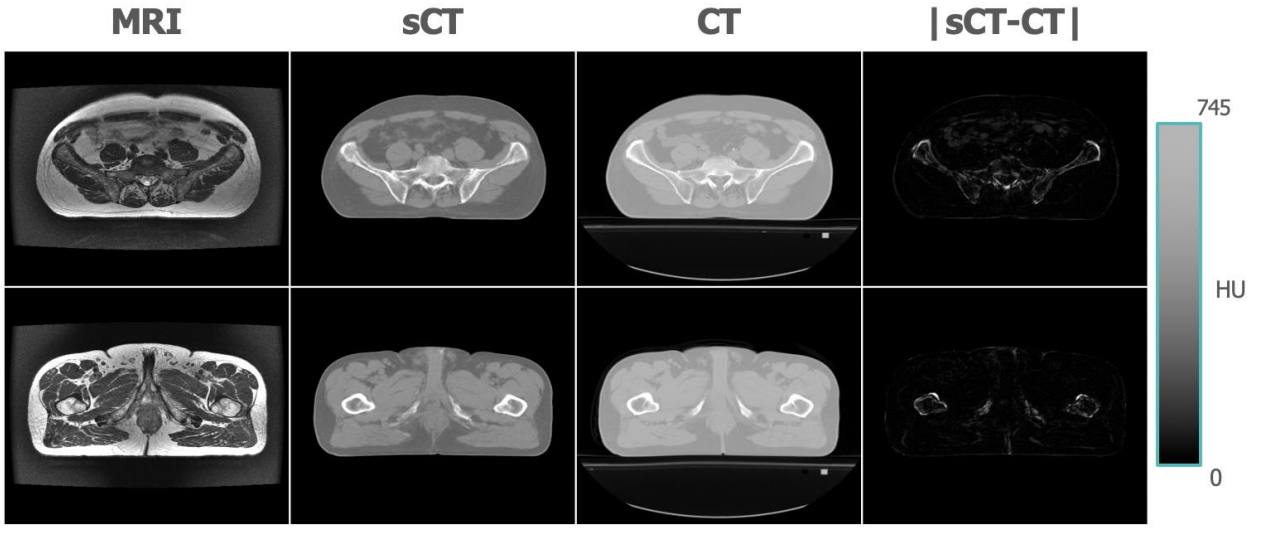

Figure 1: *MRI, sCT, CT and | sCT – CT | for an exemplary patient.*

References

1. Wang, T.-C. *et al.* High-resolution image synthesis and semantic manipulation with conditional gans. in *Proceedings of the IEEE Conference on Computer Vision and Pattern Recognition* 8798–8807 (2018).
2. Nyholm, T. *et al.* MR and CT data with multiobserver delineations of organs in the pelvic area-Part of the Gold Atlas project. *Med. Phys.* **45**, 1295–1300 (2018).
3. Maspero, M. *et al.* Dose evaluation of fast synthetic-CT generation using a generative adversarial network for general pelvis MR-only radiotherapy. *Phys. Med. Biol.* **63**, 185001 (2018).

Comparison of a deep learning method with three other methods to perform dose calculation from CBCT images in head-and-neck radiotherapy

Comparaison d'une méthode d'apprentissage profond avec trois autres méthodes pour calculer la dose à partir d'images CBCT en cas de radiothérapie ORL

A. Barateau[a], A. Largent[a], N. Perichon[a], J. Castelli[a], E. Chajon[a], O. Acosta[a], A. Simon[a], R. De Crevoisier[a], C. Lafond[a]

[a] Univ Rennes, CLCC Eugène Marquis, Inserm, LTSI – UMR 1099, F-35000 Rennes, France

Introduction: Anatomical variations occur during head and neck (H&N) radiotherapy. kV cone beam computed tomography (CBCT) images could be used to calculate the dosimetric impact of these anatomical variations and monitor the dose. This study aims to evaluate a deep learning method (DLM) to generate pseudo-CT (pCT) from CBCT and to compare this method with three existing methods in H&N cancer radiotherapy.

Methods: Fourty-four patients received VMAT for H&N cancer (integrated boost: 70-63-56 Gy). For each patient, planning CT (Bigbore, Philips) and both weekly CT and CBCT images (XVI, Elekta) were acquired. CT and CBCT images from 30 patients (30 images) were used for the training step. Weekly CTs and CBCTs were used for the evaluation for 14 patients (64 images). The DLM was based on generative adversarial architecture (GAN). The GAN DLM was compared to three other methods: i) use of a density to HU relation from phantom CBCT image (HU-D relation), ii) water-air-bone density assignment method (DAM), and iii) deformable image registration (DIR) with Admire software (Elekta, research version). Imaging endpoint was mean absolute error (MAE) of Hounsfield units (HU) from voxel-wise comparisons between pCT and reference CT. Dose uncertainties of the methods were defined as the absolute differences between DVH calculated from the reference CT and using each method, for the organs at risk and PTV. 3D gamma index analyses (local, 2%/2 mm, 30% low dose threshold) were also performed. The Wilcoxon test was used to compare the uncertainties.

Results: For the GAN DLM, the MAE in the whole body contour was 82 ± 11 HU, 69 ± 15 HU for the soft tissue and 208 ± 42 HU for the bones. The GAN DLM dose uncertainties were 8 ± 8 cGy (max=44 cGy) for the ipsilateral parotid gland D_{mean} and 5 ± 6 cGy (max=26 cGy) for the contralateral parotid gland D_{mean}. The figure shows the dose uncertainties of each method along the whole DVH for the ipsilateral PG. Significant differences with the GAN DLM are displayed with the use of the symbol *. The mean 3D gamma passrate ± SD was 98.1 ± 1.2% for the GAN DLM, 98.8 ± 0.7% for the DIR method, 97.9 ± 1.6% for the DAM and 91.0 ± 5.3% with the use of HU-D relation. The mean calculation times to generate one pCT were 30 s for the GAN DLM and DIR method.

Conclusions: GAN DLM appears particularly attractive to generate pCT from H&N CBCT images since being rapid and more accurate than the simple use of a HU-density relation curve. The method could be even more improved with a scatter correction during preprocessing.

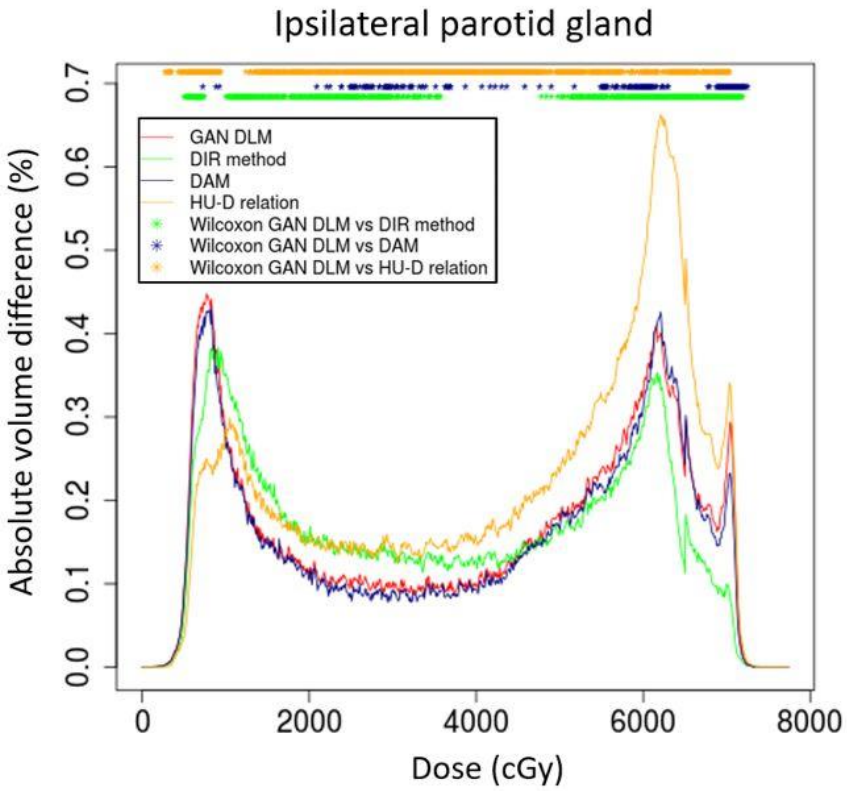

Fig. Dose uncertainties along the whole DVH for the ipsilateral parotid gland using four methods in the same cohort of patients: GAN DLM, DIR method, DAM and HU-D relation

MN3 : Médecine Nucléaire

Medical Physicist Responsibilities in Internal Radionuclide Therapy
Responsabilités du Physicien Médical en Radiothérapie Interne Vectorisée

B.Farman Ara[a]

[a]Hôpital La Timone, Service de Médecine nucléaire – CERIMED/Marseille/France

Introduction: The internal radionuclide therapy brings together therapy techniques using radiophamaceuticals and radioactive implants. Mostly used in oncology, two kinds of therapy techniques can be distinguished : selective and systemic methods.

Methods: Actors are numerous: physicians, medical phycisists, radiopharmacists, radiopharmacy preparators, technicians and nurses. Each of them is responsible of his own work. The review of different parts of the internal radionuclide therapy techniques, can lighten up the reponsibilities of medical physicists.

Results: When setting up a therapy technique, the medical physicist has an important role to play. In the case of a research protocol, he meets the sponsor and its medical-scientific team. This includes understanding of the different therapy steps and evaluating their feasibility. He participates in the writing of the therapy procedures. He controls and validates the right functioning of the dose calibrator, the presence of the needed calibration factor (if not carries out the calibration), trains the staff involved in the sources measurement. Otherwise, in case of a new routine protocol, the medical physicist and physicians make sure that all the staff involved master the different steps of this treatment.
Once a protocol is in place and staff training is completed, the inclusion of patients can be realized. It is a multidisciplinary medical decision. The following steps can be divided into 3 parts: pre-treatment, the treatment itself and post-treatment.
Pre-treatment: This step includes biological blood tests and imaging necessary for treatment. If a dosimetry needs to be performed, most commonly it is done by the medical physicist. It has to be validated by both medical physicist and physician. The treatment day and the activity to be ordered are co-validated by radiopharmacists. The recommandation about the dose calibrator remains the same. The presence of the medical physicist, within the department or institution is highly recommanded.
Treatment day : On the day of treatment, the medical physicist validates the radioactivity measurement.
Post-treatment: This step may include hospitalization and patient monitoring, single or multiple imaging like PET-CT, SPECT-CT. Once again, the post-therapy dosimetry and its comparison with the pre-treatment dosimetry, is a step that needs a medical physicist and physician common validation. Finally, the medical physicist participates to the personnal recommendations to the patient while returning home.

Conclusions: The Internal Radionuclide Therapy implies the responsibilities of the medical physicist, whenever he intervenes in the treatment of a patient. The two major steps that engage his responsibility are the well functioning of the dose calibrator and, when is technically possible, the patient dosimetry. This last point, seems to become an essential step in the most of new Internal Radiation Therapy protocols.

Evaluation and optimisation of parametric reconstruction algorithms in FDG PET imaging

Z. Chalampalakis[a], S. Stute[a] ,T. Merlin[b], M. Filipovic[a], M. Playe[a], C. Wimberley[c] , C. Comtat[a]

[a]Service Hospitalier Frédéric Joliot, CEA (SHFJ) / Université Paris-Saclay / Orsay / France
[b]Laboratoire de Traitement de l'Information Medicale (LaTIM) / Université de Brest, Institut National de la Santé et de la Recherche Médicale : UMR1101 / Centre Hospitalier Régional Universitaire de Brest / IMT Atlantique Bretagne-Pays de la Loire / CHRU Morvan / Brest / France
[c]Edinburgh Imaging, QMRI, The University of Edinburgh (QMRI) / Edinburgh / Royaume-Uni

Introduction: Recently there has been an increased interest in whole-body dynamic PET protocols for parametric imaging, for better diagnosis and prognosis in oncology. The aim of this study is to evaluate and optimise dynamic (4D) reconstruction algorithms as opposed to standard static (3D) reconstruction algorithms for improved quantification and image quality of glucose metabolic rate parametric images for FDG PET data.

Methods: Nested Expectation Maximization algorithms [1] were developed within the open source reconstruction platform CASToR to enable dynamic parametric reconstructions. Namely, the Patlak linearisation model and a spectral model [2] were implemented. The Patlak model allows the direct reconstruction of the net influx rate Ki, from which the metabolic rate of glucose can be computed. The spectral model is more generic, with no strong assumptions on the underlying kinetic model, and effectively applies time-regularisation during reconstruction to the dynamic images. A dynamic FDG Head and Neck dataset acquired with the GE Signa PET/MR was used to evaluate performance, quantification and image quality of parametric Ki images. Traditional OSEM 3D Frame-by-Frame reconstructions were performed to compare against the 4D Patlak and 4D Spectral reconstructions. For the 3D and 4D spectral reconstructions, a pixel by pixel Patlak analysis was performed on the dynamic images. A Patlak analysis was also performed at the level of a volume-of-interest (VOI) covering a tumor in the Neck Area. An image derived input function was used for all the analysis.

Results: The estimated value of Ki for the tumor VOI is 0.00042 [1/s] for the 3D reconstructions (RMSE: 0.097), 0.00040 [1/s] for the spectral reconstruction (RMSE: 0.097) and 0.00041 [1/s] for the Patlak reconstruction. The parametric Ki images generated from each reconstruction show improved contrast for the tumor compared to the standard SUV image. In addition, the 4D Patlak and spectral reconstructions provide additional contrast improvement as well as reduced noise parametric Ki images (ROI CV of 0.55 and 0.58 respectively), compared to the 3D reconstruction (ROI CV of 0.66), as visually also seen in figure 1.

Conclusions: Dynamic PET reconstruction algorithms have been developed within the CASToR platform. They have proven to provide estimates of parametric Ki images with similar accuracy to the traditional indirect Patlak estimation from static frame reconstructions, and provide images with reduced noise. These properties are desirable in parametric imaging and it is sensible to pursue use of these algorithms in whole-body dynamic imaging, where data are more sparse and noisy.

Acknowledgements: This work has received funding from the EU's H2020 research and innovation program under the Marie Skłodowska-Curie grant agreement No. 764458.

References:

[1] PMB, 55(5), 1505–1517.

[2] IEEE Nuclear Science Symposium Conference Record, 5(1), 3260–3267

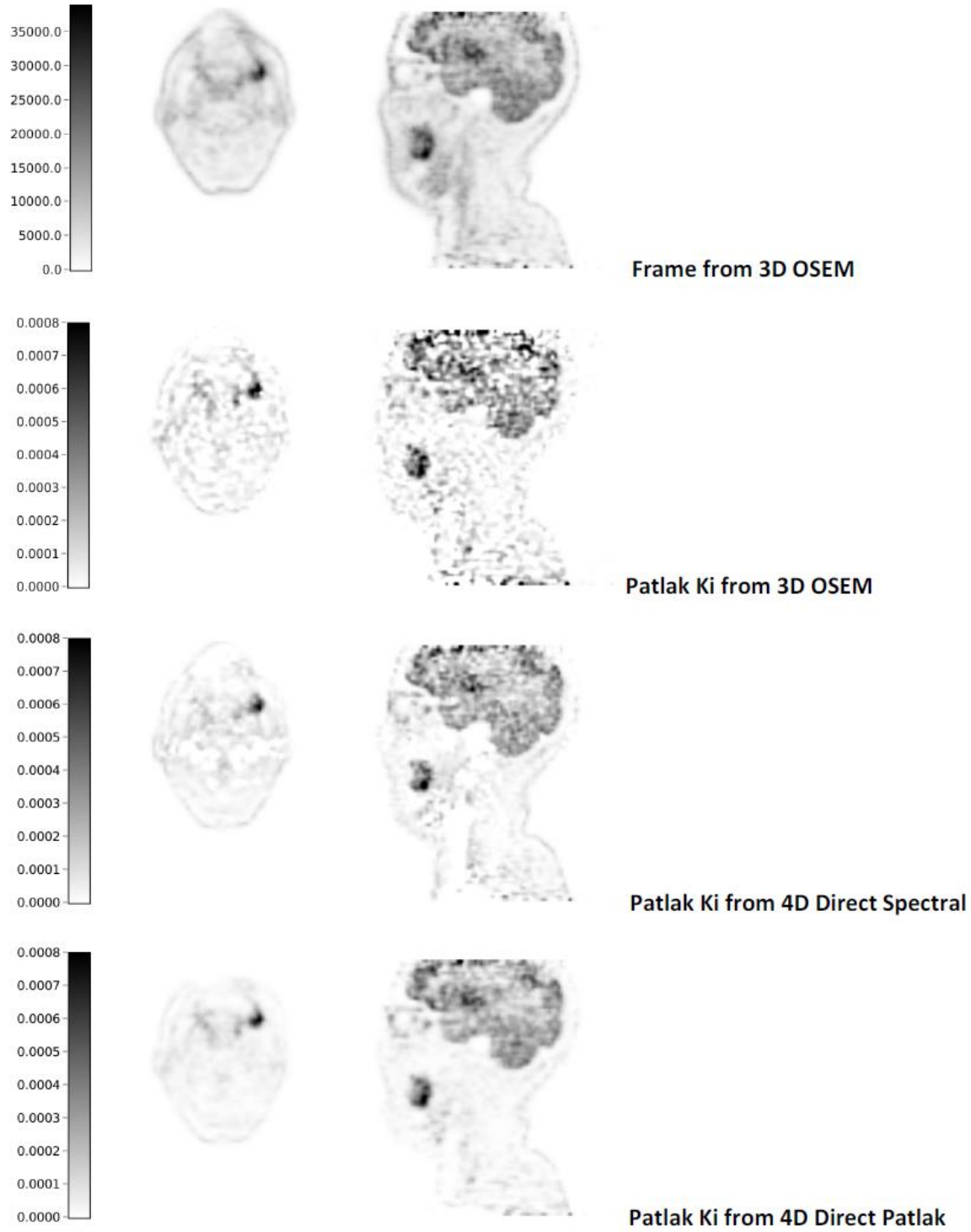

Figure1: Tumor axial and sagittal view of the last frame (duration of 5 min) and Ki parametric images from the evaluated methods.

Counterbalancing a change of acquisition time with reconstruction parameters on numerical PET
Contrebalancer le changement de temps d'acquisition avec les paramètres de reconstruction sur les TEP numériques

C. Jaudet[a], G. Foucras[a], K. Weyts[a], E. Quak[a], R. Ciappucini[a], C. Lasnon[a], A. Batalla[a], S. Bardet[a]

[a]Centre de Lutte Contre le Cancer François Baclesse / Caen / France

Introduction: New numerical positron emission tomography (PET) changes the physical properties of the detection chain[1]. We studied the relationship between acquisition time (Tacq) and reconstruction parameters on a VEREOS PET/CT camera. The aim of this study was to find the most appropriate reconstruction parameters to compensate for a modification of acquisition times in clinical settings.

Methods: We measured 5 phantoms with a signal to background ratio of 3, 4 and 6. A NEMA IEC and a Jaszczak phantoms with fillable spheres were used. The volumes of the spheres were ranging from 27 to 0.3ml. The images, with a Tacq ranging from 16s to 15min, were reconstructed with 1 to 4 iterations and 1 to 10 subsets. The standard images in our hospital are acquired with 2min per bed position and reconstructed with 2 iterations and 10 subsets. We characterized the image quality by the coefficient of variation (COV=standard deviation/ mean) in a region of interest in the background. Data fitting was performed with the statistical R software and a relationship between COV, Tacq, iterations and subsets was extracted. The entire plot had a R^2>0.99. A new set of images with a constant COV for different Tacq was then reconstructed. Detectability was measured by the difference between the maximum standardized uptake value in the sphere and the background for the new set. We then performed a comparison paired t-test of detectability between the new settings and the standard one.

Results: The COV showed an inverse square root relation with the Tacq, a feature typical of Poisson distribution. These curves varied for each iterations and subsets pair (itxsub) studied. The variation of COV was characterized and the following equation was found : COV= (5.4*itxsub+35.49) Tacq^(-0.5).A validation test of the adapted reconstruction parameter showed a COV of 0.13+/-0.1 for Tacq from 1 to 5min. The equation allowed to find the reconstruction parameters to keep a constant COV for different Tacq. The comparison of detectability distribution on the new sets compared to the standard images displayed a p-value of 0.091, 0.054, 0.043 for 1min45s, 1min30s, 1 min respectively. There was no significant difference of detectability between the standard acquisition of 2 min, 2 iterations and 10 subsets and a new set of 1m30s, 4 iterations and 4 subsets in this phantom study.

Conclusions: We characterized the relationship between acquisition time and reconstruction parameters and COV for a numerical PET. An equation was inferred and validated in phantoms to keep the COV constant while varying the acquisition time. The decrease of detectability is not significant with the new reconstruction, saving up to 30s per bed position, by changing the number of iterations and subsets in the reconstruction parameters.

References

1. Miller, Michael, et al. "Characterization of the vereos digital photon counting PET system." *Journal of Nuclear Medicine* 56.supplement 3 (2015): 434-434.

Multicentric performance assement of VERITONTM 360° CZT-camera compared to conventional Anger-cameras: a phantom study

K. Doyeux[a], E. Cassol[b], L. Imbert[c]

[a]Hôpital Bichat APHP, Department of Nuclear Medicine, Paris, France
[b]CHU de Toulouse, Department of Nuclear Medicine, Toulouse, France
[c]CHRU Nancy Hôpital Brabois, Department of Nuclear Medicine, Vandœuvre-lès-Nancy, France

Introduction: Cameras with CZT detectors constitutes a technological jump for SPECT imaging. Initially developed for dedicated cardiac cameras, this technology has been recently developed for all-purpose CZT-cameras. One of them, the VERITON camera (Spectrum Dynamics Medical), was installed last year in the hospitals of Toulouse, Nancy and Bichat. In the present study, these centers were associated to determine the performance of the VERITON CZT-camera, as compared to Anger-cameras, through analyses of phantom images.

Methods: Physical performances were compared between the VERITON camera and two Anger-cameras: the Discovery 670 (General Electric Healthcare) and Symbia T2 (Siemens Healthineers). 1) Tomographic sensitivity was determined with a cylindrical phantom filled-in with a solution of ^{99m}Tc. For each camera, this phantom was placed at the center of field of view and recorded using a body contouring mode. On the VERITON camera, additional recordings were obtained in a focus mode for which 80% of the projections may be recorded on an adjusted smaller volume of interest. Tomographic sensitivity was determined according to the number of counts recorded per second and it was expressed per MBq of the ^{99m}Tc solution. 2) Spatial resolution was assessed with the triple line insert and diffusing environment defined in the NEMA NU-1 2012 protocol. Horizontal and vertical profiles were generated for each line source on a median axial reconstructed slice. Central, tangential and radial resolutions were determined with the FWHM of gaussian fits. 3) Image quality was evaluated with a Jaszczak phantom filled-in with ^{99m}Tc and with the reconstruction parameters optimized for each camera. Contrast values were expressed for each sphere in % of the actual contrast with the formula: $(C_s - C_{BDF})/C_{BDF}$, where C_s and C_{BDF} are the mean counts values from respectively sphere and background.

Results: Tomographic sensitivities of the VERITON obtained without and with the focus mode were respectively of 100.9 and 127.6 cps/MBq, whereas lower values were obtained for Discovery 670 (60.8 cps/MBq) and Symbia T2 (73.1 cps/MBq). Central spatial resolution was also enhanced for the VERITON (< 5.0 mm), as compared with Discovery 670 (< 7.9 mm) and Symbia T2 (< 5.8 mm). Finally, the contrast coefficients of all spheres were higher with the VERITON than with the other cameras with for instance contrast values of 50.1% and 39.3% for the spheres of respectively 12.7 and 9.5 mm diameters recorded with the VERITON, whereas the corresponding values were 38.3% and 21.1% for Symbia T2. Additionally, contrast-to-noise ratio is higher for the VERITON when compared to the Discovery 670 (up to a factor 2.4 for the sphere of 12.7 mm diameter).

Conclusions: The performance of the VERITON CZT-camera is clearly higher than that of Anger-cameras, leading to consider that this camera should allow optimizing acquisition protocols and providing a significant gain for clinical routine.

Dosimetric impact of a less restrictive imaging schedule for patient dosimetry after 177Lu-DOTATATE evaluated by PlanetDose® workstation

Impact dosimétrique de la réduction du protocole d'imagerie pour les patients traités au ^{177}Lu-DOTATATE évalué par PlanetDose®

L.Pitalot[a], P.Gelibert[a], E.Deshayes[a], L.Santoro[a]

[a] Institut régional du Cancer de Montpellier (ICM), Montpellier, France

Introduction: The aim of this study was to implement the dosimetry workstation PlanetDose® (DOSIsoft) for the routine evaluation of absorbed doses to the organs at risk and the tumors during *Peptide Receptor Radionuclide Therapy* (PRRT) with ^{177}Lu and to evaluate the dosimetric influence of a less restrictive imaging schedule for patient dosimetry.

Methods: 21 patients with neuroendocrine tumors received 1 to 4 cycles of 7.2 ± 0.2 GBq of ^{177}Lu-DOTATATE. During cycles 1 and 2, SPECT/CT images were acquired at 4h, 24h, 72h and 192h after injection and reconstructed using the Xeleris software (General Electric). After the segmentation and the registration steps, a wide choice of interpolation methods to better fit the obtained time-activity data were evaluated: 3 positions of the time point T=0 intercept, 8 time-activity curve adjustments, and the possibility to take into account the physical decay after the last time point. The absorbed doses to organs at risk (liver, kidneys and spleen) and tumors were calculated and compared with time-activity curves fitted from 2, 3 or 4 imaging time points.

Results: Based on the ^{177}Lu-DOTATATE pharmacokinetics, the origin value for the time point T=0 was selected and a tri-exponential adjustment with physical decay after the last point was used for calculation of absorbed doses. The mean absorbed doses to the liver, kidneys and spleen were 4.19 Gy, 3.72 Gy and 4.96 Gy respectively after cycle 1 and 3.95 Gy, 4.12 Gy and 6.13 Gy respectively after cycle 2. The absorbed dose to tumors was 35.9 Gy after the first cycle and 26.2 Gy after the second one. A mean absolute difference of 8.5% was obtained between the absorbed doses to organs at risk calculated with 3 and 4 imaging time points and 4.3% between 2 and 4 time points. The concordance index was 0.994 between 3 and 4 imaging time points and 0.985 between 2 and 4.

Conclusions: The mean absorbed doses to organs at risk and tumors obtained with the determined settings on PlanetDose® workstation were in agreement with the literature data. We showed that a less restrictive imaging schedule can be considered with the 3 imaging time points 4h, 24h and 192h after injection.

Patient dosimetry after Peptide Receptor Radionuclide Therapy using 177Lu-DOTATATE: Comparison between two dosimetry software

Dosimétrie de patients après traitement de radiothérapie interne vectorisée au ^{177}Lu-DOTATE : Comparaison de 2 logiciels

L.Pitalot[a], D.Trauchessec[a], S.Chouaf[a], E.Deshayes[a], L.Santoro[a]

[a] Institut régional du Cancer de Montpellier (ICM), Montpellier, France

Introduction: ^{177}Lu-DOTATATE is used in peptide receptor radionuclide receptor (PRRT) to treat Neuroendocrine Tumors (NETs). The MIRD formalism is the most common method used to realize patient dosimetry. However several software packages are now available using Dose Point Kernel (DPK) and Local Deposition Method (LDM). It was shown that absorbed doses determined with LDM are in excellent agreement with those obtained using the MIRD and the kernel-convolution dose calculation approach in liver radioembolization[1]. The aim of the present study was to compare two different commercial dosimetry workstations in terms of residence times and absorbed doses to organs at risk.

Methods: 19 patients with neuroendocrine tumors received 1 to 4 cycles of 7.2 ± 0.2 GBq of ^{177}Lu-DOTATATE. During cycles 1 and 2, SPECT/CT images were acquired at 4h, 24h, 72h and 192h after injection and reconstructed using the Xeleris software[2] (General Electric). The liver, spleen and kidneys residence times and absorbed doses were calculated on the one hand with the Medical Internal Radiation Dose (MIRD) formalism using Dosimetry toolkit® (DTK) application and OLINDA/EXM® V1.0 software and on the other hand with Dose Point Kernel (DPK) and Local Deposition Method (LDM), using PlanetDose® (DOSIsoft). The segmentation, registration and dosimetry steps were carried out on PlanetDose® with parameters similar than those defined in DTK.

Results: Using PlanetDose®, a difference of 2% was obtained between the absorbed doses to organs at risk calculated with DPK and LDM respectively. The residences times obtained by LDM calculation using PlanetDose® and by the MIRD formalism using DTK showed a difference of -5% for liver, 6% for kidneys and 0.2% for spleen. In terms of the absorbed doses, the differences were: 2.9% for the liver, 7% for the kidneys and 10.3% for the spleen.

Conclusions: The absorbed doses to organs at risk obtained using the two workstations are concordant and in agreement with the literature. These results validate the use of PlanetDose® in clinical routine for patient dosimetry after targeted radiotherapy using ^{177}Lu-DOTATATE.

References

D'Arenzio, M.et *al.* Phantom validation of quantitative Y-90 PET/CT-based dosimetry in liver radioembolization. EJNMMI Res. 2017 Nov 28;7(1):94. doi: 10.1186/s13550-017-0341-9.

Santoro, L et *al*,.EJNMMI Res.Implementation of patient dosimetry in the clinical practice after targeted radiotherapy using [177Lu-[DOTA0, Tyr3]-octreotate**.** 2018 Nov 29.

Evaluation de la dose au sang en radiothérapie interne vectorisée de la thyroïde à l'iode 131 : expérience chez des patients dialysés

A. Talbot[a,b], L. Devos[a,b], C. Baillet[b], A. Beron[b], G. Lion[b], M. Vermandel [a,b]

[a]Unité de physique médicale, CHRU Lille, Lille, France
[b]Service de médecine nucléaire, CHRU Lille, Lille, France

Introduction : L'objet de cette étude est de présenter notre expérience dans la prise en charge des maladies thyroïdiennes dans le cas de patients dialysés. En effet, pour ces patients, l'élimination physiologique de l'iode 131 est beaucoup plus lente et la dose au sang, principal organe à risque exposé, est potentiellement plus élevée que pour les patients sans insuffisance rénale. Il est donc apparu pertinent pour ces patients d'évaluer de manière personnalisée cette dose afin de prévenir des effets indésirables potentiels. Notre étude porte sur 9 patients traités entre 2013 et 2019.

Méthodes : La méthode dosimétrique utilisée se base sur le formalisme du MIRD décrit dans la littérature pour les patients avec fonction rénale standard (Lassmann, 2008). Le sang est considéré comme la cible exposée par deux sources : les émissions betas de l'iode 131 présent dans le sang lui-même et les émissions gammas provenant du corps entier. La méthode nécessite d'évaluer les temps de résidence dans le sang et le corps entier. Pour cela, nous avons mis en place un protocole de mesures répétées pendant les 5 jours d'hospitalisation incluant des prélèvements sanguins et des acquisitions corps entier. Concernant ces dernières, plusieurs techniques ont été évaluées : scintigraphies corps entier antéro-postérieures, compteur thyroïdien à distance et compteur gamma suspendu en chambre d'hospitalisation. Les courbes de décroissance des fractions d'activité administrée en fonction du temps tenant compte des hémodialyses permettent d'évaluer les temps de résidence. Les facteurs S du MIRD nécessaires au calcul de dose sont issus de la littérature (Benua, 1962 – Stabin, 2005).

Résultats : Grâce à cette étude nous avons détecté un patient pour lequel la dose au sang a dépassé 2 Gy. Le suivi de ce patient n'a pas mis en évidence d'effets indésirables. L'expérience de ces mesures a permis de consolider dans notre service un protocole multidisciplinaire (médecin nucléaire, infirmier, physicien médical) reproductible et robuste appliqué dorénavant à tous les patients insuffisant rénaux pris en charge pour un cancer thyroïdien ou une hyperthyroïdie.

Conclusions : La méthodologie développée dans cette étude peut être facilement étendue à d'autres services d'irathérapie prenant en charge des patients dialysés. Cette démarche s'inscrit dans une politique plus générale de prévention des risques radio-induits et de radiovigilance.

RX1- Imagerie

Skin-dose mapping for patients undergoing interventional radiology procedures: Clinical experimentations versus a Dose Archiving and Communication System

A. Al masri[a,b], S. Carpentier[c], F. Leroy[d], S. battini[b], T. Julien[b], F. Maaloul[b]

[b]Polytech Lille/Lille/France
[b]BIOMEDIQA Groupe/Villeneuve d'Ascq/France
[c]Hopital Privé La Louvière/Lille/France
[d]INTERCARD/Lille/France

Introduction: During an 'Interventional Radiology (IR)' procedure, the patient's skin-dose may become very high for a burn, necrosis and ulceration to appear. In order to prevent these deterministic effects, an accurate calculation of the patient skin-dose mapping is essential. For most machines, the 'Dose Area Product (DAP)' and fluoroscopy time are the only information available for the operator. These parameters have been shown to be a very poor indicator of the Peak Skin Dose. We developed a mathematical model that reconstructs the magnitude, shape, and localization of each irradiation field on patient's skin. In case of critical dose exceeding, the system generates warning alerts. The reconstruction is based on the geometric and dosimetric information provided by the DICOM files for each acqusition incidence. We present the results of its comparison with clinical studies.

Methods: Two series of comparison of the skin-dose mapping of our model with clinical studies were performed. At a first time, clinical tests were performed on patient's phantoms. Gafchromic films were placed on the table of the IR machine under PMMA plates that simulate the patient. After irradiation, the film darkening is proportional to the radiation dose received by the patient's back. After film scanning and analysis, the exact dose value can be obtained at each point of the mapping. Four experimentation were performed, constituting a total of 34 acquisition incidences including all available exposure configurations. At a second time, clinical trials were launched on real patients during real 'Chronic Total Occlusion (CTO)' procedures for a total of 50 cases. Gafchromic films were placed on the back of the patients. Comparison on the dose values, distribution, and shape of the irradiation fields were performed.

Results: The comparison between the dose value shows a difference less than 15%. Moreover, our model shows a very high level of geometrical accuracy: all fields have the same shape, size and location (uncertainty < 5%).

Conclusions: This study shows that our software is a reliable tool to warn physicians when a high radiation dose is reached and then deterministic effects can be avoided.

Experimental evaluation of a dose management system-integrated 3D skin dose map by comparison with XR-RV3 Gafchromic® films

J. Greffier[1,*], N. Grussenmeyer-Mary[2], J. Frandon[1], J. Goupil[1], G. Cayla[3], B. Ledermann[3], A. Larbi[1], J.P. Beregi[1].

[1]Service d'imagerie medicale, CHU Nimes, Univ Montpellier, Medical Imaging Group Nimes, EA 2415, Nimes, France
[2]GE Healthcare, DoseWatch, R&D, Strasbourg, France
[3]Service de cardiologie, CHU Nimes, Univ Montpellier, Medical Imaging Group Nimes, EA 2415, Nimes, France

Introduction: To assess the interactive Skin Dose Map® (SDM) tool integrated to the Dose Management System DoseWatch® (GE Healthcare) with XR-RV3 Gafchromic® films for implementation in routine practice.

Methods: A post case non real time dose estimation software SDM tool was used to calculate PSD and display the patient skin dose distribution. PSD was calculated with a triangle mesh of 0.055cm² resolution on ICRP 110 anthropomorphic phantom and with a square ROI of 1cm² on flat phantom. The tool uses Radiation Dose Structured Reports (RDSR) data to model exposure events and calculate the PSD per event following recommendations defined by K. Jones et al. The PSD and SDM computed with SDM tool and displayed were evaluated in comparison with XR-RV3 Gafchromic® films positioned under the PMMA Phantom (20cm) for 13 configurations. Measurements were performed on a Philips system (Allura Xper FD10). Statistical analyses were carried out to compare PSD_{Film} and PSD_{SDM}.

Results: For the 13 configurations analyzed, the average difference between PSD_{Film} and PSD_{SDM} are 6%±6% (range from -3% to 22%) for flat phantom and 5%±7% (range from -3% to 25%) for ICRP phantom. The Lin's coefficient estimation and 95% CI are 0.979 [0.875; 0.984] for flat phantom and 0.977 [0.877; 0.985] for ICRP phantom), meaning that concordance was excellent between the measured PSD_{Film} and the computed PSD_{SDM} values. Dose map representations match for 11 out of 13 tests on PMMA Phantoms. Gaps identified are related to the table displacement during fluoroscopy events and the use of wedge filter.

Conclusion: The results found in this experimental evaluation show that SDM tool is a suitable alternative to Gafchromic® film to calculate PSD. A clinical evaluation on patients can be started in interventional radiology and cardiology.

Development and association of new metrics of dose and image quality for comparing and optimizing protocols in CT imaging

Développement et association de nouvelles métriques de dose et de qualité image pour la comparaison et l'optimisation de protocoles en imagerie scanner de diagnostic

A.C. Simon[a], N. Othman[a], G. Boissonnat[a], D. Lazaro[a], J.C. Garcia-Hernandez[a], L. Berteloot[b], D. Grevent[b], B. Habib Geryes[b], S. Gempp[c], J. Desrousseaux[c], E. Bigand[c], M. Benkreira[c], M. Vincent[c], S. Capdeville[c], J.M. Nigoul[c], B. Farman[c], E. Garnier[c], N. Nomikossoff[c]

[a]CEA, LIST/Gif-sur-Yvette/France
[b]Necker-Enfants Malades University Hospital/Paris/France
[c]Assistance Publique – Hôpitaux de Marseille/Marseille/France

Introduction: Nowadays, though Computed Tomography (CT) examinations only correspond to a small portion of medical imaging procedures (typically 10 % in France in 2012), they are credited with about 70 % of the total imaging collective dose. Reducing the dose due to CT examinations is therefore a major issue worldwide, but cannot be achieved at the expense of the image quality (IQ) needed to ensure a correct diagnosis.
Therefore, CT imaging needs to be described simultaneously using reliable metrics for delivered dose and IQ. However, such metrics are still lacking, especially for IQ. In this study, we developed and combined new metrics of IQ and patient dose in order to compare CT protocols.

Methods: For IQ evaluation, the mathematical model observer (MO) Non Pre-Whitening Eye filter (Burgess, 1994) was implemented to estimate a detectability index linked to clinical tasks such as lesion detection or discrimination. The index was calculated on CT images of a home-made dedicated phantom acquired for various irradiation and reconstruction conditions. It was then validated in the framework of a clinical study involving a dozen of experienced radiologists, on the large set on images presented in two Alternative Forced Choice (2-AFC) experiments for both tasks. After rescaling on their responses, the MO provided a Percentage of Correct answers (PC) depending on the acquisition parameters, the task and the insert size.
For dose estimation, a complete Monte Carlo model of the GE Discovery CT750 HD scanner was developed with the PENELOPE code. All the components of the scanner were estimated by physical measurements. The modelling was validated with measurements in CTDI and anthropomorphic phantoms using ion chambers and Optically Stimulated Luminescence dosimeters. Once validated, dose levels were calculated in the home-made torso-shaped phantom for every acquisition parameter used in the clinical study. Curves linking PC values calculated by the MO with the simulated dose in the phantom were then built for both detection and discrimination tasks. They thus enabled to represent the influence of irradiation or reconstruction parameters, such as voltage or reconstruction slice thickness.

Results: Values from several CT scanner standard abdominal protocols were placed on the curves after logarithmic regression and compared from the double point of view of dose and IQ. We could then deduce the better protocols in terms of reduced dose while keeping a close PC value. We showed for instance that, according to the clinical task, the patient dose could be reduced by a factor of two keeping a similar probability of correct answers by using a dual-energy protocol with adapted parameters.

Conclusions: This method paves the way for a standardized methodology enabling clinical physicists and radiologists to optimize protocols for defined clinical tasks while keeping the dose as low as possible.

RX3- Imagerie

Calculation of organ dose for pediatric patients undergoing computed tomography examinations: a software comparison

A. Al masri[a,b], N. Oubenali[c], S. battini[b], T. Julien[b], F. Maaloul[b]

[b]Polytech Lille/Lille/France
[b]BIOMEDIQA Groupe/Villeneuve d'Ascq/France
[b]Faculté d'Ingénierie et de Management de la Santé/Lille/France

Introduction: The increased number of performed 'Computed Tomography (CT)' examinations raise public concerns regarding associated stochastic risk to patients. Pediatric patients are more susceptible to radiation-induced risks than are adults owing to their rapidly growing tissues. We developed a Dose Archiving and Communication System that gives multiple dose indexes (organ dose, effective dose, and skin-dose mapping) for patients undergoing radiological imaging exams. The aim of this study was to compare the organ dose values given by our software for pediatric patients undergoing CT exams with those of another software named VirtualDose.

Methods: Our software uses Monte Carlo method to calculate organ doses for patients undergoing computed tomography exams. The general calculation principle consists to simulate: (1) the scanner machine with all its technical specifications and associated irradiation cases (Kvp, field collimation, mAs, pitch ...) (2) detailed geometric and compositional information of dozens of well identified organs of computational phantoms that contains the necessary anatomical data. The comparison sample includes the exams of thirty patients for each of the following age groups: new born, 1-2 years, 3-7 years, 8-12 years, and 13-16 years (a total of 150 patients). The parameters of the patients are very heterogeneous (various Kvp, mAs, Pitch, DLP, collimation …). The comparison protocol is the «Head» protocol.

Results: The percentage of dose difference between the two software does not exceed 20%. This difference may be due to the use of two different generations of hybrid phantoms by the two software.

Conclusions: This study shows that our software provides useful dosimetric information for pediatric patients undergoing CT exams.

Monte Carlo modelling of photon propagation in a human head model containing an enhanced-absorbing target

Modélisation par la méthode de Monte Carlo de la propagation des photons dans un modèle de tête humaine contenant une cible enrichie et absorbante

F. Vaudelle[a], J.P L'Huillier[a], M.L. Askoura[b]

[a]Univ Bretagne Loire, Ecole Nationale Supérieure des Arts et Métiers (ENSAM.), Laboratoire Arts et Métiers ParisTech Angers (LAMPA.)/Angers/France
[b]Radiation Therapy Department, Cliniques Universitaires St-Luc, Université Catholique de Louvain/ Brussel/Belgium

Introduction: Modelling the light propagation inside brain tissue structures is still a challenging task which requires the use of complex computational schemes often based on Monte Carlo method [1-3]. Because of strong tissue-scattering process (NIR infrared range: 600-900nm), deep probed structures receive much less light amount than the superficial tissues. This has the effect to impede optical measurements and efficient planning treatments. In this paper, we take an interest in noninvasive tissue arrangements for which a NIR light source strikes a human head model, and thus investigate how photons penetrate and interact with an enhanced-absorbing target located close to the CSF layer. The study especially aims at displaying the effects of tissue structure, optical properties, location and size of the inclusion, dye concentration and light source parameters on optical diagnostic and therapeutic treatment.

Methods: A 3-D Monte Carlo code was generated and adapted to the tetrahedral meshing [3] of a 3-D brain structure (Skull-bone, CSF, Grey matter and White matter layers). A spherical-absorbing target was located in the Grey matter or partially in the CSF layer. In a first step, time-resolved fluorescence measurements were analyzed in order to assess the depth location of the target. In a second step, the target absorption was enhanced by diffusing a dye with different concentrations, to create the requirements of the photodynamic therapy.

Results: Time-resolved spectroscopy measurements show the possibility to assess the depth location of the fluorescent target, whatever the concentration level of the dye (0.1-3µM). Moreover, the difference between specific mean arrival times (first moment <t>) are affected by scattering changes occurring in the CSF layer [1]. In case of continuous-wave illumination, the light delivery scheme may be optimized by playing on the source parameters.

Conclusions: Monte Carlo modelling of photon propagation inside a realistic 3-D human head model offers the possibility to develop and optimize optical diagnostic and therapeutic actions based on dye enrichment, in order to more characterize and treat various brain tissue injuries. Future investigations based on this computational tool will be reported.

References

1. Vaudelle F. and L'Huillier J.P. Time-resolved optical fluorescence spectroscopy of heterogeneous turbid media with special emphasis on brain tissue structures including diseased regions: A sensitivity analysis. *Opt. Comm.* **304** 161–168 (2013).
2. Mansouri C., L'Huillier J.P., Kashou N.H., Humeau A. Depth sensitivity analysis of functional near-infrared spectroscopy measurement using three-dimensional Monte Carlo modelling based magnetic resonance imaging. *Lasers in Med. Sci.* **25**, 431-438 (2010).
3. Fang Q. Mesh-based Monte Carlo method using fast ray tracing in Plücker coordinates. *Biomed. Opt. Express* **1** 165–175 (2010).

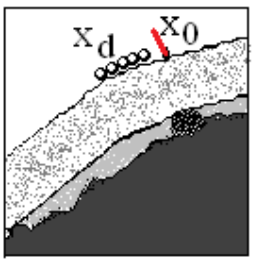

x_0: *pulsed laser source*

x_d: *detectors*

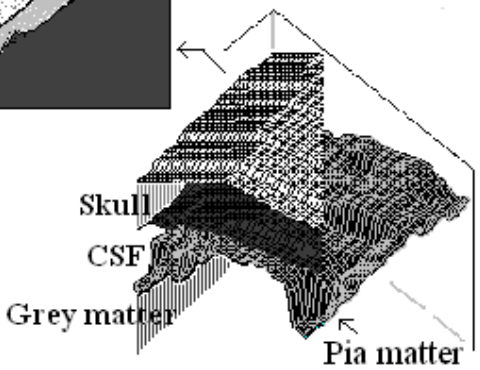

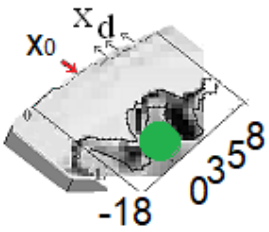

(Fang 2010)
Brainweb_Subject04

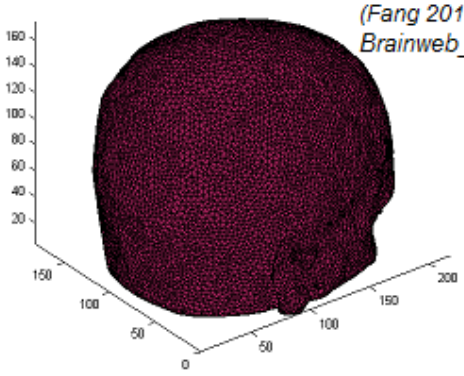

Continuous-wave laser source

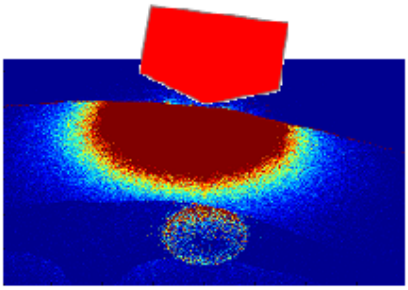

Set-up of a quality assurance program for 3T MRI images used in stereotactic radiotherapy (SRT) and radiosurgery (SRS)
Mise en place d'un programme d'assurance qualité des images IRM 3 Teslas utilisées pour la radiothérapie stéréotaxique (RTS) et la radiochirurgie (RCS)

J-B. Lacroix[a], V. Dedieu[a]

[a]Service de Physique Médicale et de radioprotection, Centre Jean Perrin, 58 rue Montalembert, 63011 Clermont-Ferrand, France

Introduction: Magnetic resonance imaging (MRI) is of particular interest for optimizing the contouring of target volumes and organs at risk, particularly for intracranial and pelvic localizations. However, MRI images suffer from specific artifacts and geometric distortions requiring the implementation of quality assurance (QA) program and the evaluation of MRI image quality impact on dose delivery and dose calculation, especially for radiosurgery techniques (SRS) or stereotactic radiotherapy (SRT). QA programs proposed by ACR or AAPM are used to monitor the quality of diagnostic radiology images, but are not suitable for checking the integrity, stability and spatial fidelity of the signal. The main objective of this study is to define a MRI image QA program that allows a fast, precise and reproducible control of the image parameters that have an impact on the dose delivery in SRT and SRS. The secondary objective is to highlight the limits and difficulties related to the QA of MRI sequences used in RCS and RTS.

Methods: A spherical MAGPHAN® SMR100 (The Phantom Laboratory) and the MRI acquisition protocols established for SRT and SRS were used. Imaging was performed by use of a 3T Discovery MR 750 (GE Healthcare) with a 16-channel head-neck-spin coil and a 3T Magnetom Vida (Siemens) with a 20-channel head-neck coil. The sequences used were 3D T1 SPGR (GE), 3D T1 MP-RAGE and 3D T2 Flair (Siemens). The methods applied to evaluate image quality parameters were based on those proposed by the ACR[1], AAPM[2], and MRI NEMA standards and were further adapted to the Magphan and to stereotaxic sequences characteristics.

Results: The parameters chosen for this QA program are: slice thickness, slice position, scan indexing, spatial linearity, signal-to-noise ratio, artifacts, uniformity, high-contrast spatial resolution and low contrast detectability. The positioning method developed for this study allow for a fast positioning (< 5min), reliable (tilt <0,5°) and reproducible (positioning with localizer images). For SPGR, the mean uniformity is equal to 95%, but it decreases up to 61% for 3D MP-RAGE and 51% for 3D Flair. Moreover, the thickness of the crossed thin-ramps is not appropriate for the measurement of millimeter slice profiles. The high resolution test plane does not provide an acceptable MTF curve. The 28 holes are not enough to obtain a 3D distortions map. Other results are within the limits fixed for this QA program.

Conclusions: This QA program allows the evaluation of geometrical limits of the applied sequences. With the appropriate methods, it is possible to performed a periodic quality control of the imager to verify its stability over time, to control possible drifts and to optimize the sequences in order to improve detection and contouring in SRT and SRS.

References

1. American College of Radiology MRI QC Manual (2015)
2. AAPM REPORT NO. 100, Acceptance Testing and Quality Assurance Procedures for Magnetic Resonance Imaging Facilities (2010)

Characterization of radiotherapy dedicated head and neck coils
Analyse des caractéristiques d'antennes tête et cou dédiées radiothérapie

P. Hinault[a,b], I. Gardin[a,c], F. Wiesinger[d] , C. Cozzini[d], P. Gouel[c], J.Poujol[b], P.Vera[a,c], D. Gensanne[e]

[a]LITIS (EA 4108), Université de Rouen Normandie/Rouen/France
[b]GE Healthcare/ Buc/France
[c]Département d'imagerie et de médecine nucléaire, Centre Henri Becquerel/Rouen/France
[d]GE Healthcare/Munich/Allemagne
[e]Département de radiothérapie, Centre Henri Becquerel/Rouen/France

Introduction: MR images acquired in treatment position are very useful in radiotherapy treatment planning to delineate target volumes and organs at risk. The use of standard receiving coils is not compatible with radiotherapy immobilization devices, thence manufacturers have developed dedicated flexible and mobile coils for acquisition in treatment position[1]. However, image quality may be affected according their positioning. The purpose of this work is to evaluate the performance in terms of image quality of a head and neck radiotherapy dedicated coil and to define the optimal set up.

Methods: This study is performed on a 1.5 T Optima MR450w GE®. The images of a homogeneous phantom filled with a paramagnetic solution are acquired by means of a 3D gradient echo sequence with two types of coils: a head & neck coil used for diagnosis and the dedicated radiotherapy coils available on our installation. As these latter are mobile, we studied the impact of their positioning on image quality, more particularly on the signal-to-noise ratio[2] and uniformity[3]. In addition, a study of geometric distortions was performed using the MAGPHAN® SMR170 phantom and the Artiscan® analysis software. The distortions were evaluated before and after the application of the 3D correction filter provided by the manufacturer.

Results: Radiotherapy coils have a signal-to-noise ratio (SNR) up to 2 times lower than the diagnosis coil, which results in a slightly lower image quality. This phenomenon is more marked as the distance (d) between the phantom and the position of the coils increases. For example, for distances of 1.2 cm and 2.4 cm, the decrease in SNR is 5 % and 10%, respectively. A 5% degradation of the SNR is also observed in the cranio-caudal direction at the junction zone between the head and sus-clavicular coils. Overall, distortions increase with the distance from the isocenter. The highest distortion obtained with radiotherapy coils before correction is 6.1 mm. When the correction filter is applied, the highest distortion obtained is 1.61 mm.

Conclusions: In the context of acquisitions in radiotherapy treatment position, this study has shown the importance of the positioning of dedicated coils to obtain optimal image quality for tumor delineation. Otherwise, signal loss and geometric distortions observed in some areas of interest can be very prejudicial to detect and delineate small and low-contrast lesions and consequently affecting the quality of radiotherapy treatment.

References

1. Liney, G. P. *et al.* Commissioning of a new wide-bore MRI scanner for radiotherapy planning of head and neck cancer. *Br. J. Radiol.* **86,** (2013).
2. Mcjury, M., Lawson, M., Page, W., Mcgrath, C. & Grey, A. Assessing the image quality of pelvic MR images acquired with a flat couch for radiotherapy treatment planning. **84,** 750–755 (2011).
3. Xing, A. *et al.* Commissioning and quality control of a dedicated wide bore 3T MRI simulator for radiotherapy planning. 1–10 (2016).

Posters - Radiothérapie

Évaluation de l'utilisation de l'outil iViewDose

V. Massaria[a], S. Guendouzen[a], A. Roque[a], N. Gaillot - Petit[a]

[a]Radiophysique Médicale/Reims/France

Introduction: Le logiciel iView Dose proposé par Elekta a été développé pour la dosimétrie in vivo et les contrôles pré-traitement en utilisant un algorithme de rétroprojection rapide qui fournit une reconstruction de dose dans le patient (ou fantôme) à partir des images EPID.

Méthodes: L'utilisation d'iViewDose a été testé en tant qu'outil de dosimétrie in-vivo et de contrôle pré-traitement (DQA) pour des traitements par radiothérapie conformationnelle (3D) du sein (calculé avec le TPS Oncentra MasterPlan®) et par arcthérapie dynamique (VMAT) de prostate (calculé avec le TPS Monaco® d'Elekta) sur l'accélérateur Elekta VERSA- HD®. Pour ce faire, une série de 30 patients traités à la prostate par VMAT et de 30 patientes traitées au sein par technique 3D conformationnelle a été étudiée. L'iViewDose n'étant pas compatible avec Oncentra MasterPlan®, les plans ont été transférés sur la station de calcul Monaco® puis recalculés. L'iViewdose réalisant sa reconstruction dosimétrique dans un milieu homogène (eau), chaque plan 3D du sein (constitué de poumon) a donc été recalculé sur le TPS dans l'eau.

Résultats: L'iViewDose est simple d'utilisation pour les traitements VMAT mais il n'est pas sans limites surtout pour les traitements 3D. L'indisponibilité de l'énergie X18 sur l'iViewDose est un frein majeur à son utilisation clinique à l'Institut puisque la majorité des traitements VMAT de prostate et les faisceaux tangentiels réduits du traitement du sein en 3D sont en X18. De plus, l'iViewDose ne permet pas la reconstruction dosimétrique des faisceaux qui s'enchaînent automatiquement à l'accélérateur en technique 3D, ni filtrés (cas du sein en 3D). Un autre problème se présente lorsque le champ de traitement dépasse le champ du panel (cas des traitements VMAT prostate + ganglions et 3D du sein mono-isocentrique) . En effet, lorsque le panel est décalé par rapport à son isocentre, l'iViewDose se recale systématiquement aux coordonnées de l'isocentre et ne prend donc pas en compte la dose en dehors du champ et crée des erreurs à ces endroits, ce qui ne permet pas une analyse pertinente. Or, il n'est pas possible de créer un rapport dosimétrique sur une région d'intérêt sélectionnée. Les traitements 3D nécessitent l'acquisition d'images de sortie pour chaque faisceau de chaque patiente, en pratique difficile à réaliser en raison de l'augmentation du temps de traitement du patient, l'analyse de la dosimétrie in-vivo s'effectuant après la séance de traitement.

Conclusions: Pour les traitements 3D, le temps machine dédié au contrôle pré-traitement est doublé par l'acquisition d'images de sortie et les contraintes sont trop nombreuses pour une seule localisation. Le logiciel iViewDose n'est pas adapté pour une utilisation en clinique pour ce type de traitement. Pour les traitements VMAT de prostate, nous n'avons pas rencontré de difficultés majeures si ce n'est l'indisponibilité de l'énergie X18 avec iViewDose.

Comparative study of the two respiratory monitoring systems for 4D-Computed Tomography

S. Dziri[a], F. Lafay[a], M. Ayadi[a]

[a]Léon Bérard Center Radiotherapy Department, France

Introduction: Respiratory monitoring systems are necessary for correlating the patient breathing signal with the Computed Tomography (CT) acquisition and for retrospectively sorted and reconstructed several phases of the 4D-CT. Two different external systems, AZ-733vi (Anzai), a pressure transducer, and Sentinel (C-rad), a surface imaging system, were installed on a Somatom Confidence CT scan (Siemens). Objectives of the study were: 1/ to evaluate the performance of the two different external surrogates in terms of signal analysis and 4D-CT image reconstruction, using a dynamic phantom, and 2/ to determine in which clinical situation one system is more suitable than the other.

Methods: Regular and irregular breathing patterns were used to compare the system performance. Three regular cos4 breathing curves were generated with the CIRS 4D phantom using three periods (5 s, 6 s, 7.5 s) and a 24 mm tumor motion amplitude in the SI direction. Irregular respiratory signals were also generated using a Matlab script. 4D-CT acquisitions of the moving phantom were performed, consecutively with each monitoring system, using the recommended Siemens protocol, based on the breathing period. For each acquisition, the 10 phases, the average and the Maximun Intensity Projection (MIP) images were reconstructed. Both systems were compared according time resolution, tumor motion amplitude and tumor volume accuracy, image profiles analysis. A fixed threshold was used for automatically delineating the tumor on the extreme phases images and on the MIP image. The tumor volume was compared to the theoretical one for each type of signal and monitoring system. Concerning the clinical part of the study, a qualitative analysis of 4D-CT images obtained on patients with one or the other system was performed.

Results: Preliminary results showed that AZ-733vi system had a better temporal resolution than the Sentinel system (25.0 ms vs 42.9 ms). Tumor amplitude deviations were up to 2mm and 4mm for regular and irregular breathing respectively. For regular breathing, the mean +/- SD absolute deviation of the tumor volume on the extreme phase was 1,6% +/-0,7% and 1,9% +/- 0,9% for AZ-733vi and Sentinel respectively. Concerning irregular breathing, this mean +/- SD absolute deviation was 4,5% +/-1,9% and 6,5% +/- 3,4% for AZ-733vi and Sentinel respectively.

Conclusions: According to these preliminary results, for regular breathing, the two systems gave similar results on tumor volume accuracy. Concerning irregular breathing, further comparisons should be done with patients-based breathing patterns. Clinically, Sentinel system advantages are the contactless measurement of the respiratory signal and the audio-caching feature. Further investigations will try to demonstrate if patients are more at ease with one system.

Dosimetric characteristics of VIPAR polymer gel for photon, electron and proton beams

V. Lagedamon[a], R. Gschwind[a], P.E. Leni[a], O.Bleuse[a,b], Y. Bailly[c], K. Laurent[c], J-M Rouvrier[a,d], M. Fromm[a], C. Grosperrin[a,d]

[a]UBFC/LCE UMR CNRS 6249, Montbéliard,France
[b]Radioterapeutická a onkologická klinika, Fakultní nemocnice Královské Vinohrady, Praha, République Tchèque
[c]UBFC/Femto-ST UMR CNRS 6174, Belfort, France
[d]HNFC, Service de radiothérapie, Montbéliard, France

Introduction: In the past few years, the development of complex radiotherapy techniques has led to the development of new dosimetric detectors based on gel, such as Fricke or polymer gels, to enhance quality control. They are able to provide 3D absorbed dose distributions with a good spatial resolution for photon radiotherapy treatment but additional studies are needed for protontherapy. The gel studied in this work must take into account the irradiation conditions and the reading mode. The great sensibility of VIPAR gel in high dose range [1,2] makes VIPAR gel a good candidate for proton irraditions (sensitive until 120 Gy).

Methods: Several studies details VIPAR gels [1,2,3]. They are composed of NVP monomers, Bisacrylamide crosslinkers, ultra-pure water, swine gelatin and additional molecules to prevent early polymerization of monomers. All samples have to be prepared 24h before irradiations and are produced under strict atmospheric condition (full of azote) to avoid impact of oxygen on gels. Then, gel dosimetric characteristics have been evaluated for the different process described as follow :
- 6X photon beams and 12 MeV electron beams provided by a Clinac 2100C of the Nord Franche-Comté hospital under reference conditions. The dose range used is 2 to 60 Gy with a constant dose rate of 400 UM/min [1].
- 3,5 MeV proton beam delivered by a Van de Graaff accelerator at Strasbourg University with an intensity of 10 nA and dose range of 8 to 80 Gy.
After irradiation (between 12 to 24h), the gels are analysed using the new optical approach developed by the laboratories [4,5]. Based on the relation between polarization ratio and absorbed dose, this system allows for determining 3D absorbed dose distribution with a high spatial accuracy of 1 micron.

Results: According to the first experiments, the stability of VIPAR gel is constant without pre-polymerization effect and gel response depend of modifications in gel composition. Experimental dose distributions are compared with Monte-Carlo simulations from GEANT4/GATE code [6]. For the photon part, a comparison of dosimetric characteristics of VIPAR gel with previous nMAG results [4] is done.

Conclusions: VIPAR gels have a great potential in photon external radiotherapy. However, additional studies are needed to evaluate LET dependency of the new VIPAR formulation in proton therapy when the LET value is higher than 4,75 keV/µm [7].

References:
1. Kozicki *et al.* On the development of a VIPARnd radiotherapy 3D polymer gel dosimeter. J. Phys. Med. Bio. 60 986 (2017).
2. Kozicki *et al*. On the development of the VIPAR polymer gel dosimeter for three-dimensional dose measurements. J. Macromol. Symp. 254, 345-352 (2007).
3. Papoutsaki *et al*. Dosimetric characteristics of N-vinylpyrrolidone based polymer gels : utilization depending on dose range. J. Phys.: Conf. Ser. 444 012068 (2013).
4. O. Bleuse, R Gschwind, Y. Bailly, K. Laurent, H. Bartova, K. Pilarova, V. Spevacek, L. Makovicka, 3D Dosimetry based on a new optical approach for dosimetry gels: use of the polarization ratio of the scattering light, Journal of Physics – Conference Series 847 (2017)
5. Bleuse O., Bailly Y., Gschwind R., Makovicka L., Laurent K., Guermeur F., Dispositif de mesure optique par lumière polarisée de doses d'irradiation absorbée par un gel dosimétrique, Dépôt de brevet FR 17 58268 (07/09/2017)
6. Jan et al. GATE V6 : a major enhancement of the GATE simulation platform enabling modelling of CT and radiotherapy. Phys. Med. Biol. 56 881 (2011)
7. Gustavsson *et al*. Linear energy transfer dependence of a normoxic polymer gel dosimeter investigated using proton beam absorbed dose measurements. J. Phys. Med. Bio. 49 3847 (2004).

Algorithme préconfiguré « Analytical Anisotropic Algorithm » utilisé pour la nouvelle machine Halcyon™ : validation de l'assurance qualité patients pour les techniques RCMI et AVMI

D. Nguyen[a], C. Sporea[a], R. Selabi[a], F. Josserand Pietri[a] , G. Largeron[a], M. Khodri[a]

[a]ORLAM / Villeurbanne-Lyon-Macon / France

Introduction : L'Halcyon™ (Varian Medical Systems) est un accélérateur linéaire de dernière génération mono-énergie (X6 FFF) que nous avons installé dans nos centres. C'est un nouveau système entièrement préconfiguré dédié aux techniques de traitement RCMI/AVMI. L'algorithme « Analytical Anisotropic Algorithm » v15.6 (AAA) a été préconfiguré pour permettre le calcul de doses délivrées aux patients. Il est également utilisé pour prédire la dose dans l'EPID pour l'assurance qualité (AQ) prétraitement des patients pour les techniques RCMI et AVMI. La personnalisation de la modélisation du faisceau n'est pas possible pour cet appareil. L'objectif de ce travail est de valider l'algorithme AAA utilisé à la fois pour générer les matrices de dose et le système Varian Portal Dosimetry (VPD) par rapport aux systèmes d'assurance qualité standard, afin de l'utiliser pour l'assurance qualité de routine.

Méthodes : Les données dosimétriques ont été collectées à l'aide de l'Halcyon 2.0 avec: la matrice de diodes 2D MapCHECK2 ™ (Sun Nuclear), la matrice de chambres d'ionisation MatriXX (IBA) et la dosimétrie portale VPD (Varian). Tous les calculs ont été réalisés dans le TPS Eclipse V15.6 avec l'algorithme AAA. Pour notre étude, nous avons généré : les 26 lettres de l'alphabet avec l'outil pinceau, 7 fentes glissantes (2, 4, 6, 10, 14, 16, 20 mm), 10 plans de traitement RCMI des cancers du sein, 15 plans de traitement VMAT (5 SBRT, 5 têtes et cous, 5 seins avec ganglions). Pour l'analyse, les fluences mesurées avec les matrices MapCHECK2 ™ et MATRIXX ont été comparées aux cartographies de dose calculée du TPS (AAA V15.6), avec les logiciels associés et les fluences prédites par VPD (AAA V15.6).

Résultats : Concernant les lettres de l'alphabet et les fentes glissantes, pour chacun des trois détecteurs, une analyse gamma 2%/2mm a été effectuée en global avec un seuil de 5%, puis local avec un seuil de 10%. Les taux moyens sont présentés ci-dessous :
MapCheck2 : γglobal = 99,04 ± 2,47% et γlocal = 98,82 ± 2,47%
Matrixx : γglobal = 99,66 ± 0,42% et γlocal = 99,11 ± 0,83%
VPD : γglobal = 99,18 ± 3,73% et γlocal = 99,15 ± 3,75%
Pour les plans de traitement des cancers du sein avec technique RCMI, les taux de réussite moyens de l'évaluation gamma local étaient de 99,9 ± 0,28% et 99,9 ± 1,68% pour la VPD, et de 99,56 ± 0,65% et de 97,49 ± 1,86% pour MapCheck2, respectivement pour les critères 3% / 3 mm et 2% / 2 mm (seuil de 10%). Pour les cas VMAT, les taux de réussite moyens de l'évaluation gamma local étaient de 99,23 ± 1,01% et de 98,14 ± 1,42% pour la VPD, et de 99,56 ± 0,65% et de 97,49 ± 1,86% pour la MATRIXX d'IBA, respectivement pour les critères 2% / 2 mm et 1% / 2 mm (seuil de 10%).

Conclusion : La modélisation de faisceaux AAA préconfigurée donne de très bons résultats et est proche des détecteurs indépendants. Elle semble assez robuste pour être utilisée dans le contrôle qualité de routine sans qu'il soit nécessaire de la personnaliser.

Rapidarc commissioning implementation in routine for six Halcyon™ and multicenter analysis using ARTISCAN™ (AQUILAB)

Implémentation du rapidarc commissioning en routine clinique sur six machines Halcyon™ et analyses multicentriques avec le logiciel ARTISCAN™ (AQUILAB)

R. Selabi[1], D. Nguyen[1], E. Da Eira[1], F. Bogalhas[1], S. Fafi[1], M. Khodri[1]

[1]Radiotherapy ORLAM/Lyon-Mâcon/France

Introduction : Le RapidArc Commissioning (RC) est une série de contrôles permettant d'évaluer les performances des appareils délivrant des traitements VMAT (Ling et al, 2008). Les paramètres testés en mode dynamique concernent le MLC (vitesse et positionnement des lames), la vitesse de rotation du bras et la variation du débit de dose. Les différences entre les appareils Halcyon (Varian Medical Systems) et les accélérateurs linéaires classiques notamment au niveau du MLC, des paramètres géométriques et mécaniques confortent davantage la mise en place du RC pour ces appareils. Cela nécessite la validité des contrôles en mode statique du MLC, du bras et la calibration de l'imageur portal. L'automatisation de l'analyse du RC permet de faciliter son implémentation en routine clinique.

Méthodes : Le RC a été réalisé sur les 6 appareils Halcyon répartis sur 4 sites. Les irradiations sont faites à partir des fichiers DICOM-RTPlan fournis par VARIAN, sans interposer de la table de traitement entre la source et l'imageur portal. Les images acquises sont analysées avec le logiciel ARTISCAN qui possède un module spécialement développé pour tenir compte des spécificités du MLC des appareils Halcyon. Les analyses automatiques sont faites suivant la méthode proposée par Ling et al. Les contrôles réalisés sont les suivants :

- Picket fence : il est fait à bras statique, en rotation puis avec introduction des erreurs dans la position des lames.
- Contrôle dosimétrique dynamique : une dose est délivrée pour un champ rectangulaire formé par le MLC en mode dynamique pendant l'irradiation et ce aux 4 positions cardinales du bras. L'intensité moyenne des pixels dans la zone irradiée doit être identique pour les 4 champs.
- Variation du débit de dose : Sur une rotation du bras à vitesse constante, le débit varie à certains angles pour délivrer la même dose à 7 fentes définies par le MLC en mode dynamique. Les images sont normalisées par rapport à un champ ouvert pour s'affranchir de la symétrie et de l'homogénéité du faisceau.
- Vitesse de rotation du bras : même principe avec variation la vitesse de rotation du bras à débit de dose constant.
- Vitesse des lames : même principe avec différentes combinaisons vitesse des lames/débit de dose, à vitesse de bras constante.

Résultats : Les résultats sont présentés au format suivant :
Paramètre évalué : moyenne sur les 6 Halycons des moyennes des pixels dans les ROI [écart relatif min ; écart relatif max]

- Picket fence : satisfaisant avec détection des erreurs pour toutes les machines
- Contrôle dosimétrique dynamique : 0,13 [-2,58% ; 4,25%]
- Variation du débit de dose : 0,14 [-0,47% ; 0,51%]
- Vitesse de rotation du bras : 0,14 [-0,29% ; 0,36%]
- Vitesse des lames : 0,03 [-0,44% ; 0,53%]

Conclusion : Après validation des résultats pour chaque machine, l'analyse multicentrique sur les 6 halcyons est satisfaisante avec très peu d'écart sur les différents paramètres évalués.

Maitrise des procédés des traitements par modulation d'intensité (Indice de complexité)

S. Jan [a,b], D. Lebhertz[b], F. Ravaud[b]

[a]Institut de cancérologie de l'Ouest / Saint-Herblain / France
[b]Institut inter-régional de Cancérologie / Le Mans / France

Introduction : Les traitements en modulation d'intensité engendrent une augmentation de la complexité du plan de traitement. Il est souvent difficile de qualifier la complexité des plans de traitement et de les comparer entre eux. L'objectif de cette étude est de pouvoir calculer des indices rendant compte de cette complexité.

Méthodes : Cette étude, réalisée avec le TPS Eclipse, sera composée de deux phases : l'une de recherche et de validation des indices de complexité et l'autre de comparaisons de 50 plans de traitements avec les indices précédemment validés.
Six indices de complexité, issus de la littérature ou construit par nous-même, sont comparés pour plusieurs plans de traitements. Chaque indice prend en compte une caractéristique physique du traitement, comme la vitesse des lames, la taille de la pénombre, l'ouverture des lames, l'irrégularité d'ouverture, etc. La comparaison des indices de complexité est réalisée sur 8 plans de traitements IMRT pour 2 localisations différentes, la prostate et l'ORL. Pour chaque localisation, 4 niveaux de complexité sont artificiellement créés, allant d'un traitement en RC3D jusqu'à un traitement en RCMI avec une optimisation poussée au maximum.
L'étude systématique est réalisée sur 50 patients, toutes localisations confondues. Les indices de complexité seront comparés à l'indice MCSv qui est retrouvé dans la littérature1 et donc pris comme référence. La concordance entre les deux indices a été évaluée ainsi qu'une comparaison des indices en fonction de la localisation.

Résultats : Les six indices de complexités créés respectent l'ordre de complexité des plans tests. On remarque que les indices qualifiant l'accélération ou l'irrégularité des lames sont très peu étalés (0.7 à 1) par rapport à ceux qualifiant l'ouverture de lame ou la pénombre (0.2 à 1).
Concernant l'étude systématique, nos indices de complexités « maison » sont concordant avec l'indice MCSv de la littérature. L'étude en fonction de la localisation montre une complexité plus élevée pour les plans ORL par rapport aux plans de prostate (environ 0.2 point d'écart).

Conclusions : Nous avons pu vérifier que nos 6 indices mettent bien en évidence la complexité du plan de traitement avec un étalement de 0.2 pour un plan très modulé à 1 pour un plan sans modulation pour pouvoir différencier les plans de traitements en fonction de leur complexité. L'étude systématique montre que les plans ORL sont plus complexes que les plans prostate.
Pour poursuivre cette étude, il faudrait estimer la corrélation entre l'indice de complexité et les résultats des contrôles qualités, pour pouvoir éliminer en amont les plans trop complexes et s'affranchir de contrôles qualités pour les plans très simples.

References
1. McNIven et al., A new metric for assessing IMRT modulation complexity and plan deliverability, Med Phys. 37, 505-515 (2010)

Characterization of a scintillation dosimetry system for in vivo dose verification in brachytherapy
Caractérisation d'un nouveau détecteur à scintillation pour la dosimétrie in-vivo en curiethérapie

F. Courrech[a], E. Meknaci[a], E. D'Agostino[b], V. Marchesi[a]

[a]Department of Medical Physics, Institut de Cancérologie de Lorraine, Vandoeuvre-Lès-Nancy, France
[b]DoseVue N.V., Agoralaan Abis, 3590 Diepenbeek, Belgium

Introduction: In vivo dosimetry allows detection of potential treatment errors. In brachytherapy, the presence of high-gradient dose distribution and potentially large dose rate depending on the type of source imposes new challenges for in vivo dosimetry. The aim of this work is to characterize a new scintillation detector for this type of measurement.

Methods: DoseVue has developed a new scintillation detector connected to an optical fiber. Measurements of characterization of the scintillator were carried out: reproducibility, linearity, correlation with the dwell time of the source. A homemade phantom was designed to deliver the dose by 4 catheters arranged around the detector. Errors were simulated on a phantom to establish the impact of a longitudinal positional deviation (or distal positional deviation) or radial movement of the catheter. These detector sensitivity measurements were performed on a high dose-rate (HDR) projector (Elekta).

Results: In a configuration delivering a homogeneous dose, a reproducibility of 0.2% has been found. Good linearity was obtained for position dwell times of 0.2s to 13.7s corresponding to a simulation of doses ranging from 10cGy to 700cGy with a correlation coefficient of 1.00. Regarding the detector's time response, dwell times by catheters showed a mean deviation of 0.12% from dwell times planned (mean time by catheters is 87.2s).
The system has shown good sensitivity in detecting longitudinal or radial movement of the catheter.

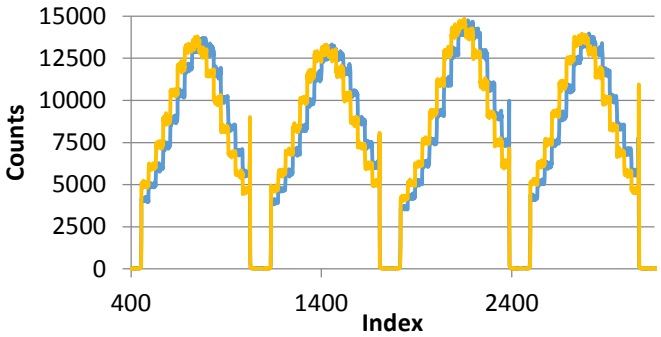

Example of detection of a longitudinal systematic shift of 5 mm of the dwell positions for an irradiation with 4 catheters (15 stop positions) using a HDR source (yellow curve: no shift, blue curve: signal obtained with the offset).

Conclusions: The small size of this new scintillator-based detector, with insertion into 6F tubes, and instant response with good reproducibility in phantom, offers possibilities for a new patient study for in vivo brachytherapy dosimetry. Real-time in vivo dosimetry could be used to provide geometric information on catheters during treatment.

Mise en place et utilisation du Module Artiscan Dynamique d'Aquilab® sur les accélérateurs Elekta®

J.M. Ponsin[a], F. Gassa[a]

[a]Centre Léon Bérard/Lyon/France

Introduction : L'irradiation avec Modulation d'intensité Volumétrique par ArcThérapie (VMAT) est de plus en plus présente et utilisée pour les traitements de radiothérapie. Cette étude a pour objectif la mise en place d'un contrôle dynamique du MLC grâce à l'utilisation du Module Artiscan Dynamique.

Méthodes : Ce module permet l'analyse des acquisitions réalisées grâce à l'imageur portal :

- Des images de fentes glissantes permettent de vérifier la stabilité de la vitesse des lames et l'influence de la gravité aux 4 angles cardinaux du bras.
- Les images de Picket Fence statique sont utilisées pour contrôler le positionnement et la vitesse de chaque lame aux 4 angles cardinaux du bras.
- Le Picket Fence VMAT sans et avec erreur permet de vérifier le positionnement et la vitesse de chaque lames lors de la rotation du bras ainsi que les erreurs introduites volontairement.
- Un contrôle permet également de vérifier l'uniformité du débit et de la vitesse de déplacement du bras en mode VMAT.
- Une acquisition est réalisée en mode Vmat, le bras tourne à vitesse constante mais le débit et la vitesse de déplacement des lames augmentent.

Les images des tests étant normalisées par le logiciel de l'imageur, ces dernières doivent être corrigées du pixel factor afin de convertir les niveaux de gris en valeur d'unité calibrée. Ce pixel facteur, différent pour chaque image, est nécessaire à l'analyse par Artiscan.
Dans une première version, certains tests étaient altérés par la non prise en compte de la réponse de l'imageur (effets de bords). Une nouvelle version introduisant une normalisation de chaque image test à une image de référence a été développée et mise en test au CLB.

Résultats : Des analyses de répétabilité et de reproductibilité ont été effectuées afin de valider la robustesse du contrôle. L'introduction d'erreurs connues dans les tests a permis de tester les performances de cette nouvelle version. Une étude a également été menée sur le pixel factor afin d'étudier son évolution et son impact sur les résultats obtenus. (Résultats en cours de finalisation)

Conclusions : Beaucoup plus robuste, cette nouvelle version désormais validée cliniquement sera déployée sur l'ensemble des accélérateurs du service.

Dosimetry audits in advanced techniques of radiotherapy – feedback on Equal-Estro experience in Tomotherapy

L'audit dosimétrique externe des techniques avancées de radiothérapie – retour d'expérience Equal-Estro en tomothérapie

A. Veres[a]
[a]Equal-Estro Laboratory, Villejuif, France

Introduction: Equal-Estro laboratory (EQUAL) has been accredited since 2004 for the dosimetry audits of radiotherapy systems in France. Until today, more than 9000 therapy beams, photons and electrons, have been tested using a remote TLD method [1-3], within a mandatory audit program of beam calibration parameters [4].
Like other national or international auditing bodies [5-7], EQUAL has developed and made available for more than 10 years novel methodologies designed for dosimetry audits of advanced radiotherapy techniques and treatment machines. It mainly concerns IMRT, VMAT, Tomotherapy and CyberKnife systems.

Methods: For advanced techniques of radiotherapy, EQUAL provides end-to-end dosimetric tests by means of phantom irradiation. The 2D images of film, irradiated in the phantom, are compared to TPS plans. TLDs are used for beam output tests, being irradiated separately form the phantom, in reference conditions.

Results: During the past five years, from 2014 to the end of 2018, 43 end-to-end tests were performed on Tomotherapy systems in France. It appears that in this period, some of the treatment units were audited more than once.
The reference beam output tests, using TLD measurements, show dose deviations in the acceptable range for all tested units.
Concerning film measurements, for more than 70% of tested units, the passing rate of gamma test is higher than 95%, for 5%-3mm gamma parameters. However, the film tests show acceptable results for over 98% of cases.

Conclusion: Starting with 2019 the tomotherapy end-to-end test is proposed with more restrictive acceptability criteria for films.

References

1. Derreumaux, S. et al., *A European quality assurance network for radiotherapy: dose measurements procedure*. Phys. Med. Biol. 40(7), 1191-208 (1995);
2. Marre, D. et al., *Energy correction factors of LiF powder TLD irradiated in high energy electron beams and applied to mailed dosimetry for quality assurance networks*. Phys. Med. Biol. 44, 3657-3674 (2001);
3. Ferreira, I. H. et al., *The ESTRO –QUALITY assurance network (EQUAL)*. Radiother. Oncol. 55, 273-284 (2000).
4. Dutreix, A. et al., Quality control of radiotherapy centres in Europe: beam calibration. Radiother Oncol. 32(3), 256-64 (1994);
5. Lehmann, J. et al., Dosimetric end-to-end tests in a national audit of 3D conformal radiotherapy, PhIRO (6) 5–11 (2018);
6. Pasler, M. et al., Novel methodologies for dosimetry audits: Adapting to advanced radiotherapy techniques, PhIRO (5) 76–84 (2018);
7. Clark, C. et al., IAEA Supported National "End-to-End" Audit Programme for Dose Delivery Using Intensity-Modulated Radiation Therapy through On-Site Visits to Radiation Therapy Institutions, Draft Document (2018).

Dosimetric measurements with Gafchromic EBT-3 films for the new 50kV Papillon+ intraoperative therapy system

Mesures dosimétriques par films Gafchromiques EBT-3 pour le nouveau système de radiothérapie per-opératoire Papillon+

C.Colnard-Hofverberg[1*],M.Gautier[1*], C.Dejean[1], J.Feuillade[1], L.Burgaud[1], A.Mana[1], B.Lhomel [1], J.Hérault[1]

[1] Centre Antoine Lacassagne/Nice/France

Introduction: The Papillon+ system is a mobile kilovoltage X-ray unit for Contact Radiotherapy with a high dose-rate delivery. The first prototype was acquired by Centre Antoine Lacassagne, in Nice France. It is operated at 50kV for partial breast intra-operative irradiation using spherical applicators of diameters between 30 and 50mm. The dose-rate at the applicators surface ranges from 10 to 46Gy/min. Methods have been developed for Commissioning and Quality Assurance prior to integration in the clinical practice. A feasibility study is presented here for using Gafchromic EBT-3 films as a tool for absolute and relative dosimetry and to assess their utility for in-vivo dose verification during treatment with the Papillon+ unit. The procedure which has been developed for handling and analyzing the films is discussed.

Methods: A Gafchromic EBT-3 films lot has been calibrated against an independent 50kV X-ray device to determine the dose calibration curve between 0 and of 30 Gy as the standard prescription dose for partial breast intraoperative therapy is 20 Gy. Absolute dosimetry was carried out with the calibrated film lot and compared with measurements using a PTW 0.02cm3 soft X-ray chamber type 23342 for validation. Homogeneity of the irradiation was estimated by using strips of films placed around the spherical applicators, on the equator as well as on the frontal side horizontally and vertically. Depth dose profiles for all applicator sizes have been acquired in a water tank with pieces of films parallel to the beam central axis. The same measurements were also made with a dedicated Ultem phantom in water and in air for comparison and to determine the effects of photon backscattering. Handling of the films was done following recommendations from the AAPM TG-55 report. Films have been digitized with an Epson 10000XL flatbed scanner and analyzed with the FilmQA-Pro software using a “One-Scan” protocol that employs two reference films to re-scale the calibration function. The green color channel was chosen for data processing because of the high dose range that is considered.

Results: Absolute dose measurements with Gafchromic EBT-3 films are in accordance with ionization chamber values. The irradiation at the breast applicators surface is homogeneous with a relative standard deviation less than 3%. Percentage depth dose measurements made in water improve with increasing applicator size. The dose at 10mm is 39.9%, 37.46%, 33.4%, and 26.25% of the dose at the applicator surface for diameters of 50, 45, 40 and 35mm, respectively. Depth dose measurements with the phantom in air showed the importance of the backscatter factor at the considered beam quality.

Conclusions: Gafchromic EBT-3 films are reliable for dosimetry at 50kV with the Papillon+ system. A reproducible and accurate method has been developed that uses Gafchromic EBT-3 films for dose measurements at commissioning and during quality assurance tests. This procedure is now used in the clinic for in-vivo dosimetry during partial breast intraoperative irradiation with the Papillon+ unit.

Evaluation of the image quality for Head & Neck (H&N) protocol in radiotherapy using a Dual Energy Computed Tomography (DECT) system

D. Agred[a], F. Lafay[a], G. Beldjoudi[a]

[a]Centre Léon Bérard / Lyon / France

Introduction: With conventional computed tomography (CCT), materials with various chemical compositions could be represented with similar Hounsfield units (HU). Dual Energy Computed Tomography (DECT) brings additional information about linear attenuation coefficient of materials. The recent acquisition of a CT scan Siemens Somatom Confidence RTPro20 in our radiotherapy department allows to acquire dual spirals at two different voltages, 80 and 140kV, and to reconstruct virtual monochromatic CT images ranging from 40 to 190keV. The objective of this study is to evaluate the image quality of DECT acquisitions for an H&N protocol and to compare the results with the ones obtained for the CCT H&N protocol, at 120kV, clinically used in radiotherapy.

Methods: DECT acquisitions were performed with the Catphan600 phantom by using acquisition parameters that give similar CTDIvol to the one obtained with the conventional H&N protocol at 120kV. Reconstruction parameters of DECT acquisitions were investigated by reconstructing monochromatic CT sets at energies ranging from 40 to 190keV by 5keV steps. The impacts of both reconstruction filter (from Qr32 to Qr49) and reconstructed slice thickness (1, 2 and 3 mm) on image quality were as well investigated. Image quality was quantified by the use of the Contrast to Noise Ratio (CNR) and the spatial resolution (SR).

Results: For a given combination of reconstructed slice thickness and filter, DECT monochromatic reconstruction gives a maximum CNR at energies ranging from 65 to 70keV depending on the considered material in the Catphan600. SR is optimal at 66 keV and is worst at other energies.
At 66keV, the reconstruction filter Qr49 (the hardest) allows to obtain a SR of 9 lp.cm-1 whereas the SR is of 6 lp.cm-1 for the Qr43 and Qr40 and worst for softer filters. However, at 66 keV, the filters Qr40 and Qr43 produce a greater CNR of respectively 101.0 ±2.5% and of 35.4 ±1.1% with respect to the Qr49 filter.
Monochromatic images at 66keV with the Qr40 filter at different slice thicknesses show a maximum CNR for the 3mm slice thickness, the SR remaining constant (6 pl.cm-1).
Combination of these reconstruction parameters (66keV, Qr40 and 3mm slices) produce a CNR on average greater by 4.7 ±2.0 % for the different material contained in the Capthan600 compared to the conventional H&N protocol (Br38 filter, 3mm slices). The SR is unchanged (6 pl.cm-1).

Conclusions: With DECT acquisition, the choice of the reconstruction parameters, and particularly the one of the reconstructed energy, allows to significantly change the SR and the CNR on images. DECT reconstruction at energy of 66keV associated with a Qr40 reconstruction filter and a reconstructed slice thickness of 3mm provide an optimal combination and improve image quality compared to conventional H&N protocol. A study on anthropomorphic phantom will constitute the last step before using DECT acquisitions in clinics to delineate organs at risks and target volumes.

Study of a new detector for stereotactic treatments: The SRS MapCheck™
Etude des performances d'une matrice dédiée au contrôle qualité pré traitement pour les irradiations stéréotaxiques.

M. Lassot[a,b,c,d], L. Drezet[a,c], O. Salomon[b,c], E. Masson[b,c], F. Mazoyer[a,c]

[a]Service de Radiothérapie, Centre Hospitalier Annecy Genevois/Epagny Metz-Tessy/France
[b]Service de Radiothérapie, Clinique Générale d'Annecy/Annecy/France
[c]Groupement Annecien de Cancérologie/Epagny Metz-Tessy/France
[d]Université Clermont Auvergne, École Universitaire de Physique et Ingénierie/Clermont Ferrand/France

Introduction: Stereotactic treatments play an important role in radiotherapy. The SRS MapCheck™ (SunNuclear) is a new detector dedicated to pre-treatment controls for the stereotactic method. It is composed of a matrix of silicon diodes. The aim of this study is to present the performance of this detector.

Methods: All measurements were performed with 6 MV filtered and unfiltered beams (FF and FFF). First, we evaluated output factors: measurements were made using fields of 1 to 7 cm^2, and compared to the values obtained with a diamond detector- *PTW 60019*. Subsequently, all measurements were made with a field of 4x4 cm^2 and 100 MU. Repeatability was studied with 20 identical acquisitions. Reproducibility was evaluated in similar conditions, but measurements were made throughout multiple days. For linearity, measurements were made with a MU number varying from 50 to 2000. Then, responses according to dose rates were monitored, varying the flow rate from 10 to 600 MU/min for the 6 MV FF beam, and from 400 to 1400 MU/ min for the 6 MV FFF beam. Next, angular responses were tested with measures realized 360° around the detector inserted into a dedicated PMMA phantom (StereoPHAN™- SunNuclear). Finally, ninety dose distributions obtained by the detector were compared to those calculated in Treatment Planning System (Eclipse™ – Varian).

Results: Concerning output factors for both beams, the deviation did not exceed 1%, compared to the diamond detector, except for fields less than 2 cm^2 where it could reach 1.8% (1x1 cm^2) for FFF beam. Regarding repeatability and reproducibility, deviation between all the measurements did not exceed 0.4%, which is much lower than the recommended 1% limit [1]. Moreover, results showed that linearity was almost perfect (linear regression coefficient R^2 = 0.9996 for FF beam and R^2 = 1 for FFF beam). No dependency with dose rate was detected for FFF beam (deviation < 0.3%), but for FF beam, a dependency of about 1% was observed for rate variations between 100 and 600 UM/min but it could be up to 3.7% for very low rates (10 UM/min). About angular responses, we can conclude that it is correct for most angles, except for angles 85° to 95° and 265° to 280°, where deviations up to 9% have been measured. On the study of dose distributions, 97.8% of cases satisfy 95% of gamma index 2% 1 mm, which respects the limits [2] very well.

Conclusions: The SRS MapCheck™ is a different way of controlling dose distributions for stereotactic treatments. This detector respects the recommendations for various criteria, but finds its limits with the study of very small fields (less than 1.5x1.5 cm^2), the use of low dose rate, and the response for specific angles.

References

1. Tromson,D. "Le diamant pour la dosimétrie en radiothérapie", *CEA - Séminaire IRFU.*(2015).
2. Miften,M. "Tolerance limits and methodologies for IMRT measurement-based verification QA: r*ecommendations of AAPM Task Group No. 218. Med. Phys*.". 45: e53-e83. (2018).

A new transparent beam profiler based on secondary electrons emission for hadrontherapy charged particles beams

Nouveau moniteur de faisceau transparent basé sur l'émission d'électrons secondaires pour faisceaux de particules chargées en hadronthérapie

C. Thiebaux[a], G. Blain[b], B. Boyer[a], E. Delagnes[c], Y. Geerebaert[a], O. Gevin[c], F. Haddad[b,d], C. Koumeir[d], F. Magniette[a], P. Manigot[a], N. Michel[b], F. Poirier[d], N. Servagent[b], T. Sounalet[b], M. Verderi[a].

[a]Laboratoire SUBATECH, IMT Atlantique CNRS-Université de Nantes/Nantes/France
[b]Laboratoire Leprince-Ringuet CNRS-Ecole polytechnique/Palaiseau/France
[c]IRFU, CEA Université Paris-Saclay/Saclay/France
[d]GIP ARRONAX/Saint-Herblain/France

Introduction: Beam profiling during patient treatment in hadrontherapy requires ultra-thin monitors to preserve the high beam quality. For detectors upstream in the line, a material budget as low as ∼15 µm water-equivalent is needed. Besides, the current trend of dose escalation to treat highly resistant tumors implies challenging requirements to the monitor in terms of radiation hardness and dynamic range.

Methods: We propose a new type of beam profiler, PEPITES, using secondary electron emission (SEE) and built with thin-film techniques and operating in the vacuum of the beam line. The beam is profiled by crossing thick nanometric patterns which emit the SEE signal. The patterns are deposited on polymeric membranes, which, in contrast with conventional systems like ionization chambers, are free from mechanical constraints and can be as thin as achievable. The thinness of the monitor disturbs very little the incident beam, which can then be delivered to the patient while keeping the profiler in the line, ensuring continuous monitoring. Also, it makes the energy loss very small allowing the monitor to tolerate higher currents than existing systems without suffering from overheating problems. Besides, the absence of mechanical efforts on the membranes makes radiation damages of less consequence than with classical systems like ionization chambers allowing to extend the operation duration of the system.

Results: A simple prototype has been successfully operated with proton and alpha beams at the ARRONAX cyclotron in a wide range of currents (100fA - 100nA) and for several energies, validating the chosen technique[1]. Secondary electrons yields have been measured within the full therapeutic energy range at the ARRONAX cyclotron and the Orsay Protontherapy Center (CPO). At the same time, several irradiation campaigns with proton beams, electron beams, gamma sources have been conducted to evaluate the radiation damages with the deposited dose (up to 10^9 Gy). No significant effect on the detector is observed, which suggest great expectations about the profiler lifetime. Tests were performed using commercial ammeters, and an integrated electronics readout device is under development.

Conclusions: PEPITES is a unique transparent beam profiler based on secondary electron emission and built using thin film techniques. The assets of this detector in the perspective of its use in hadrontherapy are numerous: good radioresistance for a long working duration, simple operations reducing installation and calibration times, a broad range of beam current and especially high flux allowing beam monitoring with dose delivery escalation. A fully working prototype is foreseen to operate at the ARRONAX cyclotron end 2020.

References

1. Boyer, B. *et al.* Development of an ultra thin beam profiler for charged particle beam. *Nuclear Inst. and Methods in Physics Research, A* (2018) (https://doi.org/10.1016/j.nima.2018.09.134).

Analysis and evaluation of a fixed vertical couch position technique in comparison with a placement based on tattoo and Couch Move Assistant on linacs Elekta Synergy S

Analyse et évaluation d'une technique de positionnement à table vertical fixe comparativement à un placement basé sur des points de tatouage et de l'assistant de mouvement de table d'accélérateurs Elekta Synergy S

M. Mathot[a], P. Henry[a]

[a]CHU de Liège, Radiotherapy department /4000 Liège/Belgium

Introduction: In our department the daily patient setup is based on tattoos and the offsets, eventually registered in the Record and Verify software MOSAIQ (version 2.6), are then applied with the Couch Move Assistant (CMA). The procedure is: for the four first days of the treatment, a Cone Beam Computed Tomography (CBCT) is taken and the correction is applied even for a displacement of 1 mm. After the four fractions, the mean of a systematic error (SE), if detected, will be calculated and applied for the following fractions. For the prostate treatment if the means is greater than 4.5 mm, the mean of the offsets will be added automatically through MOSAIQ for the rest of the next fractions. When there is prostate marker (gold seeds), a CBCT is taken daily and no SE correction is applied. Based on the publication of Petillion[1] et al. in 2015 for the whole breast radiotherapy, a fixed vertical couch position (FVCP) setup is expected to be more precise than a setup based on skin marks: because of skin mobility, imprecision of tattooing during simulation, precision of the CMA module. For a fixed couch vertical positioning, the setup would be as followed: patient setup in left-right (LR) and superior-inferior (SI) based on the skin marks. For the anterior-posterior (AP) setup, it would be based on table height measured in the Treatment Planning System (TPS). The aim of this study is to apply the same methodology for prostate treatment.

Methods: All the treatments were delivered with Elekta linacs Synergy S, all of them equipped with a CBCT. Offsets data and couch vertical position after repositioning, from 179 prostate patients, from June 2017 till December 2017 (with or without seeds, ganglia) were extracted from MOSAIQ and analyzed. Means (Σ) and standard deviations (SD) of AP were calculated for all the offsets for each patient treatment. If we use the fixed couch vertical (FVCP) protocol we calculate the offset like this: the couch vertical derived from the TPS (measurement of the height from the isocenter to the table) is subtracted from the couch vertical value after CBCT-based couch correction during treatment. Means and standard deviations of these theoretical values of the offset for FVCP are calculated and compared with those obtained in clinical conditions. We want to identify the correction of systematic error (SE) with and without applying the FVCP protocol.

Results: Based on 179 treatment analyzed and focusing the AP correction, 29 corrections of systematic error were done but 26 could be avoided with the FVCP protocol. 35 more corrections of the SE errors could have been done but it has not been due to our procedure: no SE correction in case of daily CBCT during all treatment. It concerns 31 prostate treatment with markers and the last four were prostatic beds treatments. From this 35 virtual corrections, 31 would have been avoided with the FVCP protocol. The mean of the means for all treatments without correction of the SE: No FVCP protocol: -0.08 cm (SD = 0.285); FVCP protocol: 0.01 cm (SD = 0.215). If we refer to the formula of Van Herk[2] et al. - 2.5 Σ + 0.7 σ - we may quantify the gain on the AP for the Contour Target Volume (CTV) to Planning Target Volume (PTV) margins: No FVCP protocol: 0.91 cm; FVCP protocol: 0.68 cm.

Conclusions: The advantage is in favor of the FVCP protocol in terms of precision and stability. More than 90% of the SE corrections could be avoided with the FVCP protocol: reduced AP errors positioning and workload reduction for the RTTs are the consequences.

References

1. Petillion, S. *et al.* Efficacy and workload analysis of a fixed vertical couch position technique and a fixed-action–level protocol in whole-breast radiotherapy. *J. Appl. Clin. Med. Phys.* **16,** 279–290 (2015).
2. Van Herk, M. *et al*. The probability of correct target dosage: Dose-population histograms for deriving treatment margins in radiotherapy. Int J Radiat Oncol Biol Phys. **47**(4):1121–35 (2000).

Reproducibility evaluation of breast irradiation for lateral decubitus positioning
Evaluation de la reproductibilité du positionnement des patientes pour les traitements des cancers du sein avec la technique Décubitus Latéral Isocentrique DLI

I.Birba[a], L.Mayorga[a], E.Costa[a], P.Poortmans[a]

[a] Institut Curie, Department of Radiation Oncology, Paris, France

Introduction: Accurate delivery of radiation therapy (RT) requires precision regarding patient positioning, from the treatment planning CT-Scan till the last RT fraction. Since 1990, for a selection of patients (large breast volume), we use the lateral decubitus position (DLI technique, figure 1) to deliver external beam breast irradiation, to decreasing the dose to the ipsilateral lung and the heart maintaining target volume coverage. In DLI, the patient lies on the affected side with the breast placed on a wedge developed exclusively for this technique. The aim of this study is to evaluate the reproducibility of patient positioning in DLI.

Methods: We evaluate the reproducibility of positioning with the DLI technique, by analysing double exposure MV images of the mediolateral (in DLI this is anteroposterior considered the treatment machine) beam of 30 patients. The Image Guided Radiotherapy (IGRT) protocol prescribes to realize the image weekly. Using these images, we measured three distances (figure1):
- Distance 1 (D1) from the pulmonary margin to the internal field limit
- Distance 2 (D2) from the outer edge of the breast to the outer field limit
- Distance 3 (D3) from the inferior mammary fold to the lower field limit
We recorded 600 measures using the treatment images and compared those with the DRR.

Results: Results of distance D1 are presented in Figure 2. Three categories of patients emerge from the study:
- Category 1 (blue color): Patients with a low standard deviation (STD) of D1 around a deviation to DRR Δ_{DRR}=0cm: [-0.5cm; +0.5cm], representing 53%. Good positioning reproducibility, so the IGRT protocol with 1 image per week is sufficient.
- Category 2 (black color): Patients with a low STD of D1 around Δ_{DRR}=0cm: [- 1.0 cm; ~ - 0,5 cm] U [~ +0,5 cm; 1.2 cm], representing 13%. Good positioning reproducibility, after the application the IGRT protocol by registering and correcting for the deviation on the first day, followed by 1 image per week. As a PTV margin of 5mm is used, the target volume remains covered.
- Category 3 (orange color): patients with a large STD of D1 not around Δ_{DRR}=0cm, representing 34%. Breast repositioning is variable, requiring an adapted IGRT protocol with a daily imaging and online correction protocol.

Conclusions: This study allowed us to thoroughly evaluate positioning reproducibility of the DLI technique. A categorized modification of the IGRT protocol allows improving the technique and decreasing the PTV margin. Rather reassuring, more than half of our patients have an excellent repositioning with just weekly imaging and for the other half an adapted IGRT protocol. DLI technique is a good alternative to IMRT for large breasts. The study continues evaluating possible factors influencing patients' positioning, in particular these of category 3, including correlation with the interval between surgery and radiation therapy; breast edema; patient's relaxation; seroma/hematoma resorption; patient's age or breast size.

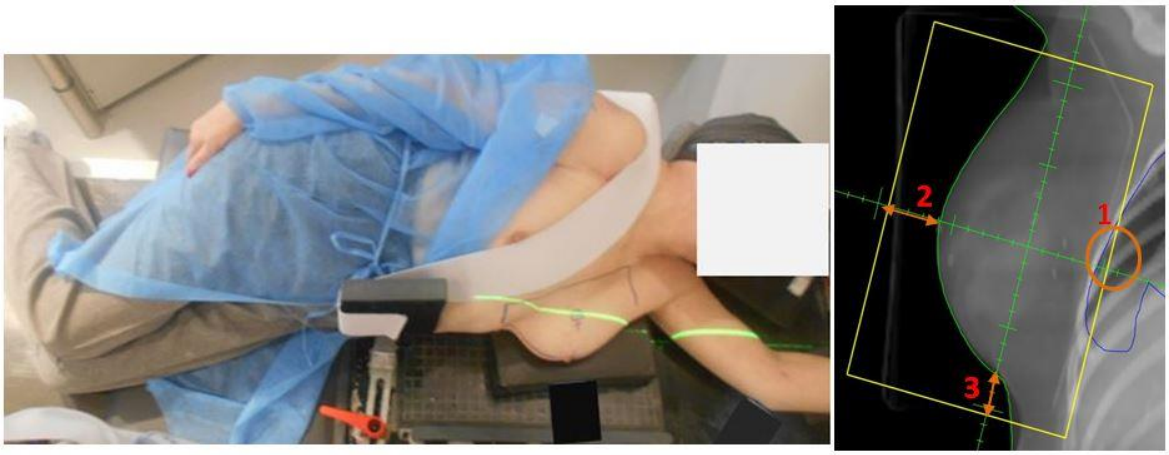

Figure 1. Patient position with the DLI technique and the three distances D1, D2, D3 measured on the Digital Reconstructed Radiographs DRR

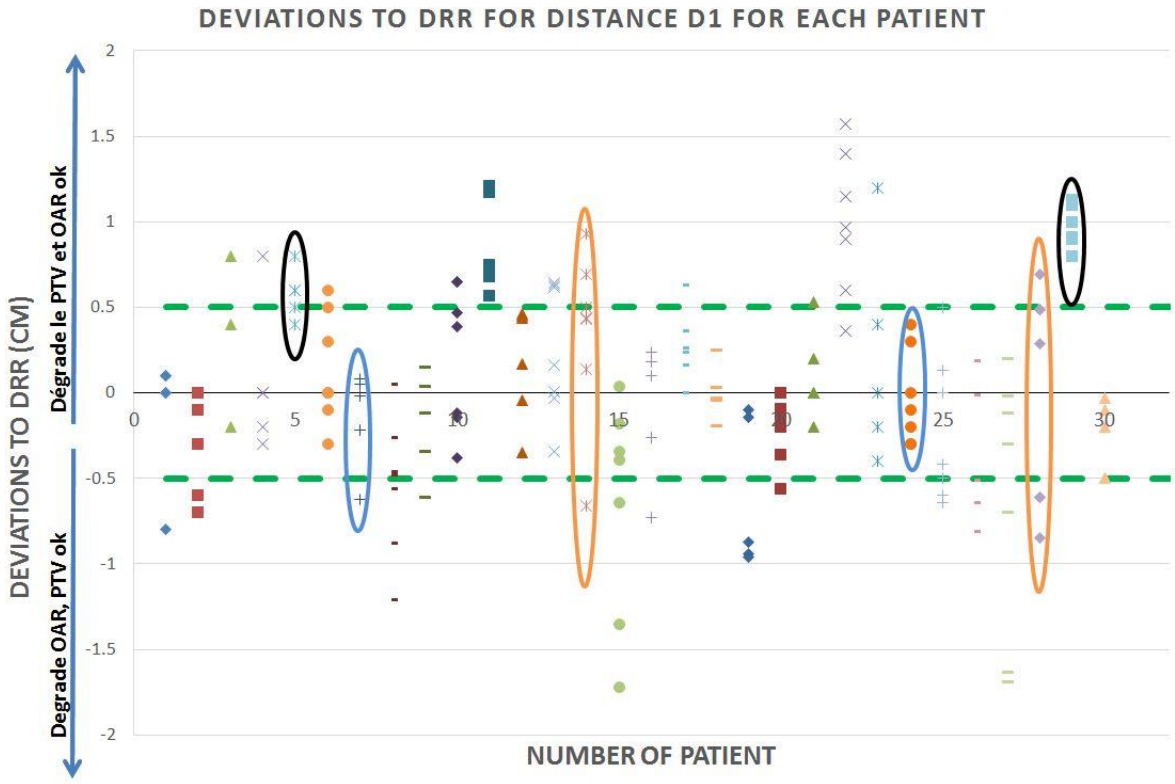

Figure 2. Deviations to DRR for distance D1 for each patient.

Relations between radiation dermatitis degrees during radiation therapy and dose levels, for different regions in breasts and chest walls
Relations entre les degrés de dermatite d'irradiation au cours de la radiothérapie et les niveaux de dose, pour différentes régions des seins et des parois thoraciques

M. Moussallem[a, b, c], H. Rima[a, b], S. Ayoubi[a, b]

[a]Radiation Oncology Department, Centre de Traitement Médical du nord / Zgharta / Lebanon
[b]Centre Hospitalier du Nord / Zgharta / Lebanon
[c]Doctoral School of Sciences and Technology, and Faculty of Public Health, Lebanese University / Tripoli / Lebanon

Introduction: Despite the use of planning maximal dose threshold constraint in radiation therapy (RT) treatments, radiation dermatitis in breast cancer continue to be among the most common side effects during treatment. In order to minimize dermatitis, we have divided previous general maximum dose constraint threshold (107 % of prescribed dose) to different specifics thresholds associated to different specifics regions in breasts and chest walls.

Methods: One hundred consecutive patients treated with tangential-field RT by 50 Gy in 25 fractions were included. Patients were divided in five groups: (i) “chest walls”; (ii) “breast with inframammary folds”; (iii) “small breast” (less than 700 cc); (iv) “medium breast” (between 700 and 1200 cc); and (v) “large breast” (greater than 1200 cc). Furthermore, each group was divided in two subgroups: inferior quarter site and the remained site. At the last treatment fraction, for all patients, in each site, the maximum skin radiation reaction grade value (scored from 0 to 10) with the associated site planned maximum dose value (in % from the prescribed dose) were collected in order to find relations between the two values.

Results: 46, 16, 23, 15 and 0 patients were suited respectively with groups (i), (ii), (iii), (iv) and (v). Only group (ii) sites, were represented by significant (R^2 > 0.5) mathematical regression fitting curve (Figure 1). The inframammary breast folds’ sites were the most sensible regions to radiation in group (ii), and the maximum dose level in these sites should not exceed the 105 % of the 50 Gy prescribed dose. However, all other regions in breasts or chest walls can tolerate higher maximum doses, they can achieve in some cases approximately 112 % of the prescribed 50 Gy, without causing any skin dermatitis.

Conclusions: In order to reduce radiation dermatitis, the old general constraint threshold should be divided in different thresholds according to different regions in breasts and chest walls. Special attention should be taken to inframammary folds to not exceed 105 % of the prescribed dose. However, future studies with larger patient number including individual radiation test sensibility were recommended in order to achieve greater precision for dose thresholds constraints values especially for patients without inframammary folds.

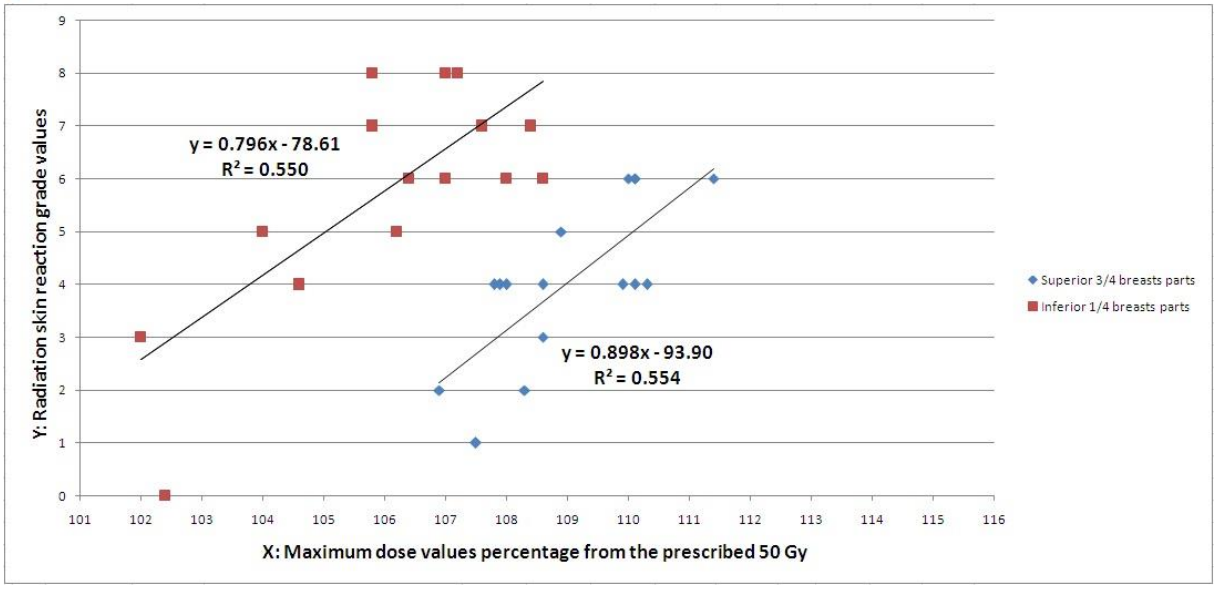

Figure 1. Curves related to the two subgroups sites (inferior ¼ breasts parts who represent inferior inframammary folds in this group and superior ¾ breasts parts) of the "breast with inframammary folds" patient group (ii). Curves showing the variation of the maximum radiation skin reaction grade values (Y) in each site versus the correspondent planned maximum dose values percentage (X).

Transmission of the MLC, comparison between measurement and calculation with Eclipse™ according to the field size and depth

Transmission du MLC, comparaison entre mesure et calcul avec Eclipse™ en fonction de la taille du champ et de la profondeur

F. Mazoyer[a,c], L. Drezet[a,c], O. Salomon[b,c], J. Kristiansen[a,c], E. Masson[b,c]

[a]Service de Radiothérapie, Centre Hospitalier Annecy Genevois/Epagny Metz-Tessy/France
[b]Service de Radiothérapie, Clinique Générale d'Annecy/Annecy/France
[c]Groupement Annécien de Cancérologie/Epagny Metz-Tessy/France

Introduction: The multi-leaf collimator (MLC) is an essential component of linac to deliver intensity modulation treatments need to be properly modeled in the treatment planning system (TPS). For this purpose, Eclipse TPS (Varian) uses a two-parameters approach: Transmission factor (T) and Dosimetric Leaf Gap. LoSasso [1] and Wasbø [2] identified a variation in T for 6 and 15 MV beams for field sizes between 5 and 14 cm² and few depths. This study proposes to compare the T values measured and calculated according to these parameters with a larger range, for 6 MV beams with and without flattening filter (FF and FFF) and 18 MV.

Methods: The transmission ratio is defined as the ratio of leakage and scatter dose in MLC leaves over the open field dose [1]. We measured it on a TrueBeam (Varian) for field sizes ranging from 3 x 3 cm² to 15 x 37.5 cm². We used 0.3 cc ion chamber (PTW 31013) to obtain a representative average of the two components of the MLC's transmission (interleaf and under leaf). The ion chamber is inserted in a solid water phantom perpendicular to the MLC leaves and placed at the isocenter. The default depth was 5 cm for 6 MV beams and 10 cm for 18 MV beam. We also measured T for a referent field size from 5 to 20 cm depths. Same conditions were reproduced in Eclipse and calculated with a 1 mm grid size and AcurosXB 13.6.

Results: This experiment revealed significant differences between the measurements and the calculation. In the Eclipse simulation, T results are constant for any fields size and depth. It depended only on energy and are in accordance with the values optimized during the TPS configuration. The measurements indicated an increase in T with the field size from 1.14% to 1.43% for the 6 MV FFF, 1.36% to 1.77% for the 6 MV FF and 1.42% to 1.94% for the 18 MV. For the 6 MV (FFF and FF), we measured an increase in T with depth from 1.22% to 1.43% and 1.44% to 1.61% respectively. For the 18 MV beam, we observed a slight decrease but not significant (1.55% to 1.51%).

Conclusions: This study confirmed and completed the descriptions of LoSasso [1] and Wasbø [2]. We revealed a dependence of the MLC transmission factor with field sizes and depth that is not modelled in Eclipse TPS. Calculated doses are underestimated in smalls fields and inversely. This dependence was more significant when energy increases. This study could explain the dose differences obtained during sliding gap irradiation by Kim [3].

References

[1] LoSasso TJ *& al.* Physical and dosimetric aspects of a multileaf collimation system used in the dynamic mode for implementing intensity modulated radiotherapy. *Med Phys*. **25**(10):1919-27 (1998)
[2] Wasbø E. *& al.* Dosimetric discrepancies caused by differing MLC parameters for dynamic IMRT. *Phys Med Biol*, **53**, 405-415 (2008)
[3] Kim *& al.* Relationship between dosimetric leaf gap and dose calculation errors for high definition multi-leaf collimators in radiotherapy. *Physics and Imaging in Radiation Oncology. **5**, 31-36 (2018)*

Impact of iMAR® algorithm (Siemens) and extended field of view reconstruction on HU numbers accuracy and dose calculation in radiotherapy treatment plans

R. Hermouet[a], N. Delaby[a], S. Laffont[a], C. Lafond[a]

[a]Centre Eugène Marquis, Rennes

Purpose: Definition AS64 CT (Siemens) provides an artifact reduction algorithm (iMAR®) which allows to reconstruct the missing data considering the material type which created the artifact. This correction can modify the image by changing the volumes and the HU numbers. The diameter of the scan field of view is only 50 cm long. It's then possible to reconstruct an extended field of view when the patient size is larger. Uncertainty on HU numbers is 50 HU when the field of view diameter is extended to 65 cm. Beyond this diameter, Siemens doesn't ensure their accuracy. These options are particularly interesting for radiotherapy. The aim of this study is to determine the influence of these algorithms on HU numbers, volumes and dose calculation.

Methods: Images of phantom CIRS062 were acquired with different positions (0 to 20 cm from the center of the FOV), and were reconstructed with or without the extended field of view. The HU numbers were measured with the TPS Pinnacle v9.10 (Philips). The impact on dose calculation will be evaluated on CIRS062 and anthropomorphic phantom. CT images of patients with dental fillings were reconstructed with or without the iMAR® algorithm. The HU numbers were measured in different volumes of interest. The influence on dose computation will be studied and compared to a manual correction of artifact densities. The same study will be realized on CT images of patients which don't need an artifact correction.

Results: When the phantom CIRS062 was moved 10 cm from the center, the external contour is correctly reconstructed (deviation of 0,03 % on the reconstructed slice surface). The deviation on mean HU numbers reaches 16 HU (2,18 %), which is faithful with the deviations given by Siemens (50 HU). For a translation of 15 cm, the contour is not correctly reconstructed (deviation of 5,17 %). The deviation on mean HU numbers reaches 74 HU (27 %). For the iMAR® study, E.Bär et al. [1] showed that the deviation on dose computation could reach 5 % in an anthropomorphic phantom. They also determine a 5 % dose difference in the PTV between corrected and uncorrected patients. Our results will be confronted to the literature.

Conclusion: These reconstruction algorithms show a real interest during the planning dosimetry in radiotherapy, by improving image quality and accuracy. However, their implementation in clinical routine requires to analyze their influence on volumes contouring and on dose computation.

References

[1] E.Bär et al, Improving radiotherapy planning in patients with metallic implants using the iterative metal artifact reduction (iMAR) algorithm, 2015

Impact dosimétrique des erreurs de reconstruction manuelle d'un applicateur de curiethérapie interstitielle Venezia

S. Briand Maroubi[a], E. Toalombo Montero[a], F. Gassa[a]

[a]Centre Léon Bérard / Lyon / France

Introduction : Le Venezia™ est un applicateur gynécologique utilisé en curiethérapie interstitielle et intracavitaire. La reconstruction de l'applicateur se fait grâce à l'imagerie TDM/IRM pour le repérage de la 1ère position et du trajet de la source de traitement. Le TPS Oncentra® V3.1.6 propose une bibliothèque pour simuler le trajet de la source et pour reconstruire automatiquement cet applicateur. Cependant, une reconstruction manuelle est toujours possible.
L'objectif de cette étude est d'évaluer l'impact dosimétrique sur la couverture des volumes cibles (VC) et sur la dose aux OARs en comparant la reconstruction manuelle et automatique du Venezia ainsi que l'impact d'une erreur de reconstruction des aiguilles paramétriales.

Méthodes : Dans un premier temps, 5 patientes sont réparties en 2 groupes : 3 avec une imagerie IRM et 2 avec TDM. La dosimétrie de référence est réalisée à partir de la reconstruction automatique des applicateurs. Une reconstruction manuelle de chaque applicateur est effectuée.
Dans un second temps l'étude s´est portée sur 20 patientes pour lesquelles des offsets de 1.5, 2.5 et 5.0 mm sont appliqués lors de la reconstruction manuelle des aiguilles paramétriales. Les plans sont recalculés afin d'évaluer l'impact dosimétrique des erreurs de reconstruction de l'applicateur. Les temps d'arrêt de la dosimétrie de référence sont utilisés.
Pour ces 2 parties, la couverture des VC et l'impact sur les OARs sont déterminés en relevant les critères D90 pour le CTV HR-IR et D2cc pour la vessie, le rectum et le sigmoïde après conversion en EQD2 et cumul de doses avec la RTE (formalisme Tridicol).

Résultats : Pour la 1ère partie de l'étude, 130 positions de sources sont évaluées pour comparer l'écart entre la reconstruction manuelle et automatique. La variation moyenne 3D était de 3.8 à 1.1 mm (1 SD) pour l'IRM et 2.5 à 0.9 mm (1 SD) pour le TDM. L'impact dosimétrique est faible : CTV HR : +2.7% à l'IRM et +2.2 % pour le TDM ; rectum : 1.6 % à l'IRM et 1.3 % pour le TDM ; sigmoïde : 1.7% à l'IRM et 1.6 % pour le TDM ; vessie 1.8% à l´IRM et 0.3% pour le TDM.
Dans la 2ème partie de l'étude, l'application d'un offset (+) ou (-) jusqu'à 2.5mm n'apporte aucune différence significative en terme de couverture sur les VC et les OARs. Pour un offset de +/- 5mm, la vessie reste dans les tolérances Tridicol (D2cc < 90Gy). En ce qui concerne le rectum, dans le sens (-) on remarque un dépassement de dose (D2cc >70Gy) lorsque la contribution du temps sur des aiguilles interstitielles est supérieure à 30% du temps total de traitement. Sur le CTV HR, une perte de couverture (D90<85Gy) pour 35% des patientes pour lesquelles un temps hétérogène dans l´application paramétriale a été observée.

Conclusions : D'après les résultats préliminaires, l'impact dosimétrique lors de l'introduction des erreurs de reconstruction manuelle de l'applicateur de curiethérapie interstitielle Venezia n'impacte pas de façon significative la couverture des VC ni la dose aux OARs.

Utilisation de plans d'expériences pour évaluer l'influence de l'angle du collimateur, du nombre d'arcs et du nombre de points de contrôle sur la distribution de dose et la complexité de plans de traitement VMAT de cancers ORL

M. A. Khalal[a], M. Edouard[a]

[a]Département de radiothérapie, Institut Gustave Roussy, 114 rue Édouard-Vaillant 94805 Villejuif, France

Introduction : Lors de la réalisation des dosimétries VMAT, certains paramètres sont fixés avant la phase d'optimisation du plan mais ont un impact sur les possibilités de modulation et la complexité du plan. C'est le cas de l'angle de collimateur, le nombre d'arcs ou encore le nombre de « control points ».
Nous souhaitons déterminer l'impact de ces paramètres en pondérant l'analyse entre atteindre les objectifs dosimétriques et limiter la complexité des plans. Pour une telle étude paramétrique, l'approche classique consiste à fixer les (n-1) paramètres et à faire varier le $n^{ième}$ paramètre. Cette approche est couteuse en temps car on se retrouve ainsi avec un nombre important de tests à réaliser. Pour pallier à ce problème, nous avons mis en place une méthodologie basée sur les plans d'expériences (PEX) [1] largement utilisée en industrie. Cette méthode consiste à réaliser des mesures en faisant varier plusieurs paramètres à la fois dans le but de réduire le nombre de tests à effectuer tout en gardant un maximum d'information.

Méthodes : L'étude porte sur une vingtaine de patients atteints d'un cancer ORL et traités par VMAT. La planification du traitement est réalisée avec le TPS RayStation. Pour chaque patient, on souhaite étudier l'impact des paramètres suivants: l'angle de collimateur (15°/30°/45°), le nombre d'arcs (deux/trois/option dual Arcs qui redistribue différemment la fluence entre les arcs) et enfin l'espacement entre les points de contrôle (2°/3°/4°) sur des indices de couverture des PTVs (D98%, D2%, indice d'homogénéité, indice de conformation), protection des OAR et complexité de modulation (MCSv et LTMCS) [2].
Une étude complète nécessiterait de faire 3*3*3 = 27 plans pour chaque patient soit 540 plans. Le plan d'expérience que nous avons utilisé est basé sur une table de Taguchi de type $L_9(3^4)$. Le nombre de plans à réaliser est ainsi réduit à 9 par patients. Nous avons automatisé la génération des 9 plans par patient par l'utilisation de scripts disponibles sur RayStation.

Résultats : Les plans sont générés automatiquement par script. Un second script est utilisé pour le calcul des indices dosimétriques et de modulation directement sur le TPS. L'analyse des résultats est en cours.

Conclusions : Le script dans les TPS combiné à l'utilisation d'un plan d'expérience permettent d'effectuer des études paramétriques avec un coût humain considérablement réduit. Cette étude va permettre de définir 3 paramètres dosimétriques influençant la modulation de plans VMAT pour obtenir le meilleur compromis entre objectifs dosimétriques et complexité du plan.

Références

1. Dufreneix, S. *et al.* Design of experiments in medical physics: Application to the AAA beam model validation. *Physica Medica.* **41,** 26–32 (2017).
2. Masi, L. *et al.* Impact of plan parameters on the dosimetric accuracy of volumetric modulated arc therapy. Medical Physics. **40,** 071718 (2013).

Evaluation of dosimetric data of patients treated at the Jean Bernard Center between 2016 and 2018 for prostate cancer

Evaluation des données dosimétriques des patients traités au centre Jean Bernard entre 2016 et 2018 pour un cancer de la prostate

F. Ravaud[a], D. Lebhertz[a], F. Denis[a], Y. Metayer[a]

[a]Centre Jean Bernard (ILC), Le Mans, France

Introduction: This contribution aims to present the analysis of a dosimetric database containing around 700 patients treated for prostate cancer between 2016 and 2018. Currently, the quality of dosimetry is determined based on clinical goals coming essentially from Recorad[1]. In this work we seek to improve our validation criteria for intensity modulation (IMRT/VMAT) treatments.

Methods: In order to collect the individual dosimetric data from Eclipse TPS, we have created a program that allows both validating individual dosimetry based on criteria defined in the center and storing them in a SQL database. A validation sheet and an associated database are created for the various prostate cancer prescriptions (from low risk to high risk cancer). A program has been designed to allow easy and immediate analysis of collected data.

Results: Our results show that the clinical goals used in the center are for the most part easily achievable in modulation intensity technique, enabling us to establish new optimized criteria based on our practices. In addition, we compared dose indicators for each participant of our team, radiotherapist or dosimetrist. This analysis shows at the same time a good homogeneity of practices in the team and a good stability of these practices over time. Finally, we were able to compare the dosimetric data of a patient with rectal complication to the overall data and verify that they did not predispose him to the observed complications.

Conclusions: The statistical analysis of our patient database allowed us to check the stability of our dosimetric process for intensity-modulated prostate treatments. Moreover, this analysis allowed us to increase our clinical goals which should reduce for patients the risks of side effects.

References

1 MA. Mahé, I. Barillot & al., Recorad : Recommandations pour la pratique de la radiothérapie externe et de la curiethérapie, Cancer Radiothérapie, **20** (2016), pp. S1-S270

L'arrivée du MRIdian de Viewray au sein d'un service de radiothérapie

I. Bessieres[a], A. Petitfils[a]

[a]Service de Physique Médicale / Centre Régional de Lutte contre le cancer - Centre Georges-François Leclerc / Dijon / France

Introduction : En 2019, trois centres français de lutte contre le cancer s'équipent d'une machine de radiothérapie de nouvelle génération, le *MRIdian* développé par *Viewray* embarquant un appareil IRM sur un accélérateur linéaire. Cette communication a pour objectif de faire un retour de l'expérience dijonnaise des principales étapes ayant permis l'aboutissement du projet.

Méthodes : De la commande à la validation clinique en passant par les travaux du bunker, la réception et l'installation du *MRIdian*, plusieurs étapes clefs ont été menées. Du fait des dimensions inhabituelles de la machine et de la conjugaison des risques électromagnétiques aux risques radiologiques, la conduite de ce projet a requis une organisation particulière et une collaboration soutenue entre les différents acteurs.

Résultats : Des travaux d'aménagement du bunker d'une durée de trois mois ont été nécessaires. L'installation et l'*acceptance* par *Viewray* de la machine se sont étalées sur près de deux mois. La validation pour une utilisation clinique aura nécessité deux mois.

Conclusion : Finalement, une année complète se sera écoulée entre la commande et la première utilisation clinique du *MRIdian* au cours de laquelle il aura fallu sans cesse adapter notre organisation au caractère singulier de cette machine et de sa réception.

Implementation and evaluation of offline adaptive radiotherapy (ART) based on pelvic CBCT (XVI-Elekta) with Dynamic Planning (DP) module of pinnacle 16.2

G. Guibert[a], C. Tamburella[a] P. Weber[a]

[a]Radio-Oncologie/Chaux-de-Fonds/Suisse

Introduction: For pelvic radiotherapy treatment, organs at risk distention (bladder, rectum) could impact target position (prostate) and therefore treatment quality. The delivered dose to organs and the disease recurrence risk could increase. Pinnacle Dynamic Planning module (DP) allows dose evaluation on daily-acquired CBCT but a proper HU-density calibration curve is needed for accurate dose calculation. Before clinical use, several aspects are evaluated; dose calculation accuracy on CBCT images, rigid registration quality and overall displacement compared to treatment, and OARs auto-segmentation.

Methods: HU to physical-density calibration curve for pelvis M20 CBCT image (XVI 5.0.2) was measured using a CIRS phantom setup (model 062M). A typical prostate VMAT plan is made on a heterogeneous phantom (bony and soft tissue anatomy). The dose distribution difference (DVH, mean dose…) between CT and CBCT phantom images is evaluated with DP. For 10 patients treated in pelvic area, the average displacement after a rigid registration, calculated both by the XVI system and by DP, is compared. Different DP parameters (cross correlation and mutual information algorithms, box limitations or not) are tested. Dice Score resulting from OARs propagation on CBCT for 3 deformable registration smoothing parameters (Gaussian filter) is compared.

Results: DVHs calculated on CBCT and CT phantom images show a total overlap. Moreover, mean dose difference between CBCT and CT dose is less 1% for PTV and less 4.8 % for OARs (1.3 Gy in absolute dose). Max dose difference is less 3% both for PTV and OARs. The CBCT calibration curve is therefore clinically validated. The "propagated isocenter" resulting from DP rigid registration between CBCT and CT corresponds to the treatment position. If the registration proposed by DP is kept then the difference of average distance (in 3D) between IGRT and DP is less 1 mm whatever algorithm or box size. Concerning the OARs auto propagation, no trend really emerges, except for some cases where CBCT bladder filling is near the CT, in this case Dice Score reaches 0.8 even 0.9.

Conclusions: By using a specific calibration curve it is possible to include routinely CBCT image in the adaptive radiotherapy loops. Nevertheless CBCT images are used in a context of partial ART meaning no re-optimization with DP on CBCT are performed. DVH observation is a good indicator to evaluate at first glance anatomical change on dosimetry and can be used as a decision tool for replanning on a new conventional CT. "CBCT dose" results of recomputed beams on the real isocenter (e.g. “dose of the day”) and is not the result of a warping of intial dose distribution. DP is a module integrated to the TPS, only needs to export CBCT. All structures, constraints, beam setup are automatically imported when DP is launched.

References

1. Hinault, P. *et al.* Adaptive radiotherapy:Evaluation of the dose actually delivered to the patient in a treatment of prostate cancer radiotherapy. *Physica.Medica* **32,** 344(2016).

First French clinical experience with the Calypso® system using the real-time tracking for the prostate treatment

D. Cirella[a], J. Prunaretty[a], P. Debuire[a], N. Aillères[a], A. Morel[a], S. Simeon[a], S. Valdenaire[a], P. Fenoglietto[a]

[a]Institut du Cancer de Montpellier, Service Radiothérapie/Montpellier/France

Introduction: The Calypso® 4D localization system (Calypso® Medical Technologies, Seattle, Wa) is a real-time electromagnetic tracking system. It is used to continuously monitor implanted Beacon® transponders. It is a real-time target tracking system that takes into account both inter- and intrafractional target motion. The purpose of the study was to report the intrafraction prostate displacement using the Calypso® system through a randomized phase II study (RCMI-GI).

Methods: The RCMI-GI study will include 166 patients into arm 1 and arm 2 in 1:1 ratio. 83 patients will be treated with standard set-up margins (1 cm all around the prostate except 5 mm in the posterior direction) and conventional IGRT protocol (daily CBCT). For the other ones, the treatment will be performed with reduced margins (3 mm all around the prostate) using the Calypso® system. The prescribed dose is 80 Gy in 40 fractions. To date, 21 patients were treated in arm 2 using VMAT and Calypso®. At the beginning of each fraction, a CBCT was performed and “Set zero and track” function of the Calypso® was applied. A 3 mm-gating threshold was used during the treatment. The displacements ≥ 3 mm in all directions were evaluated qualitatively and quantitatively.

Results: A total of 787 sessions were analyzed. An intrafraction motion ≥ 3 mm was detected for 77 fractions. Visually, the shifts were unpredictable and varied from a continuous drift to a transient evolution. For each patient, from 0% to 23% of fractions were impacted by a displacement ≥ 3 mm. 12,4% of movements were in the lateral direction, 48,8% in the axial direction and 38.8% in the longitudinal one. The mean time of the treatment interruption was ranged from 00:01 to 09:52 (mm:ss) and increased the mean session time of 24.7% in comparison with a fraction without motion. 46% of 77 fractions required couch shift corrections using kV imaging and explained a longer treatment.

Conclusions: The intrafraction motions of the prostate are unpredictable and not negligible during the treatment. The Calypso® system performs an accurate and continuous monitoring of the target and allows a safe margin reduction.

Volumetric modulated arc therapy breast irradiations with a monte carlo algorithm: performances obtained with monaco calculations for single and bilateral irradiations

Irradiations mammaires par techniques volumétriques à l'aide d'un algorithme monte carlo : performances obtenues avec les calculs de monaco pour des irradiations simples et bilatérales

C. Bouyer[a], V. Plagnol[a], C.Vignolo[a], I. Plagnol[a], E. Bruno[a]

[a]Centre Catalan d'Oncologie/Perpignan/France

Introduction: Some breast irradiations are intricate in 3D techniques due to patients' morphology or volumes to irradiate. With the development of VMAT techniques, more and more breast irradiations are planned with volumetric arc therapy. In most studies, a AAA or similar algorithm is used (Boman, 2017; Fogliata, 2015). A small number of studies is done with a more realistic algorithm: the weakness of such studies is the low number of patients (Seppälä, 2015). To estimate achievable constraints and improve our practices with a MonteCarlo-based algorithm, we collected data for VMAT breast irradiations and analyzed the dosimetric performances.

Methods: Two irradiation fractionations have been studied: 50Gy in 25 fractions and 39,9Gy in 15 fractions. For time, esthetic fibrosis, and late damages all breast irradiations are calculated for 39.9Gy. As hypo-fractionation efficiency is not yet proven in some cases, chest walls and triple negative patients are planned for 50Gy.
We have separated patients into 7 categories: right breast, left breast, complete right breast (breast with axillary, internal mammary and supra-clavicular lymph nodes), complete left breast, complete left chest wall, complete right chest wall, bilateral breast. Plans were generated with a MonteCarlo-based algorithm (Monaco V5.11.02) for at least 10 patients per category. A statistical uncertainty per control point of 2.5% with a dose grid of 0.25cm was used for each planned treatment. To enable a 1cm air jaws aperture, an autoflash margin of 1cm was applied. To crop PTVs from body surface, a surface margin was applied: 0.5cm for axillary and supra clavicular PTVs and 0.3cm for internal mammary nodes PTV and for breast PTVs.
Our optimization process consists in protecting organs at risk at the expense of PTVs coverage. Anyway, no dosimetry was accepted without respecting at least those constraints:

Homolat. lung	Controlat. lung	Controlat. breast	Heart	PTV coverage	107% of dose
V15<50%	V10<50%	V5<50%	V30<46%	>95%	<2%
V20<35%	V15<20%	Max 60Gy			

Table 1: constraints

All patients' were treated on a Synergy accelerator with an Agility MLC.

Results: All collected data were compared depending on irradiation categories.

	right breast (39.9Gy/15)	left breast (39.9Gy/15	complete right breast (39.9Gy/15)	complete left breast (39.9Gy/15)	complete left chest wall (50Gy/25)	complete right chest wall (50Gy/25)	bilateral breast (50Gy/25)
D_{mean} heart	2.63 ±0.72	4.42 ±1.83	4.34 ±1.37	5.75 ±2.22	7.57 ±1.13	7.79 ±1.14	6.93 ±1.33
V5 heart	3.24 ±5.4	27.13 ±26.9	27.5 ±24.16	61.7 ±21.98	77.06 ±13.5	82.72 ±10.5	80.49
V5 sein contro	10.62 ±10.4	16.53 ±15.4	29.36 ±7.4	40.6 ±7.15	44.2 ±8.3	43.9 ±7.1	/
Breast PTV coverage	96.94 ±1.03	95.99 ±0.56	96.66 ±0.85	95.7 ±1.75	96.5 ±1.3	96.7 ±0.8	96.32 ±0.87

Table 2: Achieved constraints

As expected, heart constraints are better for right breast irradiations than for left-side, especially for the V5. Irradiations without nodes also showed better heart and contralateral breast protection.
The absence of significant difference between left and right complete chest wall irradiations could be explained by the delineated volumes which are oversized in chest wall cases (no mammary landmark).
If we normalize to a same prescription dose, we obtain similar constraints for complete breast and complete chest wall plans. Results also indicate that reachable constraints for bilateral irradiations are similar to ones for chest walls.

Conclusions: This study is useful to improve our practices as, now, reachable constraints are known. We are planning to enrich this study on a permanent basis to include all new patients by an automatic data collection.

Validation of the beam modelling of the multileaf collimator InCise2 on the Cyberknife M6 in the TPS Precision

N.Chazeau[a], K.Herlevin-Gerard[a], F.Courrech[a], I.Buchheit[a], V.Marchesi[a]

[a]Unité de radiophysique médicale, Institut de Cancérologie de Lorraine – Alexis Vautrin –Vandoeuvre-lès-Nancy, France

Introduction: Stereotactic treatment in the ICL are realized on a Cyberknife M6 with the collimation systems in fixed circular fields and by Iris. This work falls in the project of the commissioning of the multileaf collimator InCise2 and presents the validation of the beam modelling of the MLC InCise2 for the calculation model Finite-Size Pencil-Beam (FSPB) of the TPS Precision.

Method: The modelling of the MLC for the FSPB algorithm in the TPS Precision v 1.1.1.1 needs the acquisition of open beams profiles (without collimator) according to the axes X, Y and the diagonals (45° and 135°), orthogonal profiles, TPR and OF for MLC fields sizes included between 7,6 x 7,7 mm² and 115 x 100,1 mm². The validation of the modelling consists to comparing, for simple shapes of fields, with a normal beam angle to the entrance surface of the medium, calculated and measured dose distribution in a homogeneous phantom *Stereotactic Dose Verification Phantom* (Standard Imaging) by ionization chamber (PinPoint PTW 0,015cc) and by radiochromic film (Gafchromic EBT3), then patient treatment plans characteristic complex shapes of dose distributions with MLC (eroded, perimeter, random and conformal shapes). Many criteria of gamma index in dose and distance were tested (from 3%,2mm to 1,5%,1,5mm).

Results: For field sizes included between 7,6 x 7,7 cm² and 30, 8 x 30,8 cm² more than 95% of the points respect the criteria of the global gamma analysis 1,5%,1,5mm with an average 97,47% and a standard deviation of 1,86%. The average gamma is 0,42 with a standard deviation of 0,04. Dose measurement in the field 7,6 x 7,7 mm² is the only over 2% (-8,5%) compared to the TPS dose calculated, which can be explained by the important detector size compared to the field size. The average difference of the dose measurements of the other fields compared to TPS values is 0,6% with a standard deviation of 0,9%.

Conclusion: The first results allowed validate the modelling of the FSPB algorithm for simple shapes of fields. Now, it remains to validate the complex shapes of field and the measure in heterogeneous medium to validate the modelling of the Monte-Carlo algorithm too.

Evaluation of the ITV (Internal Target Volume) contouring tool on imaging Deviceless 4D-CT (GE) of a dynamic phantom in the case of lung cancer thanks to MIRADA software

Fanny Lacroix[1], Julie Desrousseaux[1], Jérôme Champoudry[1], Xavier Muracciole[1], Stéphanie Gempp[1]

[1]Service de Radiothérapie CHU Timone, Marseille - *Hôpital La Timone - AP-HM - 264 Rue Saint Pierre 13385 Marseille Cedex5 - France*

Introduction: The purpose of this study is to compare differents semi automatic contouring tools of ITV on imaging Deviceless 4D-CT in the case of lung moving tumor.

Methods: 8 4D-CT acquisitions (with a GE Scanner Discovery RT, with Smart Deviceless 4D option) have been realized on the CIRS Dynamic Thorax phantom (Model 008A/008PL), with 8 different respiratory cycles, simulated by CIRS motion control v1.1.2 dedicated software. For each respiratory phases, the GTV has been contoured manually by a single operator. Then by combining these 10 GTV the ITVref has been obtained. Different MIRADA tools have generated various ITV, which have been compared to the ITVref:

- Thanks to MIRADA's ITV auto-segmentation module (Auto-ITV), a semi-automatic delineation of the ITV was generated from each GTV of each 10 respiratory phases. Once these 10 Auto-ITV obtained, a comparison in terms of volume and centroid position (X, Y, Z) was performed to determine the phase from which the generated Auto-ITV was most similar at ITVref: it's the ITVauto.
- On the MIP reconstruction obtained from 4D-CT images (thanks to Advantage4D (GE) software) the lesion was delineated manually, it's the ITVmip.
- MIRADA allows the MIP reconstruction of 4D-CT images, with the manual contour of the lesion on these images we obtain the ITVmip_mir.

For these 3 ITV, the relative uncertainties in terms of volume and the absolute uncertainty of the centroid position with the ITVref were calculated. The difference in shape were evaluated thanks to the DSC: Dice Similarity Coefficient. Then a ROC analysis was done.

Results:

- *Determination of ITVauto:* Regarding the 8 4D-CT acquisitions, the lowest mean relative uncertainty in terms of volume between the Auto-ITV generated from the GTV phase 70% of respiratory cycle and the ITVref is 5.5% (for other Auto-ITV generated uncertainty range from 10 to 20%). In addition, for this Auto-ITV 70% the difference in position of the centroid with the ITVref for 6 out of 8 cases is zero or less than 1 mm for one direction. For the rest of our study, the ITVauto corresponds to the Auto-ITV generated from the GTV phase 70% of the respiratory cycle.
- *Comparison ITVauto, ITVmip, ITVmip_mir with ITVref:* The comparison in terms of volumes for ITVauto, ITVmip, ITVmip_mir compared to ITVref gives respective relative uncertainties of 5.5% [min 0% - max 13.9%], 8.4% [min 4.5% - max 13.6%], 11.1% [min 0% - max 18.2%]. Whatever the case considered, the centroid position of the ITVref is confused (within 1 mm) with the positions of the centroids of the 3 different ITV generated. If contours are identical, the DSC is equal to 1. For 5 cases out of 8, the ITVauto method has the best DSC, with values ranging from 0.896 to 0.964 and an average value equal to 0.941.

The ROC analysis for the 3 ITV generated revealed that for 4 cases out of 8, ITVauto has the best benefit / risk ratio. Whereas for other 4 cases, the best benefit / risk ratio is discussed between the 3 methods of delineation of the ITV.

Conclusion: The ITV auto-segmentation tool from the 70% respiratory phase proposed by MIRADA seems to be the most representative method of ITV delineation for lung lesions motion on a dynamic phantom. In view of this study, an evaluation on a cohort of patients will verify and validate this result in the case of lung cancer.

Using a reduced data set of measurements for CyberKnife M6 commissioning: a safe way to save time without accuracy loss?

A. Rignon[a], Y. Barbotteau[a], F. Allot[a]

[a]Centre de Radiothérapie de CLAIRVAL / Marseille / France

Introduction: Considering clinical activity and treatment types, the accelerator section of a Cyberknife (Accuray) has to be renewed every 18 to 36 months.
This replacement leads to new commissioning and new models. This crucial process impacts patient care capability for a long time. Actually, the data measurements, models and dosimetric verifications, have to be done for every clinically used algorithms and collimation types:
- fixed cones and IRIS (variable aperture size collimator) are used with RayTracing and Monte Carlo algorithm
- MLC is used with FSBP (Finite Size Pencil Beam) and Monte Carlo algorithm.
Aware of this issue, Accuray henceforce offers to acquire a reduced data set for save time during the commissioning process. This study aims at verifying that this new method does not induce an accuracy loss in dose to patient calculation.

Methods: Only A-type algorithms are concerned by this data set shrink: RayTracing (fixed and iris collimators) and PencilBeam (MLC). Monte Carlo algorithm is not concerned. Accuray proposes to remove 2 out of the 5 depths required for profiles measurements. Considering the 3 collimator systems, these are 116 less profiles to measure in a water tank. For each collimator-algorithm couple, 2 models have been created: one from the standard 5 depths data set and another from the reduced 3 depths data set. The 2 models comparison has been run following 2 steps. First, using single beam treatment plans calculated on a homogeneous rectangular phantom. Calculated profiles at missing depth are compared to measure. Then, RTDose files have been used to run a 3D gamma index comparison (1% local /1mm). Secondly, several realistic treatment plans were calculated for cranial, spinal and pelvic localizations using both models. RTDose files have been used to run a 3D gamma index comparison (1% local/1mm) the same way. 3D gamma index comparisons have been made with a in-house software written in Python. A batch-mode was implemented allowing a fast and exhaustive analysis.

Results: Whether analyzing realistic or simple treatment plans, differences appear between the models made with the 2 data sets. Yet, these differences are clinically admissible.
Profiles are measured at a constant source-detector distance. Depth-related profile variations are smooth enough to be well interpolated under these conditions.

Conclusions: Estimated time sparing with this reduced data set of measurements is up to 3 to 4 days, with no relevant accuracy loss in dose to patient calculation.

Application of the TRS-483 correction factors on output ratios measurements for 8 detectors in stereotactic radiosurgery with cones

Application des facteurs correctifs issus du TRS-483 sur les facteurs d'ouverture du collimateur mesurés avec 8 détecteurs en radiothérapie stéréotaxique.

T. Cardon[a], R. Amblard[a], N. Garnier[a], R. Villeneuve[a], Anaïs Gerard[b], Mourad Benabdesselam[c], B. Serrano[a]

[a]Princess Grace Hospital Center, Medical Physics Department, Monaco
[b]Centre Antoine Lacassagne, Medical Physics Department, Nice, France
[c]Institut de Physique de Nice, Côte d'Azur University, Nice, France

Introduction: The purpose of this work is to assess correction factors performances from TRS-483[1] for output ratio (OR) determination in clinical 6 MV with flattening filter (WFF) Clinac and 6 MV flattening filter free (FFF) Truebeam stereotactic radiosurgery mode for cone irradiation using EBT3 films as reference[2].

Methods: Correction factors are applied to OR measurements for 10 cones with diameters between 30 to 4 mm on the Clinac 2100C (Varian) for a 6 MV WFF and 6 cones with diameters between 15 to 4 mm on the Truebeam STx Novalis (Varian) for a 6 MV FFF beam. Measurements were done in a water tank (MP3 phantom PTW) respectively at a 10 and 1.5 cm depth with a distance source water tank of 100 and 98.5 cm in WFF and FFF conditions. The detectors used were ionization chambers: Pinpoint and Pinpoint 3D (PTW), diodes: SRS, P, E (PTW) and Edge (Sun Nuclear), Microdiamond (PTW) and EBT3 radiochromic films. The OR measured by each detector were corrected by Alfonso formalism[3]. The $OR_{corrected}$ are compared to EBT3 radiochromic films OR_{film} considered as the reference. OR were normalized with a 30 mm cone diameter for 6 MV WFF and with a 3 x 3 cm² field for 6 MV FFF. For the 8 detectors, the OR repeatability was very high: r = 0.99. The mean uncertainty of EBT3 films response was estimate lower than 2.6 % (2σ).

Results: The TRS-483 correction factors on output ratios measurements for the detectors studied here are not available for all the cones sizes and depends on the type of detectors. However, whatever the detector and the cone size, when the correction factors are available, differences between $OR_{corrected}$ and OR_{film} are less than 1% and 2% respectively in WFF and FFF measurement conditions. The most interesting detectors, which are usable for cones diameters sizes up to 6 mm, are the diodes E and SRS. Their responses is less than respectively 0.8 % at 10 cm depth and 1.8 % at 1.5 cm. Only the Microdiamond has correction factors in the TRS-483 down to the cone diameter of 5 mm with a result less than 0.5%.

Conclusions: When available, the application of output ratio correction factors in stereotactic cone radiosurgery using a 6 MV WFF or FFF allows, for all the detectors studied, to obtain corrected OR without significant difference with our EBT3 film reference. Despite not being for the Truebeam in the TRS-483 conditions of 10 cm depth. For the 4 mm diameter cone, the TRS-483 do not provide any correction factors.

References

1. International Atomic Energy Agency, Dosimetrie of Small Static Fields Used in External Beam Radiotherapy. Rapport n°483, 211 pages, Vienne (2017).
2. Girardi A. et al. Small field correction factors determination for the IBA razor nano chamber and the IBA razor chamber. Physica Medica. **52,** 151-152 (2018)
3. Alfonso R. *et al*. A new formalism for reference dosimetry of small and nonstandard fields. Med. Phys. **35 (11),** 5173-81 (2008).

Output ratios measurements in stereotactic radiosurgery using cones with a 6 MV FFF beam: comparison between 8 detectors

Comparaison des facteurs d'ouverture collimateurs mesurés avec 8 détecteurs en radiothérapie stéréotaxique utilisant des collimateurs coniques en 6 MV FFF

T. Cardon[a], N. Garnier[a], R. Amblard[a], R. Villeneuve[a], Anaïs Gerard[b], Mourad Benabdesselam[c], B. Serrano[a]

[a]Princess Grace Hospital Center, Medical Physics Department, Monaco
[b]Centre Antoine Lacassagne, Medical Physics Department, Nice, France
[c]Institut de Physique de Nice, Côte d'Azur University, Nice, France

Introduction: The purpose of this work is to assess 8 detectors performances for output ratio (OR) determination, in clinical 6 MV flattening filter free (FFF) beam of the Truebeam STx Novalis stereotactic radiosurgery linear accelerator for cone irradiation using EBT3 radiochromic films (Ashland) as reference[1, 2, 3].

Methods: We study 6 cones with diameters between 15 to 4 mm on a Varian linear accelerator with a 6 MV FFF beam. Measurements were done in a water tank (MP3 Phantom PTW) at a 1.5 cm depth with a distance source detector of 100 cm. The evaluated detectors were ionization chambers: Pinpoint (PTW), Pinpoint 3D (in axial and radial position) (PTW), diodes: SRS, P and E (PTW), Edge (Sun Nuclear), microdiamond (PTW) and EBT3 radiochromic films. The OR were normalized with a 3 x 3 cm² field and compared to EBT3 films as reference detector. For all of the 8 detectors, the OR repeatability was very high: r = 0.99. The mean uncertainty of radiochromic films response was estimate lower than 2.6% (2σ).

Results: Pinpoint and Pinpoint 3D in axial position both underestimate OR. Results of measurement comparisons with film can reach out to respectively -1.7% and -2.7% for cone diameter ≥ 10 mm until -10.3% and -16.7% for smaller cones. This phenomenon is enhanced in radial position for Pinpoint 3D: up to 26% for the smaller cone. Non-shielded (SRS and E) and shielded (P and Edge) diodes overestimate OR respectively up to 2.2% and 3.2% for cone diameter ≥ 10 mm. This overestimation can reach out to 7.1% and 5.4% for smaller cones. Microdiamond is the closest to radiochromic films whatever the cone size with a maximum overestimation of 2.3% for the 6 mm diameter cone.

Conclusions: Among all detectors studied, microdiamond is the more accurate active detector for the OR determination of stereotactic cones despite its sensitive surface size. Pinpoint, Pinpoint 3D and diodes, respectively due to inappropriate size of sensitive volume and composition do not seem appropriate without corrective factors below 10 mm diameter cone.

References

1. Morales JE. *et al*. A comparison of surface doses for very small field size x-ray beams: Monte Carlo calculations and radiochromic film measurements. Australas. Phys. Eng. Sci. Med. 37, 303-9 (2014).
2. Garnier N. Amblard R. Villeneuve R. *et al*. Detectors assessment for stereotactic radiosurgery with Cones. J. Appl. Clin. Med. Phys. **19 (6)**, 88–98 (2018).
3. Girardi A. *et al*. Small field correction factors determination for the IBA razor nano chamber and the IBA razor chamber. Physica Medica **52**, 151-152 (2018)

Dosimetric study before implementation of stereotactic treatment conditions on a future VersaHD linear accelerator: impact of table rotations in VMAT and DCA

M.Zinutti [ab], A.Moine[b], J.Terrinha[b], L.Maillot[b], M-H.Mercier[b]

[a]Institut Universitaire du Cancer Toulouse /Toulouse/France
[b]Institut de cancérologie de Bourgogne/Chalon sur Saône/France

Introduction: This study was conducted in the context of a forthcoming VersaHD accelerator installation for patients treated with intracranial stereotactic treatment conditions. The future MLC was implemented in our TPS. The aim of this work was to quantify the interest of table rotation for two treatment techniques: Dynamic Conformal Arctherapy (DCA) and Volumetric Modulated Arc Therapy treatment (VMAT).

Methods: CT images from old patient treatments were selected. Ten patients with tumor size from 2.04 to 67.27 cm^3 close or not from OARs were included.
For each patient, four treatment planifications were performed with or without table rotation in VMAT and DCA techniques. Thus, for each of the two techniques, a plan with a 360° gantry rotation without table rotation and a plan with three partial gantry rotations with three table rotations were compared. All plans were normalized such as 98% of the PTV was covered by the 27 Gy isodose (prescribed on the 80% isodose in three fractions).
Several parameters were considered: the Paddick conformity index IC, the gradient index IG, the ICRU83 homogeneity index HI, total UM number and dose criteria received by the target and organs at risk.

Results: While mean IG index is lower with table rotations for both techniques (VMAT and DCA), no significant differences were observed on IC and HI (see table 1).
Healthy brain irradiated volume is smaller with table rotations plans for both techniques ($V_{12GyDCA}$=3.35%±3.03 and $V_{12GyVMAT}$=3.71%±3.03 with table rotations respectively against 4.58±4.18 and 4.75±3.79% without table rotations).
For target volume above 20cm^3, healthy brain dose criteria are not achievable for all plans.
Brain stem protection is better in VMAT: $D_{0.5cc}$=6.05±4.62 and 6.68±5.15Gy with and without table rotations respectively against 7.09±6.28 and 9.32±7.63 in DCA. VMAT plans with table rotations better protect all the OARs except for cochlea.

Conclusions: Table rotations lead to a better protection of OARs in intracranial stereotactic treatment conditions. Their impacts are not significant with dosimetric index. VMAT plans with table rotations are better in case of a PTV close to OARs like brain stem. However, DCA plans with table rotation are a suitable solution for a PTV far from OARs.

	Parameter	Plan 1: DCA 360° gantry rotation without table rotation	Plan 2: DCA with three partial gantry rotations with three table rotations	Plan 3: VMAT360° gantry rotation without table rotation	Plan 4: VMAT with three partial gantry rotations with three table rotations
Index	$CI_{Paddick}$	0,79 ± 0,07	0,78 ± 0,06	0,82 ± 0,10	0,85 ± 0,06
	$GI_{Paddick}$	4,25 ± 1,96	3,20 ± 0,66	5,36 ± 2,29	4,75 ± 2,18
	HI_{ICRU83}	0,19 ± 0,07	0,22 ± 0,04	0,24 ± 0,04	0,23 ± 0,03
Target	UM number	1282,40 ± 151,12	1161,51 ± 135,84	1424,50 ± 213,30	1344,30 ± 155,35
	Dmax PTV	33,98 ± 1,93	34,31 ± 1,44	35,31 ± 1,42	34,80 ± 0,65
	D99% PTV	26,77 ± 1,60	26,44 ± 0,17	26,52 ± 0,38	26,57 ± 0,26
	PTV Volume (cm^3)	20,81 ± 22,96			
Organ at risks Protection	Dmean healthy brain	2,48 ± 1,72	2,18 ± 1,48	2,34 ± 1,56	2,17 ± 1,47
	Healthy brain volume (cm^3)	1386,85 ± 119,00			
	V12Gy healthy brain (cm^3)	63,06 ± 58,46	46,18 ± 42,64	64,92 ± 51,73	50,82 ± 41,41
	V12Gy healthy brain (%)	4,58 ± 4,18	3,35 ± 3,03	4,75 ± 3,79	3,71 ± 3,03
	V23,1Gy healthy brain	10,73 ± 10,45	9,84 ± 9,78	10,70 ± 9,37	9,81 ± 8,47
	Dmax right optique nerve	2,64 ± 2,76	1,92 ± 2,06	1,78 ± 1,80	1,43 ± 1,70
	$D_{(0,2cc)}$right optique nerve	2,11 ± 2,51	1,44 ± 1,53	1,46 ± 1,56	1,16 ± 1,36
	Dmax left optique nerve	2,75 ± 3,00	2,01 ± 2,58	2,51 ± 3,32	1,95 ± 2,99
	$D_{(0,2cc)}$ left optique nerve	2,24 ± 2,76	1,63 ± 2,13	1,98 ± 2,88	1,60 ± 2,67
	Dmax rigth lens	1,46 ± 1,65	0,74 ± 0,57	0,94 ± 1,05	0,68 ± 0,55
	Dmax left lens	1,47 ± 1,81	0,83 ± 1,00	1,27 ± 2,50	0,82 ± 1,40
	Dmax Chiasma	4,54 ± 5,02	3,79 ± 3,81	2,66 ± 2,82	2,42 ± 2,77
	Dmax right Cochlea	2,38 ± 4,03	3,18 ± 4,05	3,19 ± 4,95	3,37 ± 4,16
	Dmax left Cochlea	2,94 ± 4,19	3,89 ± 6,77	4,48 ± 6,74	4,19 ± 5,87
	Dmax Brain stem	11,44 ± 9,26	10,15 ± 8,87	9,64 ± 8,40	9,33 ± 8,34
	$D_{0,5cc}$ Brain stem	9,32 ± 7,63	7,09 ± 6,28	6,68 ± 5,15	6,05 ± 4,62

Table 1: Results of different parameters for four treatment plans.

Towards a new dosimetry reference quantity for stereotactic radiotherapy: the dose area product
Développement d'une nouvelle grandeur de référence pour les traitements en conditions stéréotaxiques: le produit dose-surface

J. Jurczak[a], B. Rapp[a], S. Dufreneix[b], J. Gouriou[a], F. Delaunay[a], J-M Bordy[a].

[a]CEA, LIST, Laboratoire National Henri Becquerel (LNE-LNHB), Gif-sur-Yvette, France.
[b]Department of Medical Physics, Integrated Center for Oncology, Angers, France.

Introduction: Traceability of delivered doses in external radiotherapy is based on the national reference of absorbed dose to water at a point. Appropriate for conventional radiotherapy, this approach requires correction factors that burden the uncertainty budget for stereotactic irradiations, on the rise in the last few years. To obviate this difficulty, the LNHB suggested replacing the concept of point dose by the dose area product (DAP). In that way, a previous thesis in the laboratory has proven the feasibility of this concept from the metrological point of view[1,2].

Methods: This project is part of a PhD started in January 2019. The field sizes lower or equal to 15 mm diameter defined by specially designed collimators, multi-leaves and jaws will be investigated, as well as the transfer of the DAP national dosimetry reference of the LNHB towards the clinical user thanks to a large-area plane-parallel chamber specially designed by the LNHB and its use for the commissioning of medical linear accelerators (LINAC).

Results: Once this transfer dosimeter manufactured and tested, it will be used to characterize the radiations fields, in particular through parameters such as tissue phantom ratios and output factors (OF), whose accuracy is essential for the calculation of the treatment planning systems (TPS). For the OF, a comparison will be made between the obtained values if one consider the absorbed dose to water at a point (IAEA 483 protocol) or the DAP, the latter being considered to provide more accurate values because intrinsically not influenced by the electronic equilibrium problems inherent in stereotaxy. The comparison will allow validating or not the results based on the point dose used until now.

Conclusion: This project is aimed at promoting the use of DAP for small field sizes to, in fine, improve the dosimetric accuracy of treatments. One of the objectives, as long as TPS algorithms don't accept DAP as input data, is to propose to the clinical user a conversion protocol between the two quantities leading to more reliable traceability of the absorbed dose for the LINAC commissioning.

References

1. Dufreneix S. Etablissement de références dosimétriques dans les faisceaux de rayons X hautes énergies et de très petites sections (<1 cm²) pour la radiothérapie. Paris-Sud University, 2014.
2. Dufreneix S, Ostrowsky A, Le Roy M, Sommier L, Gouriou J, Delaunay F, *et al*. Using a dose-area product for absolute measurements in small fields: a feasibility study. *Phys. Med. Biol.* **61**, 650–662 (2016).

CyberKnife quality assurance - a manufacturor-independent tools based on a portative high energy imager

Y. Barbotteau[a], M. Crespin[b], A. Rignon[a], F. Allot[a]

[a]Centre de Radiothérapie de CLAIRVAL / Marseille / France
[b]Centre de Radiothérapie de BEAUREGARD / Marseille / France

Introduction: The CyberKnife® (Accuray) is a highly complex robotic radiosurgery system. As such, CyberKnife should follow a comprehensive QA program. Two significant reports, the AAPM-TG-135 and the Canadian TQT Guidelines for CyberKnife, and the manufacturor recommendations allow to establish an appropriate QA program. However, most of the tests are quite simple as they are based on water tank or Gafchromics® films measurements. It's all the more surprising that for classic LINACs, elegant and accurate solutions using the embedded portal imager have been around for years. This study aims at demonstrating the feasibility of using a portative high energy imager to perform QA controls on the CyberKnife by comparing quality controls based on measurements done with this imager and quality controls based on standard methods.

Methods: This study has been performed with a CyberKnife M6 model with 3 collimator systems: fixed cone (from 5 to 60 mm), Iris (variable apertures from 5 to 60 mm) and MLC Incise 2. To reach the required accuracy, high spatial resolution and energy response were the main criteria of choosing the portative imager. Other parameters such as imager size, pixel depth and frame rate have to be consistent with the CyberKnif e beam characteristics. Thus, the multipurpose radiography flat panel detector referenced as XRD 0822 of Perkin Elmer was selected. The main characteristics of this detector are:
- energy ranging from 20 keV to 15 MeV,
- pixel size 0.2 mm,
- active surface of 1024 x 1024 pixels (200 x 200 mm2),
- depth pixel 16 bits,
- frame rate up to 30 frames per second.

An in-house software, written in C language, was developed to operate the image acquisitions with the high energy imager and to convert them in DICOM format. This software corrects all acquired images by taking into account dead pixels, dark current and uniformity of the imager response. For IRIS and fixed cone, the following parameters are analyzed: absolute field size diameter, beam symmetry, beam circularity, beam homogeneity and constancy of the output factors. For MLC Incise 2, picket and garden fence tests are performed.

Results: The imager stability and its intrinsic performances are good enough to ensure the reliability of the results. Constancies tests are consistent with the water tank measurements despite the fact that in-water dose is compared to in-silico dose. After having carefully selected the grey level threshold, geometrical measurements such as field size diameter and circularity are consistent too.
Picket and Garden fence tests results are compared to the ones performed with Gafchromics films (which are analyzed with RIT113 software) and more accurate and objective results were found using the imager.

Conclusions: Portative high imager is an adequate device to perform automatic and accurate QA controls for CyberKnife system. Further investigations are in progress for the possibility of using this device for patient QA.

Mise en place du scanner 4D réduit et utilisation des densités effectives pour la stéréotaxie pulmonaire

A. Hadj Henni[a], S. Thureau[a], E. Anger[a], J. Maire[a], E. Labbe[a], R. Lejeune[a], G. Bulot[a], R. Zidi[a], Y. Lauzin[a]

[a]CRLCC Centre Henri Becquerel Normandie-Rouen, Rouen, France

Introduction : Dans le cas des traitements stéréotaxiques pulmonaires, l'AAPM TG 101 recommande l'utilisation d'une grille de calcul avec une résolution inférieure à 2mm et une résolution longitudinale des coupes scanographiques équivalente. Avec ces contraintes, l'utilisation d'un scanner 4D (CT4D) sur l'ensemble du thorax pour création d'un ITV est impossible dû au trop grand nombre de coupes. L'objectif est de diminuer la zone d'exploration du scanner 4D et de réaliser la planification dosimétrique sur un scanner 3D en respiration libre (CT3D_RL) avec des coupes de 1.25mm. Cependant cette « stratégie ITV » implique dans le volume cible, une tumeur mouvante de forte densité entourée de tissu à faible densité. Cette densité dynamique rend le calcul de dose sur le CT3D_RL imprécis. La publication de D.Wiant et al. « On the validity of density overrides for VMAT lung SBRT planning » propose de « forcer » les densités dans l'ITV et dans la couronne (PTV- ITV) pour améliorer le calcul de dose par l'algorithme AAA. Nous proposons dans ce travail, et en nous basant sur cet article, d'évaluer l'effet de différentes configurations de densités forcées sur la qualité de la planification dosimétrique.

Méthodes : Ce travail utilise 10 patients traités pour un cancer bronchique non à petites cellules en stéréotaxie par arcthérapie volumétrique (VMAT, Eclipse AAA 13.6, PRO3, Varian®). L'étude évalue l'écart du calcul dosimétrique entre la planification réalisé sur notre scanner moyenné de référence reconstruit à partir d'une acquisition 4D (CT4D_Moy) et différentes configurations sur scanner CT3D_RL : CT3D_RL, CT3D_RL en fixant les densités à l'intérieur du PTV à 0UH (CT3D_RL_PTV0), CT3D_RL en fixant les densités à l'intérieur de l'ITV à 0UH (CT3D_RL_ITV0), CT3D_RL en fixant les densités à l'intérieur de l'ITV à 0UH et la couronne (PTV – ITV) à – 200UH (CT3D_RL_HP200). Les doses au volume cible (PTV) et aux organes à risques ont été évaluées à l'aide des Histogrammes Dose-Volume.

Résultats : L'analyse des résultats dosimétrique ne montre pas d'écart significatif en termes de couverture et d'homogénéité pour le PTV et de contraintes aux organes à risques quelque soit la configuration.
Un relevé du PDL (Produit Dose Volume) pour les 2 protocoles (1 CT4D réduit et 1 CT3D en 1.25mm vs 1 CT4D en 2.5mm) réalisés sur fantôme anthropomorphique montre une diminution d'un facteur 2 de la dose délivrée.

Conclusions : La méthode CT3D_RL_HP200 proposée par l'article de Wiant et al. est validée dosimétriquement par comparaison à notre scanner moyenné de référence (CT4D_Moy). Cette configuration nous permet l'acquisition de coupes scanographiques de 1.25mm et une diminution de la dose délivrée au patient en réduisant la zone d'exploration du scanner 4D centrée uniquement sur le volume cible. L'étape suivante consistera, en utilisant notre fantôme respiratoire et des films gafchromic EBT3, à vérifier la concordance entre calcul et mesure pour ces différentes configurations.

Traitements stéréotaxiques intra et extra crâniens dans un environnement Elekta

V. Plagnol[a], C. Bouyer[a], I. Plagnol[a], C. Vignolo[a], E. Bruno[a]

[a]Centre Catalan d'Oncologie / Perpignan / France

Introduction: En 2016, le Centre Catalan d'Oncologie a mis en place les traitements hypofractionnés dits « stéréotaxiques » pour les patients atteints de pathologies crâniennes ou extra-crâniennes (pulmonaires et osseuses principalement). Nous avons effectué une collecte des données dosimétriques des patients traités avec ces techniques. Cela nous a permis de déduire des seuils d'alertes ainsi que des critères de validation dosimétriques à respecter avant chaque traitement.

Méthodes: Le Centre Catalan d'Oncologie évolue dans un environnement Elekta. Notre système de planification dosimétrique est le logiciel Monaco d'Elekta. Pour la mise en place de la technique stéréotaxique, nous avons travaillé avec la version 5.11.02. Les calculs de dose du logiciel sont basés sur la méthode Montecarlo. La grille de calcul utilisée est de 2mm et la précision de dose imposée est de moins de 2% par point de contrôle. Nous nous rapportons systématiquement à un formalisme de dose dans le milieu. La balistique est effectuée en technique VMAT avec un traitement scindé en deux parties. La machine qui délivre les traitements est un Synergy avec un multilame Agility de la marque Elekta, le tout piloté par le système Mosaiq (Version 2.64). Pour les tumeurs mobiles, nous utilisons Symmetry (Elekta) comme système de positionnement. Après un certain nombre d'études à blanc, nous avons entre autres relevé pour l'ensemble des planifications effectuées, les éléments dosimétriques suivants : l'indice de conformité (indice de Paddick), l'indice d'hétérogénéité, le nombre d'unités moniteur par Gray délivré, le taux de couverture du PTV, etc… De plus, les résultats des contrôles qualité patient pré-traitement effectués systématiquement ont été consignés pour différents critères de gamma index avec le système delta 4 de Scandidos. Un contrôle par mesure ponctuelle ionométrique est également effectué pour chaque patient.

Résultats: En avril 2019, nous avions effectué 266 dosimétries pour 221 patients différents depuis la mise en place de cette technique. L'analyse des données nous a permis de déduire un indice minimum de conformité IC à respecter pour les différentes localisations traitées : Poumons (156 cas) : IC>0.85 ; Vertèbre / Os (29 cas) : IC >0.85 ; Encéphale (72 cas) : IC > 0.90. Nous nous sommes également fixés des critères « d'attention » à respecter pour le nombre d'Unités Moniteur par Gray : Poumons (156 cas) : NbUM/Gy < 400 ; Vertèbre / Os (29 cas) : NbUM/Gy < 450 ; Encéphale (72 cas) : NbUM/Gy < 250. Pour le delta 4, nous avons décidé de fixer la validation à 95% des points de mesure acceptés avec les critères d'indice gamma local 2% / 2mm. Avec la méthode ionométrique, la mesure doit être inférieure à +-5% par rapport aux données de calcul.

Conclusions: La collecte des données et leur analyse ont permis d'encadrer notre pratique pour les traitements de radiothérapie hypofractionnés quelque soit la personne effectuant la dosimétrie. Une corrélation entre certains indices dosimétriques ou de qualité et la validation de la dosimétrie a été établie.

Impact of the PTV density on the treatment planning for lung SBRT patient

M. Savanović[a,b], D. Jaroš[c], K. Keraudy[a], F. Huguet[a], J.N. Foulquier[a]

[a]Department of Radiation Oncology, Tenon Hospital, 75020 Paris, France.
[b]Faculty of Medicine, University of Paris-Saclay, 94276 Le Kremlin-Bicêtre, France.
[c]Affidea. International Medical Centers. Center for Radiotherapy. 78000 Banja Luka. Bosnia and Herzegovina.

Introduction: The aim of this study was to evaluate the impact of the planning target volume (PTV) density on the treatment planning for lung cancer patient who underwent Stereotactic Body Radiation Therapy (SBRT).

Methods: Treatment of the lung SBRT patients using dynamic conformal arc (DCA) therapy depends on the proximity of OARs. The prescribed dose was 60 Gy to the PTV (± 80%) in 4 to 8 fractions. The gross tumor volume (GTV) was created from reference CT scan. Internal target volume (ITV) was generated from maximum intensity projection (MIP) to take into consideration overall tumor motion in all respiratory cycle. The PTV was created from the ITV by adding uniform margin of 3 mm. Due to tumor motion PTV encompasses more volume with low density. Additional volume for planning was created to ensure the PTV coverage, due to low density. Treatment was planned in Pinnacle 9.10 calculated using the Collapsed Cone Convolution (CCC) algorithm, for two to four partials DCA. The dose was delivered using linear accelerator TrueBeam Novalis STx. Evaluation of the PTV coverage was retrospectively analyzed depending on PTV density, for forty patients (16 female and 24 male) who underwent lung SBRT. The aim of this study was to evaluate complexity of the treatment planning for the PTV density smaller or greater than 0.5 g/cm3 (without overriding density). Respecting constrain for the PTV coverage (D98%>95%), we compared changes in the dose prescription, maximum dose, number of the monitor units (MU), margin volume and irradiated volume covered with 30 Gy (V_{30Gy}). The comparison of median values was performed using the non-parametric Wilcoxon test (significance level: $p<0.05$).

Results: Median density values of the PTV with lower density was 0.33 (0.20-0.44) g/cm3, for 20 patients; while 20 patients with higher density had the median PTV density of 0.58 (0.50-0.84) g/cm3. Median values of the PTV coverage for lower and higher density was 98.2 vs 98.7 % ($p<0.046$), respectively. Lung density was 0.21 vs 0.29 g/cm3 ($p<0.001$), dose prescription was 83 vs 90 % ($p<0.0001$), maximum dose was 74.43 vs 68.22 Gy ($p<0.0001$), number of the MU was 2206 vs 1787 ($p<0.033$), margin volume was 31.72 vs 27.62 cc ($p<0.045$) and V_{30Gy} was 117.26 vs 87.67 cc ($p<0.012$). Margin volume was 15 vs 10 times ($p<0.026$) larger than GTV volume.

Conclusion: Large tumor motion increases the ITV and decreases density in the PTV. Adding larger margins, the PTV coverage was ensured but irradiated volume was increased. To obtain similar PTV coverage, for the PTV with lower density, we need larger margin and more MUs, which can lead to higher maximum dose.

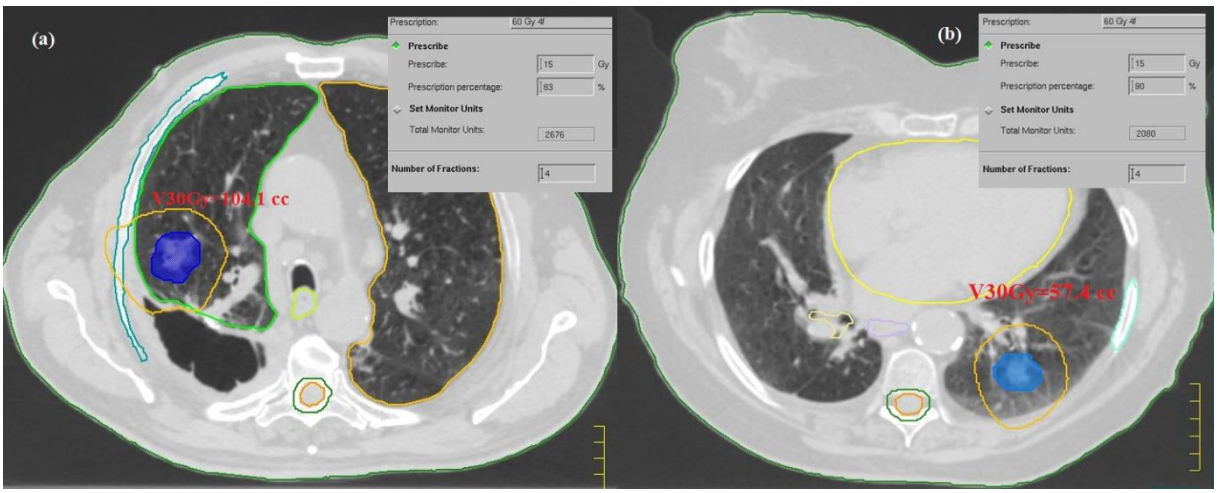

Figure1. The impact of the PTV density on the treatment planning was presented for two cases with PTV density 0.33 g/cm3 (Figure 1. (a)) vs 0.58 g/cm3 (Figure 1. (b)), with dose prescription, number of MUs and volume of 50% isodose line.

Posters – Médecine Nucléaire

3D phantom and immobilisation device printing in imaging
Impression 3D de fantôme et de système de contention en imagerie

L.Bonnor[a], H. Austins[a], A. Batalla[a] , S. Collet[a], C. Bertaut[a], L. Lechippey[a], P. Berejny[a], L. Guerin[a], K. Sebe-Mercier[a], C. Jaudet[a], C. Loiseau[a]

[a]Centre François Baclesse / Caen / France

Introduction: In medical imaging field, tools for optimizing dedicated examination, quality control and quantification are essential. This ensures monitoring, maintains optimum performance and personalized dose assessment. To meet these needs, we have developed a 3D printing protocol able to create realistic models and custom-made support [1].

Methods: We used a Tevo Tornado printer and PETG and PLA polymer plastics to ensure waterproofing and biocompatibility requirements. This technique consists of a layer-by layer deposition of 0.1mm of molten material. We have printed:
- Three rat phantoms created from the animal's scan acquisition. Containing pulmonary, renal, hepatic cavities and 4 spheres simulating tumors of different sizes;
- A patient support for thyroid examinations with pinhole collimator.
A comparison of the properties of the polymers was carried out as well as an optimization of the printing parameters. We have chosen PETG, which is more adapted to the constraints of nuclear medicine. It is rigid, hydrophobic and waterproof. A cubic mesh was used for isotropic reasons. The mesh density of the "rat" phantoms was optimized during printing to get close to the density of water with CT energy. Different densities are tested: 20%, 80% and 95%. We use a Philips Brilliance 40 scanner and the following acquisition parameters: 80kV, pitch 0.828, collimation 40x0.625mm, voxel of 1x1x1 mm3, matrix 512x512, FOV 500mm. The full uniformity within a region of interest is calculated. The phantom waterproofing is evaluated (4 measurements over a month) based on the segmented volume of water in the cavities. The support cushion for thyroid examinations is created from two filaments of different elasticity to limit the patient's head movements and improve comfort. Tolerance assessment is based on the success of the examination (400 seconds duration) on 20 patients.

Results: The average Hounsfield number values in a region of interest in the abdomen are -840, -162 and 55.6 HU respectively. This is not exactly 0 UH but it allows to segment the water of the cavity. The integral uniformity values are 32%, 53% and 47%. This is quite low but inherent of this printing technique. The water volumes in the cavities are from 5.5 to 0.16 ml. Their variation of filling is less than the measurement inaccuracy of 5%, which supports its use with radionuclides in preclinical applications. The support cushion was used on 20 patients with a 100% tolerance.

Conclusion: We printed different phantoms made of cavities and compatible with the constraints of nuclear medicine. A support cushion has been created for thyroid examinations with pinhole collimator and used on patients with a 100% tolerance. 3D printing represents an undeniable advantage in imaging for quantification and dosimetry as it is closer to clinical condition than available commercial phantom.

References:
1. Tiffany Beaumon et al. Development and test of sets 3D printed age-specific tyroid phantoms for 131I measurements. Phys. Med. Biol. 62 4673-4693 (2017).

Implementation of the PET-CT Qualimagiq software module to automate the analysis of the quality control of the Philips Gemini PET-CT scanner according to NEMA standards
Implémentation du module logiciel PET-CT de Qualimagiq pour automatiser l'analyse du contrôle qualité d'un TEP-CT Gemini Philips selon les standards NEMA

G. Guibert[a], C. Tamburella[a], S. Tual[a], L. Do Carmo[a], G. Amzalag[a], P. Weber[a]

[a]Radio-Oncologie, Hôpital neuchâtelois/La Chaux-de-Fonds/Suisse

Introduction: At the installation of a PET-CT scanner, acceptance tests are performed by the manufacturer. After these initial tests, the final user will perform regularly constancy tests to follow the stability of the performances of the installation. The objectives of all these tests are to ensure that the facility specifications meet the legal and constructor criteria and moreover to establish reference values. The PET-CT module of software package Qualimagiq from Qualiformed analyses images acquired to evaluate the PET-CT performances, in compliance with the international standards [1], it was implemented for the first time on a Philips Gemini PET-CT. It allows achieving an automatic routine image quality control. For both PET and CT, the parameters are spatial resolution and image quality (contrasts, noise, homogeneity). For the PET, tests are completed by the accuracy of the attenuation maps and corrections. Finally, the calibration check of the system is done by measuring the mean SUV.

Methods: Different test objects or phantoms are scanned in clinical conditions, either for the CT modality only, either for the PET only, or for both. The PET-CT Software module has been installed on the Qualimagiq platform already used to automate quality controls on our radiation therapy treatment machines. Algorithms analyze DICOM images acquired for quality controls with many image processing methods but all are applied after the detection of the phantom in the image to avoid the influence of its misalignment with the imager. This detection is mainly based on circular object detection because this geometry is preserved by an image zoom which really improves the spatial resolution of the analysis. The software configuration is supported by Qualiformed. The users can modify in Qualimagiq the analysis settings at any time and save them during the process. The algorithms identify images to be analyzed thanks to specific keywords contained in the DICOM header.

Results: For each test the pdf results file is divided in two parts. The qualitative analysis shows the cold, hot or contrasted regions of interest on the image. If the delineation of the analysis ROI is well focused on the target in the phantom then the setup is valid whereas an offset indicates some mistakes. Graphs and data tables containing value ±SD, units and their tolerances are then not reliable. References values are extracted from these tables.

Conclusions: The PET-CT module of the Qualimagiq software package from Qualiformed answers to the QA program according the NEMA standards. The principle of algorithm analysis based on geometric shape detection is relatively intuitive, even though the module configuration represents an important task. The data analysis is fast and the report traceability is systematic (machine, operator, date).

References

1. Performance measurements of PET. NEMA Standards Publication NU 2-2012. Rosslyn, USA: National Electrical Manufacturers Association. 2012.

NEMA performance evaluation of a digital PET / CT
Evaluation des performances NEMA d'une TEP/TDM numérique

A. Belly-Poinsignon[a], C. Michel[a], C. Provost[c], M. Mohamad Alabdoaburas[a], F. Matloob[b], C. Savary[b], L. Champion[b], R. Belshi[a]

[a]Service of medical physics/Saint Cloud/France
[b]Service of nuclear medicine /Saint Cloud/France
[c]Service of radio-pharmacology/Saint Cloud/France

Introduction: Institut Curie, at the Saint Cloud site, installed a Philips VEREOS digital PET/CT in August 2018 in its nuclear medicine service. Acceptance tests, evaluating the physic performances of the system, were carried out according to the NEMA NU2-2012 protocol1. Acquisitions were made using available scanning procedures in the console. Generated values, of physic parameters, were then calculated from the Matlab© program implemented in the system.

Methods: Performance measurements were assessed with 18F radionuclide. Spatial resolution was measured using a point source. Sensitivity was evaluated using successive acquisitions of a homogeneous line-source placed inside metal sleeves of different diameters. Count-rate performance of the system was calculated from acquisitions of a 1.3 GBq line-source placed in a cylindrical polyethylene phantom. Finally, image quality was evaluated with a NEMA/IEC body phantom, containing refillable spheres of 10, 13, 17, 22, 28 and 37 mm (diameter) for a contrast spheres:background of 4:1. We compared our results with the performances obtained for equivalent equipment and for old generation analog PET/CT (relevant parameters).

Results: Range results of spatial resolutions (FWHM), at 1 cm and 20 cm from the center of field-of-view, were 4.03 to 4.68 mm for axial direction, 3.97 to 5.76 mm for radial direction and 3.97 to 4.91 mm for tangential direction. For 0 and 10 cm, we obtained an average sensitivity of 5.4 cps/kBq. Peak NEC was 167.86 kcps @ 56.67 kBq/ml and corresponding diffused fraction was 31.4 %. Relative error of count rate was 6.05 %. Contrast recovery coefficients varied between 55 % and 93 % for the 4 hot spheres (diameter 10, 13, 17 and 22 mm) and between 81 and 88 % for the 2 cold spheres (diameter 28 and 37 mm).

Conclusions: Achieved results are in agreement with expectations and show significant performance gains thanks to digital technology. Nevertheless, some parameters such as sensitivity must be correlated with time-of-flight PET performance. The performances are measurable with the manufacturer protocols without additional software.

References

1. NEMA-NU2 (2012) Performance Measurements of Positron Emission Tomographs, Nema Standard Publications

Posters - Imagerie

Etude dosimétrique suite à l'installation du système PHILIPS Clarity en neuroradiologie interventionnelle

J.B. Maurice[a,b], A. Kazemi[c], J.P. Pruvo[c], M. Vermandel[a,b]

[a]Unité de physique médicale / CHRU Lille / France
[b]Service de médecine nucléaire / CHRU Lille / France
[c]Service de neuroradiologie / CHRU Lille / France

Introduction : Le CHU de Lille est un centre de référence national en neuroradiologie interventionnelle, notamment pour la prise en charge en phase aiguë d'accidents vasculaires cérébraux ischémiques. Une des techniques employées, la thrombectomie mécanique, consiste à retirer le caillot à l'aide d'un dispositif mécanique introduit par voie endovasculaire sous contrôle radioscopique. La prise en charge en urgences et la complexité du geste peuvent engendrer des doses importantes à la peau du patient.

Méthodes : En mars 2018, la technologie Clarity (PHILIPS) a été installée sur une salle interventionnelle Allura Xper FD 21/10 (PHILIPS, 2008) permettant un traitement des images en temps de réel conduisant notamment à réduction du bruit. Tout l'environnement de travail a été adapté pour faciliter le geste du radiologue et diminuer la dose délivrée au patient : optimisation des protocoles par les opérateurs, l'ingénieur d'application et le physicien médical et installation d'un écran de grande taille configurable pour un meilleur confort visuel. Pour estimer l'impact de cette technologie sur la dose délivrée aux patients, nous avons déterminé les niveaux de référence interventionnels (NRI) pour cette salle avant et après l'upgrade à partir des données dosimétriques (Produit Dose-Surface) de 1003 interventions (respectivement 591 et 412 interventions avant et après l'upgrade) sur une période de 20 mois.

Résultats : Nous observons une diminution de 76 %, 70 % et 60 %, respectivement pour les NRI des interventions d'artériographie cérébrale diagnostique, de thrombectomie mécanique et d'embolisation d'anévrisme intracrânien. Les NRI pour ces 3 types d'intervention sont ainsi de 18 Gy.cm², 37 Gy.cm² et 75 Gy.cm². Ces valeurs sont très inférieures aux recommandations nationales (SFPM, 2017). Les PDS maximaux avant et après l'upgrade de l'installation sont respectivement de 338 Gy.cm² et 177 Gy.cm² pour la cohorte de patients.

Conclusions : Notre étude permet de confirmer la réduction de doses délivrées aux patients après l'installation du système Clarity. L'ordre de grandeur des doses délivrées est ainsi inférieur au seuil d'apparition de radiodermites ou d'alopécie (hors cas des ré-irradiations) pour notre échantillon de patients. La prise en charge des patients en neuroradiologie interventionnelle est donc nettement améliorée. Cette étude continuera en 2019 en intégrant le kerma dans l'air, le temps de scopie et le nombre d'images de graphie, ce qui permettra d'affiner nos résultats.

Références :
Rapport 32 : Niveaux de référence en radiologie interventionnelle, Société Française de Physique Médicale, Juin 1017

The setting up and the use of gafchromic film to evaluate the patient skin dose in interventional radiology
La mise en place et l'utilisation de film gafchromic pour évaluer la dose à la peau délivrée au patient en radiologie interventionnelle

Y. Bousserief[a], A. Fernandez[a], T.Blanpain[a], Dr.L.Faroux[a], Pr.D.Metz[a]

[a]51100/CHU Reims/France

Introduction: The use of X-rays involve stochastics et deterministics effects. The risk or deterministics effects appeare for absorbed skin dose about 3 Grays (Gy) delivered at one time. Moreover, the Authority of Safety Nuclear demand a patient's medical following when the skin dose exceed 3Gy. However, the devices, used in interventional radiology, just give us 2 indicators: the Airkerma and the Kerma Surface Product. That's why, in the hospital centre of Reims, we decide to use gafchromic films (GAFCHROMIC ISP modèle XR-RV3) to evaluate the patient skin dose in the service of cardiological exploration.

Methods: First of all, the calibration has to be done. For this calibration, gafchromic film is divided in multiple pieces of identical size (5cmx9cm). Then a piece of film is positionned in a support next to a detector (Unfors Xi of RaySafe), un the support too. The detector allow to know the delivred dose. Une piece of film is not irradiate in order to be use as a telltale, to estimate the background noise. The others are irradiated at differents doses with a step of 0,1Gy from 0 to 1Gy, a step of 0,5Gy from 1 to 6Gy. Next, each piece of film is readen, 24h later, thanks to a flatbed scanner (Epson Expression 10000XL) and connected with the delivred dose to make a calibration curve. Afterward, the calibration done, tests will be made on the most irradiant technique of the service, the chronic coronary occlusion treatment, by placing the film under the patient. The film will be read and the dose evaluate and compare with the indicators.

Results: The test on the patient has not started yet. The first results obtained with films will be compare for different parameters like the Body Mass Index (BMI), the operator, the surgical approach… Moreover, the dose obtained thanks to the film will be compare with the dose estimate through the software VirtualDoseIR.

Conclusions: It is difficult to conclude at this step of the research. However, gafchromic films seem to provide advantages like the estimation of the dose at the end of the treatment, the maximal skin dose delivred to the patient and the dose distribution mapping. The dose will be estimate just after the exam. This study will allow to determine the type of patient at risk (with the pathology, the BMI…) and to select the necessity of the use of a film for futur exams.

Dose tracking software implementation within a interventional radiology and cardiology department
Mise en place d'un logiciel de suivi de dose en radiologie et cardiologie interventionnelles

V. Plagnol[a], PM. Blayac[a], P. Maquin[a], F. Pey[a], L. Brunagel[a], B. Caron[a], J. Duriez[a], G. Garcia[a], R. Morales[a], Y. Roque[a]
[a]SCM Coradix - Centre Pierre Louis Tapias / Perpignan / France

Introduction : In 2017, the interventional radiology and cardiology department has set up a system for archiving and monitoring doses (DACS). This approach, part of the quality policy of the imaging center, had anticipated the requests of the decision n ° 2019-DC-0660 of the Autorité de Sureté Nucléaire (French Nuclear Safety Authority) which gave rise to the Decree of February 8, 2019. The DACS enabled us the analysis of the doses delivered during radioguided interventional practices and to deduce local reference levels.

Methods: The activity of the interventional radiology and cardiology department represents approximately 5000 examinations per year in three rooms: an interventional cardiology room, a hybrid room (interventional cardiology and radiology) and an electrophysiology room. The equipment are from GEMS manufacter, two JEDI 100 Vascular and a motorized Elite Cardio. Currently, this last table is not connected to the DACS. The dose management software used is Radimetrics from Bayer, which we know well because it has already been connected, for over 2 years, with all the CT scanners of our group. The implementation of the software was easy. The link with the terms is direct and does not go through the PACS. We collect in real time and in continuous flow all the data concerning each examination. Until then, an ad hoc study of two cases per year was carried out to establish reference levels. These studies were therefore based on a limited number of cases and had certain limitations due to the workload it represented.
With Radimetrics, all examination parameters data are recorded as well as the skin dose map delivered to the patient which is performed in real time without any further manipulation. Alerts have been institute, they relate to the dose area product, the dose at the reference point, the time of scopy but also the patient peak skin dose.

Results: As soon as the dose management software was installed, we were able to establish alerts, in accordance with the national recommendations on the management and follow-up of patients in interventional radiology and cardiology. Until then, the precious presence of radiologic technologists in the department allowed us to be alerted, now everything is done automatically.

Once the number of examinations has been sufficient, we have determined the local reference levels for all acts performed. Warning and alerts thresholds have been implemented in the software. The inter-operator practice can also be analyzed.

Conclusions : The presence of a DACS in a department of interventional radiology and cardiology is very important. This simplifies the detection of patients requiring follow-up. It allows a precise and direct knowledge of the peak skin dose delivered to the patient. For multiple exams on the same patient, we will have a cumulative dose mapping of his exams. Finally, local reference levels are based on a large sample and can be determined for all procedures.

Gestion de la magnéto-protection des travailleurs en Imagerie par Résonnance Magnétique

S. Aktaou[a], A. Al masri[a,b], K. Guerchouche[a], F. Maaloul[a]

[a]BIOMEDIQA Groupe/Villeneuve d'Ascq/France
[b]Polytech Lille/Lille/France

Introduction : Dans le service d'Imagerie par Résonance Magnétique (IRM), tous les travailleurs participant à la préparation du patient, sa mise en place, aux actions de nettoyage du tunnel, … sont susceptibles d'être exposés aux champs électromagnétiques (CEM) émis par l'appareil. L'exposition aux CEM peut provoquer chez les travailleurs des effets radio-biologiques indésirables. Le décret n° 2016-1074 du 3 août 2016 détermine les modalités spécifiques de protection contre l'exposition aux CEM dans les services d'IRM. Le but de cette communication est de proposer un processus organisationnel afin de rendre plus facile l'intégration de ces modalités de magnéto-protection dans la gestion et la maitrise du risque.

Méthodes : L'étude a été menée auprès de sept services d'IRM utilisant des aimants de 1,5 et 3 Tesla. Nous avons effectué pour chaque puissance une évaluation de l'exposition en mesurant les deux champs électromagnétiques (statique et dynamique) à différents points de l'appareil d'IRM à la fois à l'intérieur et autour de la salle d'examen. Les valeurs de mesures ont été comparées aux valeurs déclenchant l'action (VA) définies dans le décret national permettant de délimiter des zones à risque au sein du service. Finalement, nous avons croisé nos résultats avec les références britanniques et américaines (ceux de l'agence britannique de réglementation des médicaments et des soins de santé (MHRA) et la société américaine de radiologie (ACR)).

Résultats : Suite aux résultats de mesures des CEM et leur comparaison aux recommandations des sociétés savantes consultées, un système de zonage adaptatif aux besoins des différents services d'IRM à travers le pays a été proposé. En effets, trois zones à risque ont été identifiés au sein des services d'IRM. Ceci a permis l'élaboration d'un guide de bonnes pratiques liées à la magnéto-protection des travailleurs en IRM.

Conclusions : Le guide établi par notre étude est un standard qui permet aux intervenants dans le service d'IRM de se protéger contre le risque lié aux champs électromagnétiques.